Università degli Studi di Ferrara

DOTTORATO DI RICERCA IN

"SCIENZE BIOMEDICHE E BIOTECNOLOGICHE"

CICLO XXXIV°

COORDINATORE Prof. Pinton Paolo

Transcriptomics and cancer: beyond messenger RNA

Settore Scientifico Disciplinare MED/06

Dottoranda

Dott.ssa Crudele Francesca

Tutore

Prof. Volinia Stefano

Anni 2018/2021

INDEX

INTRODUCTION

Non coding RNAs (ncRNAs) represent a large portion of the human genome which is not translated into proteins, mediating transcriptional gene modulation [1]. Many non-coding RNAs contribute to the alteration of biological functions in normal cells, leading to progression and malignant phenotype in cancer [2]. Among them, the class of Ultra-conserved regions (UCRs) are DNA elements of more than 200 base pairs long, without insertion or deletion and extremely conserved in the orthologous loci of vertebrates, in particular human [3], mouse, and rat genomes [4], but Single Nucleotide Polymorphisms (SNPs) in UCRs are related to cancer susceptibility [5]. Their expression is altered in leukemia [6], liver cancer [7], glioma [8], and neuroblastoma [9], which might be modulated either by promoter hyper-methylation or by interactions with microRNAs (miRNAs) [10]. The Transcribed-UCRs (T-UCRs) are a class of non-coding RNAs and are involved in gene expression regulation transcription [11] and splicing [12] during development processes. There is a considerable overlap between T-UCRs and long non-coding RNAs (lncRNAs) [13, 14]. The biological functions of lncRNAs are ascribable to control and regulation of cell cycle, metabolism, immune response [15], differentiation [16], and transcription/translation [17], but they can also regulate cancer onset, progression, or survival of patients [18–21]. MiRNAs, a group of small non-coding RNAs, act as regulators of gene expression: they can enable oncogenes or inactivate onco-suppressors in solid cancers [22]. CircularRNAs (circRNAs) are convalently closed and single strand RNAs (ssRNAs) present in human cells with tissue- and cell-specific expression[23]. Since their discovery[24], they have been considered as aberrant products of splicing. Recent advances in RNA sequencing and circRNA-specific decoding tools allowed their quantification and characterization. Their biogenesis is specifically regulated and circRNAs may exert their functions in various ways, for example by acting as miRNA ('sponges'), as protein inhibitors (‘decoys’) or by being translated into proteins. Different studies have recently shown that tens of thousands of potential circRNAs are transcribed from the human genome[25, 26] and that their expression can be modulated in breast cancer and other cancers or leukemias[27–29].

CHAPTER 1: THE CODING POTENTIAL OF CIRCULAR RNAS IN HUMAN CANCER SAMPLES

The full functional role of circRNAs in cancer is still under debate[30] and several studies asserted that circRNAs can act as templates for translation. For example, Abe et al. demonstrated that a pool of circRNAs comprise boundless Open Reading Frames (ORFs) that can be translated in a protein concatemer by a mechanism called "rolling cycle amplification"[31]. Furthermore, Chen et al. confirmed the cytoplasmic localization of circRNAs in eukaryotic cells[32]. Different research groups explained two cap-independent mechanisms of circRNAs translation: the internal ribosome entry sites (IRES)-mediated translation and N6-methyladenosines (m6A)-mediated translation[33, 34]. To date, an increasing number of studies have also been investigating the coding potential of circRNAs[35–37] and the role of the peptides encoded by circRNAs and long non-coding RNAs in glioblastoma[38], colorectal cancer[39] and neurodegenerative disease[40]. In this paper, we studied the coding potential of the circRNAs sourced by MiOncoCirc, a pan-cancer compendium of more than 160,000 cancer circRNAs detected through a poly(A)-independent method and gene-body targeting: exome capture RNA-seq[28, 41]. We then studied the expression of a focused group of circRNAs with strong potential for novel protein isoforms in a wide range of human cancers and cell lines.

1.1 METHODS

Cancer circRNA selection. The MiOncoCirc dataset includes RNA-Seq data from a large number (n=2036) of cancer samples, derived from several tumor types (prostate adenocarcinoma, breast cancer, lung cancer, pancreatic cancer, liver cancer, etc.) and controls[28]. From the MiOncoCirc compendium (about 160,000 circRNAs), after excluding the read-through circRNAs (rtCircRNAs) located between two different genes, we selected the circRNAs with absolute count higher than 40, i.e., expressed in at least 40 different human samples (n=47,415). We then used the genomic coordinates of these circRNAs in conjunction with GENCODE (v. 33) to determine all different spliced isoforms. To account for alternative splicing events for each circRNA, the different transcripts corresponding to these circRNAs, and at least 150 nucleotides long, amounted to 56819 were considered. Using TransDecoder (v.5.5.0) we predicted for each circRNA transcript, and retained for further analysis, the circular ORFs (circORF) encoding for at least 50 ammino acids, starting with a methionine and ending with a stop codon.

In-silico characterization of polypeptides predicted from circRNAs. Using protein-BLAST (ver. 2.9.0) we determined the homologies between the polypeptides encoded by a circORF and by the respective linear isoforms (from Ensembl, release-101), with an e-value lower than 1e-10. In addition, we considered only the

protein isoforms validated in the Consensus Coding Sequence (CCDS) dataset at NCBI. Next, we used a Python script to isolate all circRNAs encoding for proteins with a mismatch of at least 1 amino acid at the amino- and/or carboxy- terminus, when compared to their CCDS isoforms. Upon comparison with the CCDS isoforms, we annotated the predicted circRNA proteins as having “canonical” or “internal” starting methionine and a “premature” or “canonical” stop codon.

The domain structure of circRNA encoded proteins. Then, we investigated the domain composition of the circRNA protein by using HMMER HmmScan (https://www.ebi.ac.uk/Tools/pfa/hmmer_hmmscan/). We compared the domains of each circRNA protein with those of each parental isoform (GENCODE, v. 33). We developed a Python script to identify the predicted circular proteins which had domain mismatches with the linear isoforms, in particular: i) different order (the circular RNA protein has the same domains but in a different order), ii) partial overlap only (missing one or more domains when compared to the parental isoforms), iii) partial overlap and one or more additional domain (i.e., missing a domain and presenting a circular RNA predicted domain that is not present in the linear isoforms), iv) same parental domain structure with additional domains, v) no overlap with the domain structure of parental isoforms.

Expression profile of circRNAs with unique protein coding potential in cancer. Finally, we investigated the cancer expression of the circRNAs with predicted unique polypeptides, focusing on those differing in primary structure when compared with the parental isoforms. We used the exome capture RNA-Seq data collected in MiOncoCirc [28] from clinical samples, cell lines and normal tissues (n=2036) [42–44]. Data were expressed as log2 reads per million (RPM); 15330 circRNAs with low variation in cancer and normal samples were retained using an IQR threshold of 0.5, of which 1308 code for proteins different from the linear isoforms. Samples with overall high expression of circular RNAs (n=1018) were filtered using the median of total log2 RPM counts as threshold.

Functional characterization of the circRNA with unique encoded proteins and expressed in cancer. The genes encoding the circRNAs differential expressed in cancer and with coding potential were studied for statistical over/under representation (FDR<0.05) using PantherDB (http://pantherdb.org/).

Identification of novel peptides in PeptideAtlas compendium. The novel terminuses from coding circRNAs, not aligned with linear counterparts, were used to find any match with Peptide Atlas (build: Human 2021-01), a compendium of peptides collected by mass spectrometer experiments from human and other organisms[45, 46].FASTA36[47] (version 36.3.8h Aug, 2019) was used to align the novel terminuses with Peptide Atlas database. We used BLASTP 2.13.0+ and the database RefSeq Select proteins as reference to check the similarity between the carboxy-terminus and peptides from Peptide Atlas.

1.2 RESULTS

1.2.1 Coding potential for novel proteins in cancer circular RNAs

With our work, we aimed to understand what the coding potential of circRNAs was, in cancer, for each human gene. Additionally, we looked for the most substantial alterations when compared to the canonical linear (parental) isoforms. Our hypothesis being that circRNAs possess the capacity to encode for unique and novel protein isoforms, that while still belonging to the locus parental protein family, are functionally different isoforms. Such functional relevant changes could include full or partially novel polypeptides, but also modifications of the parental domain structure. Figure1.1 illustrates the bioinformatics cascade leading to the identification of coding circRNAs, with novel protein structures and differentially expressed in cancer.

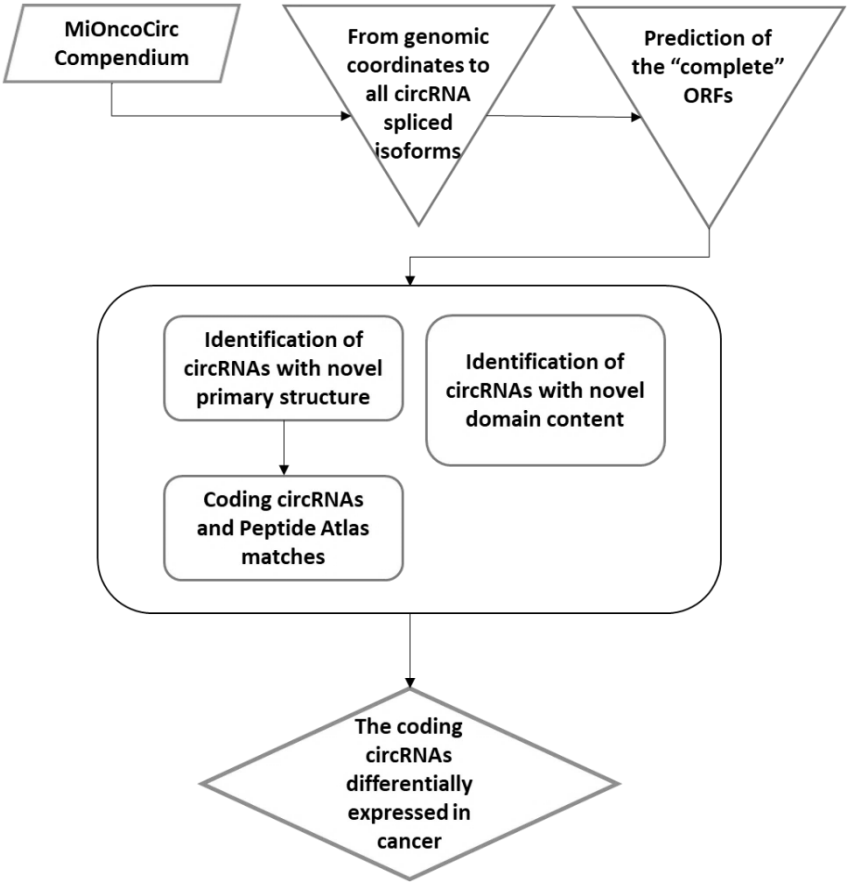

Figure 1.1 The flow chart representation of the study. The diagram synthesizes the bioinformatics analysis flow which led to the identification of the circRNAs with novel coding potential (structurally divergent proteins from those encoded by the linear mRNAs) and differentially expressed in a set of human cancer types. Legend: ORF: open reading frame.

Thus, we predicted the proteins from “complete” circular ORFs (circORFs), i.e., starting with AUG, terminating with a stop codon, and considered thereafter only those at least 50 residues long. Next, we looked for novel sequences among these circORF encoded proteins. Essentially, for each gene, we focused on the longest circORF proteins (n=4361) bearing a partial overlap (e-value lower than 1e-10) with their standard protein counterparts (from CCDS). Most of these novel protein coding circORFs started at the canonical AUG and were thus preceded at 5’ by the proper ribosome binding site (77.2%), followed by a minority of internal AUG (18.8%), while the remaining portion (4%) started with a novel 5’ extension encoding a completely new amino-terminus. On the contrary, the largest portion of these circRNA predicted human proteins had a novel sequence only at the carboxy-terminus (88.3%), while the minor parts ended with a premature termination (5.1%) or with the canonical stop codons of the linear protein (6.6%). Among them a small percentage of the predicted circORF proteins possessed both novel N and C termini (1.6%). Figure 1.2 illustrates the annotation of circORF terminuses-based.

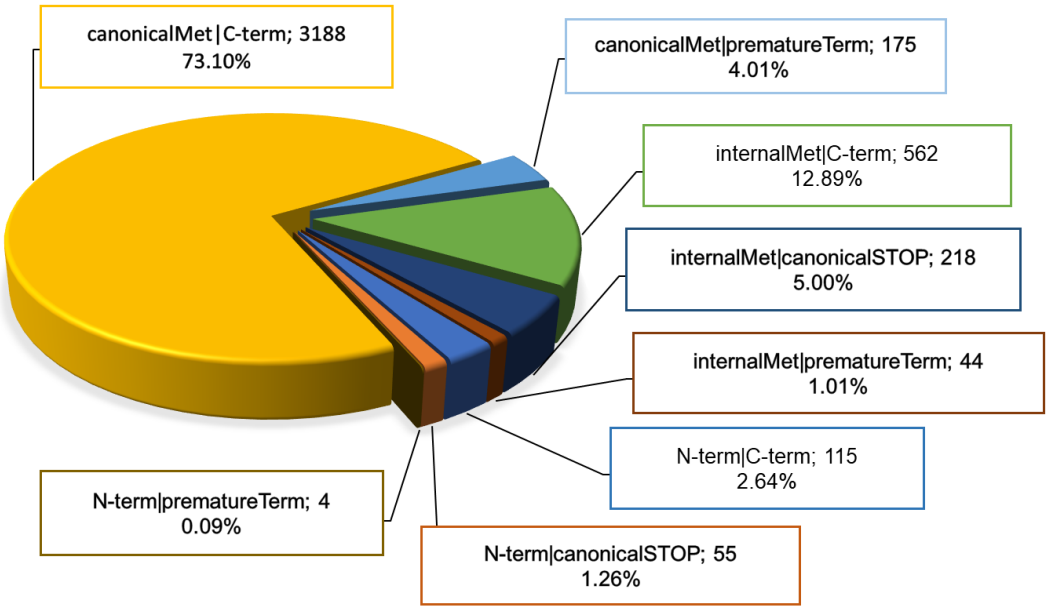

Figure 1.2 The percentage of circORFs characterized by novel or unexpected terminuses. This pie chart illustrates the number and the relative percentage of the circORFs with novel or unexpected combination of terminuses compared to all linear counterparts. The circORFs annotated as “canonicalMet|canonicalSTOP” are not included in the pie chart.

The distribution of the length for the predicted novel peptide extensions, respectively at amino- and at carboxy- terminus, alongside the descriptive statistics, are plotted in Figure 1.3

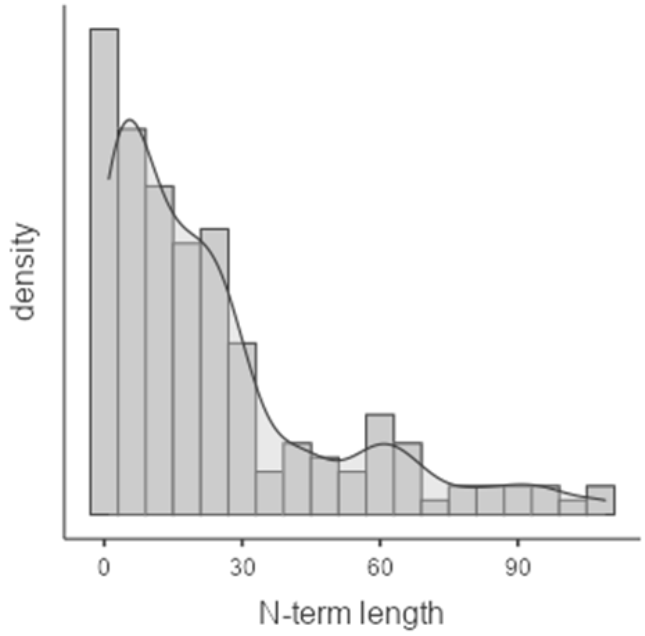

N-term length	
Valid	174
Mean	24.1
Median	16.0
Std. Deviation	25
Minimum	1
Maximum	109

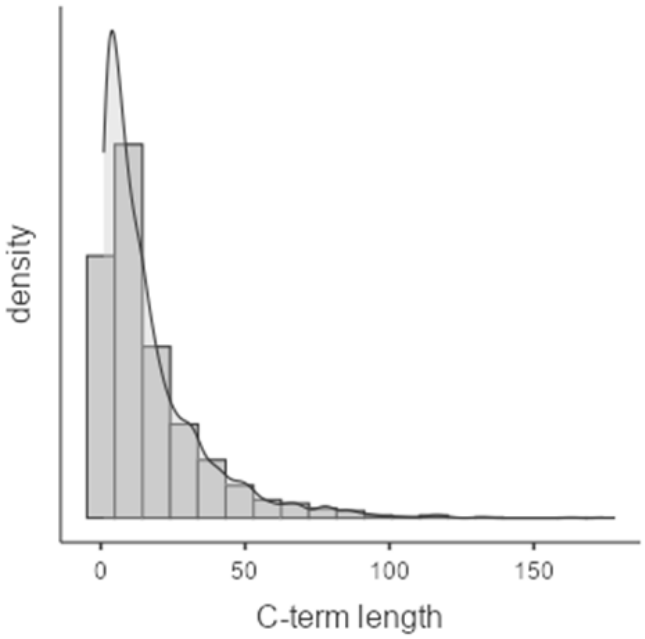

C-term length	
Valid	3865
Mean	17.0
Median	11.0
Std. Deviation	18.6
Minimum	1
Maximum	174

Figure 1.3 Density of the amino- and carboxy- terminus lengths from circRNAs with coding potential and the relative statistics.

The average length of the extra peptides (mean = 24.1 Aa) was slightly higher for those at N-terminus than those at C-terminus (mean =17.0 Aa).

In addition to changes in the primary structure of circRNA proteins, we also looked for specific differences in their domain structure. Although most of the circRNA predicted proteins shared the exact domain structure with their linear isoforms, still about a fifth of them showed unique structures (n=1,179). The most frequent structural alteration in circular RNA proteins was domain loss: when compared to their linear mRNA products 931, circORF were lacking one or more domains.

Different domains' order was also apparent (n=120); additionally, there were instances of: i) inclusion of an extra domain (n=50), ii) coincidental domain loss and inclusion of extra domains (n=58), and iii) circORF proteins with completely novel domain structure (n=20) (Figure 1.4)

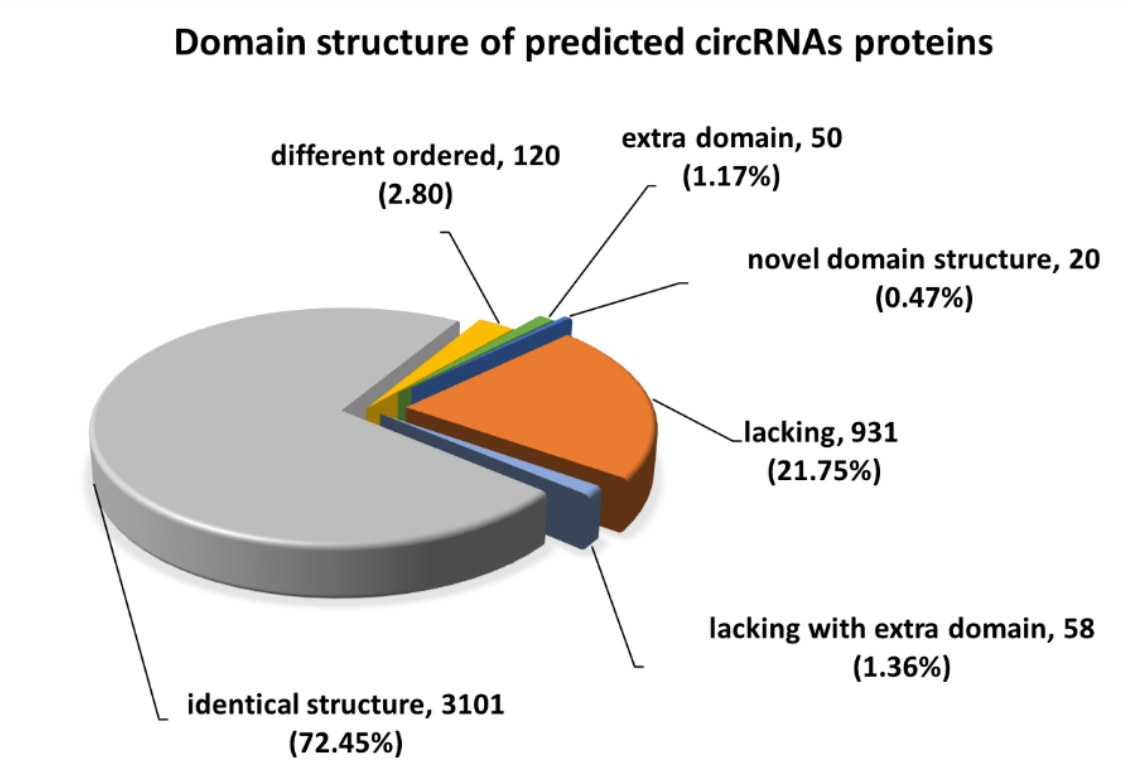

Figure 1.4 Domain structure of predicted circRNA proteins compared with the parental linear isoforms.

1.2.2 CircRNAs terminuses annotated in Peptide Atlas database.

To support our study, we compared the amino- and carboxy- terminuses with Peptide Atlas database. We found that 82 novel terminuses overlapped with a peptide, at least 10 amino acids long, reported in Peptide Atlas database (Table S9). Most of them (n=77) are aligned with a peptide related to the linear counterparts, although the primary sequence of the entire circRNAs resulted as original. Of interest, 3 of them present a carboxy-terminus aligned with a peptide sequence referred to a protein different from that parental. (Table 1.3)

CircularID	PeptideAtlas_ID	Term_len	Overlap_len
ENST00000474710.5_114380216_114380940_ZBTB20	PAp05139612	26	10
ENST00000474710.5_114350273_114380940_ZBTB20	PAp05139612	25	11
ENST00000382181.2_417525_422238_RBCK1	PAp07107667	20	20

Table 1.3. Coding circRNAs with C-Term overlapped a peptides referred to a different protein from parental. The Table reported: circID composed by the transcript_ID,

chromosome, start-end of chromosome and gene symbol; PeptideAtlas_ID, the length of the carboxy-terminus and the number of the amino acids overlapped.

In particular, the carboxy-terminuses of the circZBTB20 overlapped with peptides 10 and 11 amino acids long which referred to PELI3 protein while circRBCK1 C-terminus overlapped with a peptide 20 amino acid long and is not significantly related to a linear protein (evalue≥ 0.43).

1.2.3 circRNAs with unique coding potential and expression in cancer

To proceed further with the study of circRNAs roles in different cancer types, cell lines and normal samples, the expression profiles of circular RNAs with either original amino/carboxy predicted peptides or novel domain content were investigated in 1018 human samples from the MiOncoCirc compendium. We focused on the samples with high circRNA level (using the median of the total circRNA expression as threshold) and identified 629 circRNAs, with highly variable expression across the cancer and control human samples (IQR > 0.5).

Then, to reveal possible cancer associated roles of peptide circRNAs, we performed a differential expression analysis: 183 circRNAs showed a significant difference in their expression when cancer and cell lines were compared with normal samples (BH adjusted p-value <0.05) (Table 1.1)

chr_start_end	gene	circRNA_annotation	logFC	AveExpr	adj.P.Val
chr15_89113724_89155534	ABHD2	C-term|canMet	-0.49	-4.385732	0.0302275
chr18_21656860_21659343	ABHD3	C-term|intMet	0.57	-4.525312	0.0009348
chr2_64551442_64553409	AFTPH	C-term|canMet	1.24	-3.041979	3.08E-09
chr13_42285985_42308609	AKAP11	C-term|canMet	0.31	-5.046138	0.038654
chr6_151348710_151353752	AKAP12	canSTOP|consStr|intMet	-1.75	-4.742102	2.71E-15
chr1_243613670_243843282	AKT3	C-term|canMet|lackDom	-0.76	-3.279219	0.0195457
chr18_9182381_9221999	ANKRD12	C-term|canMet|consStr	0.49	-0.259885	0.0015594
chr4_41013582_41033304	APBB2	C-term|canMet	-0.52	-5.075323	0.0004876
chr4_36210389_36214480	ARAP2	C-term|canMet	0.36	-4.730431	0.0439487
chr4_36228581_36229645	ARAP2	C-term|canMet|lackDom	0.80	-2.917314	0.0094205
chr10_31908171_31910563	ARHGAP12	C-term|canMet|lackDom	-0.58	-0.187338	0.0038982
chr1_17580552_17588479	ARHGEF10L	C-term|canMet	-0.50	-4.495813	0.0471641
chr8_130214555_130358143	ASAP1	C-term|intMet	0.70	-4.692733	0.0023677
chr1_161846448_161863312	ATF6	C-term|intMet	-0.46	-4.157255	0.0165754
chr6_16326393_16328470	ATXN1	C-term|canMet|consStr	-0.71	-1.068755	0.0262745
chr8_102838743_102843747	AZIN1	C-term|canMet|consStr	0.35	-4.880319	0.0190586
chr21_29321220_29321514	BACH1	C-term|canMet|consStr	0.48	-5.040842	0.0005401
chr16_87975047_87984259	BANP	C-term|canMet	0.80	-2.547534	1.28E-05
chr2_214767481_214792445	BARD1	lackDom	0.32	-4.862828	0.0363578
chr7_33146241_33177591	BBS9	C-term|canMet|consStr	-0.75	-4.095965	0.0003354
chr13_102807145_102834552	BIVM	C-term|canMet	-0.54	-5.012002	0.0001445
chr3_113249721_113250833	BOC	C-term|canMet|lackDom	-1.47	-4.911996	2.22E-12
chr11_13413529_13445181	BTBD10	consStr	-0.44	-4.230596	0.0116871
chr11_93747296_93759858	C11orf54	consStr	-1.01	-4.769626	1.17E-13
chr11_93747296_93757465	C11orf54	C-term|canMet|consStr	-0.50	-4.721407	0.0017755
chr7_90726566_90790652	CDK14	C-term|canMet	-0.53	-4.013187	0.0214184
chr1_179986168_179997175	CEP350	C-term|canMet	0.40	-4.704762	0.0094095

chr3_138570317_138572984	CEP70	C-term|canMet	-0.67	-3.251803	0.0035151
chr15_57437984_57442478	CGNL1	C-term|canMet	-1.55	-4.775137	9.54E-14
chr20_41512845_41551360	CHD6	C-term|canMet	-0.76	-3.920032	0.000124
chr8_60741258_60743097	CHD7	C-term|canMet	0.92	-2.893806	0.0009427
chr16_53155925_53157541	CHD9	C-term|canMet	-0.46	-4.070529	0.0213699
chr10_124038514_124046724	CHST15	C-term|canMet|lackDom	1.12	-3.435645	7.33E-05
chr12_70278131_70319364	CNOT2	C-term|canMet	0.36	-4.690489	0.0392907
chr2_207555627_207577655	CREB1	canMet|consStr|premTerm	0.25	-5.181895	0.025331
chr20_495718_508660	CSNK2A1	C-term|canMet|consStr	0.32	-4.785032	0.0370166
chr4_1228198_1241519	CTBP1	consStr	0.35	-5.022798	0.0118515
chr4_1225359_1241519	CTBP1	consStr	0.56	-3.268335	0.0108594
chr14_59263440_59291306	DAAM1	consStr	0.66	-4.476877	0.0116871
chr15_65752378_65756472	DENND4A	C-term|canMet	0.36	-4.986049	0.0271981
chr19_47352753_47362693	DHX34	C-term|canMet|inslackDom	0.34	-5.111878	0.004739
chr22_38552665_38568289	DMC1	C-term|canMet|consStr	0.32	-5.044676	0.033584
chr1_224952669_224968874	DNAH14	C-term|canMet	0.63	-4.834016	0.0036914
chr20_63928334_63931022	DNAJC5	canMet|consStr|premTerm	1.05	-3.099577	2.28E-05
chr21_37420298_37472880	DYRK1A	C-term|canMet	0.67	-2.153783	8.37E-05
chr17_47326225_47345098	EFCAB13	C-term|canMet	0.30	-5.030541	0.0270689
chr6_130926604_130956499	EPB41L2	C-term|canMet	-1.77	-3.291045	6.02E-08
chr6_130955104_130956499	EPB41L2	C-term|canMet|lackDom	-0.94	-3.411731	0.000558
chr1_50567076_50596216	FAF1	C-term|intMet	0.53	-4.623733	0.0046739
chr2_201016990_201024039	FAM126B	C-term|canMet|consStr	0.41	-4.894143	0.0032404
chr6_70475409_70502791	FAM135A	consStr|intMet|premTerm	-0.54	-5.141151	2.02E-05
chr4_186706562_186709845	FAT1	C-term|canMet|lackDom	-1.73	-3.500236	1.75E-05
chr11_128758114_128782023	FLI1	C-term|canMet|lackDom	0.74	-4.418677	0.0005382
chr11_128758114_128768272	FLI1	C-term|canMet	0.74	-4.722216	1.58E-05
chr11_128758114_128772985	FLI1	C-term|canMet|lackDom	0.80	-4.23791	0.0003691
chr3_172112451_172251541	FNDC3B	C-term|canMet	0.65	-4.087266	0.0053531
chr3_172112451_172226947	FNDC3B	C-term|canMet	0.91	-3.624134	0.0002726
chr6_108663454_108664889	FOXO3	canSTOP|consStr|intMet	0.48	-4.390282	0.0302275
chr11_62638982_62639731	GANAB	C-term|N-term	0.63	-4.576324	0.0002095
chr16_67685456_67685802	GFOD2	C-term|canMet|consStr	-0.33	-5.09809	0.00951
chr16_4332214_4333519	GLIS2	C-term|canMet	-1.43	-3.455216	7.33E-05
chr9_4286037_4286523	GLIS3	C-term|canMet	-1.22	-3.761582	9.16E-05
chr1_1804418_1839238	GNB1	C-term|canMet|consStr	0.46	-4.946419	0.0008211
chr1_1815755_1839238	GNB1	C-term|canMet	0.88	-4.377537	1.56E-06
chr3_120750522_120751000	GTF2E1	C-term|canMet|consStr	0.75	-4.273575	8.37E-05
chr1_113940381_113941459	HIPK1	consStr	0.49	-4.714052	0.0035151
chr11_33286412_33328633	HIPK3	C-term|canMet|consStr	-0.85	-4.794648	1.68E-08
chr11_33286412_33287511	HIPK3	C-term|canMet|consStr	-0.76	1.2523144	3.46E-07
chr14_21230318_21234229	HNRNPC	C-term|canMet|consStr	0.61	-2.054603	8.59E-05
chr19_5016256_5041251	KDM4B	C-term|canMet|consStr	0.49	-4.760458	0.0038446
chr3_183643479_183672484	KLHL24	C-term|canMet|consStr	-1.17	-3.875801	1.26E-07
chr3_183650295_183651276	KLHL24	C-term|canMet|lackDom	-1.08	-4.135783	9.74E-07
chr3_183643479_183665039	KLHL24	C-term|canMet|lackDom	-0.93	-4.917762	1.32E-11
chr3_183643479_183651276	KLHL24	C-term|canMet|lackDom	-0.92	-2.320361	1.18E-05
chr3_183650295_183672484	KLHL24	C-term|canMet|consStr	-0.91	-4.830024	2.47E-08
chr18_6237963_6312056	L3MBTL4	consStr	-0.39	-4.894219	0.0237472
chr8_70637814_70641050	LACTB2	canSTOP|intMet|lackDom	0.52	-4.751059	0.0018406

chr13_21045684_21046230	LATS2	C-term|canMet	0.26	-5.108883	0.0471641
chr12_51049033_51058128	LETMD1	consStr	0.39	-5.037293	0.0053016
chr1_211778917_211793190	LPGAT1	C-term|intMet|lackDom	-0.89	-2.898406	7.33E-05
chr9_128907156_128909321	LRRC8A	C-term|canMet|lackDom	0.39	-4.797147	0.0237472
chr1_235830225_235833667	LYST	C-term|canMet	0.99	-4.289698	1.18E-05
chr2_127335869_127343194	MAP3K2	C-term|canMet|lackDom	0.33	-4.909315	0.0245962
chr10_48401611_48410168	MAPK8	C-term|canMet|lackDom	-0.83	-3.690764	7.13E-06
chr10_48401611_48404981	MAPK8	C-term|canMet|consStr	0.34	-5.032031	0.0131476
chr3_15411244_15415942	METTL6	canSTOP|intMet	-0.34	-4.549952	0.0439487
chr10_72562894_72566794	MICU1	C-term|canMet	0.66	-4.277828	0.0001851
chrX_10566887_10567603	MID1	C-term|canMet|lackDom	-0.49	-4.821469	0.0370166
chr14_45246742_45247377	MIS18BP1	C-term|canMet	0.60	-4.632662	0.0009348
chr9_13216773_13250372	MPDZ	C-term|canMet|lackDom	-0.61	-5.244745	3.46E-09
chr14_67269700_67303599	MPP5	C-term|canMet|inslackDom	-0.65	-4.167631	0.0023819
chr8_17743603_17755961	MTUS1	C-term|canMet	-1.02	-3.749651	0.0020531
chr15_72045723_72046634	MYO9A	C-term|canMet|consStr	-0.46	-4.272792	0.0235015
chr2_24643965_24683128	NCOA1	C-term|canMet|lackDom	-0.35	-5.171066	0.0015594
chr8_70213902_70216764	NCOA2	C-term|canMet|novDomStr	0.80	-4.251356	0.0002095
chr16_69695135_69695379	NFAT5	canSTOP|intMet	0.43	-5.099029	0.0094205
chr7_44645326_44666851	OGDH	C-term|N-term|intMet	0.21	-5.226649	0.0371473
chr3_16294855_16303592	OXNAD1	N-term|canSTOP|consStr	-0.45	-4.891907	0.0008146
chr5_139363758_139364743	PAIP2	C-term|canMet	0.46	-2.923203	0.0473368
chr8_51831443_51861246	PCMTD1	C-term|canMet|consStr	0.50	-4.676568	0.0035151
chr8_51845660_51861246	PCMTD1	C-term|canMet|inslackDom	0.61	-3.22871	0.0090118
chr1_65913244_65918835	PDE4B	C-term|canMet	-0.92	-2.168724	0.0218573
chr2_172568740_172596023	PDK1	canSTOP|intMet|lackDom	0.60	-3.827937	0.0413559
chr2_172570725_172596023	PDK1	canSTOP|intMet|lackDom	0.86	-4.254683	0.0005713
chr3_52412810_52414587	PHF7	C-term|canMet	0.60	-4.935128	0.0002867
chr11_86022366_86031611	PICALM	lackDom	0.53	-2.742188	0.0235181
chr1_151427822_151442205	POGZ	C-term|canMet	-0.68	-4.645183	5.63E-05
chr2_169603641_169614724	PPIG	C-term|canMet|consStr	-0.30	-4.99646	0.022186
chr4_120710308_120811449	PRDM5	canSTOP|inslackDom|intMet	-0.49	-5.08842	0.001252
chr5_145796441_145826200	PRELID2	C-term|consStr|intMet	-0.52	-4.818658	0.0025646
chr17_76312869_76313891	PRPSAP1	intMet|lackDom|premTerm	0.30	-5.018328	0.0354732
chrX_37386598_37426000	PRRG1	C-term|canMet|consStr	-0.51	-4.862536	0.0061932
chr14_73147794_73173707	PSEN1	C-term|canMet|consStr	0.47	-4.05029	0.015728
chr9_112262434_112297916	PTBP3	C-term|canMet	0.67	-3.483643	0.0024167
chr9_112268048_112297916	PTBP3	C-term|canMet	0.76	-4.151604	0.0001875
chr1_31915894_31919658	PTP4A2	C-term|canMet	-1.04	-4.079046	6.40E-09
chr6_57193841_57210445	RAB23	C-term|canMet|consStr	-1.76	-3.782838	7.05E-13
chr9_122957010_123020459	RABGAP1	C-term|canMet|lackDom	-0.60	-4.878676	7.89E-05
chr20_34072065_34078553	RALY	N-term|canSTOP|consStr	0.46	-3.739214	0.0302275
chr18_22936753_22949713	RBBP8	C-term|canMet|consStr	0.41	-4.954841	0.0095139
chr9_122877470_122897576	RC3H2	C-term|canMet|consStr	0.26	-5.005121	0.0460611
chr1_24514313_24514567	RCAN3	C-term|canMet	0.86	-4.182852	0.0039913
chr12_123498543_123499536	RILPL1	C-term|intMet	-1.44	-3.917493	1.51E-07
chr3_149846010_149912083	RNF13	C-term|canMet|consStr	0.54	-4.284257	0.0043536
chr3_149846010_149921227	RNF13	C-term|canMet|consStr	0.61	-1.869947	0.0004017
chr3_149846010_149895560	RNF13	C-term|canMet|consStr	0.64	-4.458735	0.0002031
chr6_7176654_7189322	RREB1	C-term|canMet|consStr	-0.63	-4.197698	0.0005813

chr9_35546429_35548535	RUSC2	C-term|canMet	-1.09	-3.570149	2.84E-05
chr3_18378169_18420991	SATB1	C-term|canMet|lackDom	-0.96	-3.006262	0.0024167
chr19_1147308_1154402	SBNO2	C-term|canMet	0.68	-4.659693	0.000176
chr17_1636708_1637062	SCARF1	C-term|intMet	0.86	-3.367628	0.0042192
chr4_82878729_82881937	SEC31A	C-term|canMet	0.49	-3.891134	0.0081947
chr15_90217438_90219891	SEMA4B	C-term|canMet	1.02	-3.381823	1.67E-05
chr19_38119305_38119882	SIPA1L3	C-term|consStr|intMet	0.47	-3.556298	0.048752
chr3_170359698_170391260	SKIL	C-term|canMet|consStr	0.28	-5.122669	0.0317195
chr3_170359698_170361429	SKIL	C-term|canMet|consStr	0.66	-3.420161	0.0086743
chr16_68266592_68275249	SLC7A6	canMet|consStr|premTerm	0.33	-5.119774	0.0070669
chr2_40428472_40430304	SLC8A1	C-term|canMet|consStr	-1.38	-1.036732	1.10E-05
chr5_136147831_136154163	SMAD5	C-term|canMet|consStr	-0.91	-4.208213	1.18E-05
chr3_43299753_43303792	SNRK	C-term|canMet|lackDom	-0.66	-3.309134	0.0028126
chr17_48112030_48113401	SNX11	C-term|canMet|consStr	0.61	-4.739841	0.0008211
chr1_204112914_204114605	SOX13	C-term|canMet	-1.24	-4.759379	5.64E-10
chr12_120782654_120810886	SPPL3	consStr	0.35	-4.932789	0.0148738
chr2_85861180_85870258	ST3GAL5	C-term|canMet	0.47	-4.701199	0.008974
chr20_49135832_49166285	STAU1	C-term|canMet|consStr	-0.52	-5.194811	4.00E-08
chr1_172555868_172591071	SUCO	consStr	0.26	-5.16473	0.0271981
chr6_149369908_149379518	TAB2	C-term|canMet|consStr	0.63	-4.048325	0.0032404
chr20_61997549_62014707	TAF4	C-term|consStr|intMet	0.35	-4.862109	0.0284723
chr17_29482196_29498521	TAOK1	C-term|consStr|intMet	0.21	-5.222167	0.0270689
chr17_29482196_29491865	TAOK1	C-term|consStr|intMet	0.41	-5.040318	0.0032404
chr8_123077110_123101007	TBC1D31	consStr	0.32	-5.148498	0.0036642
chr8_123077110_123105464	TBC1D31	consStr	0.56	-3.212711	0.0120199
chr8_123077110_123120188	TBC1D31	C-term|canMet|consStr	0.60	-4.308365	0.0045704
chr8_123077110_123109620	TBC1D31	C-term|canMet|consStr	0.86	-3.669245	7.33E-05
chr11_121045673_121053732	TBCEL	C-term|canMet	0.50	-4.775702	0.0020531
chr1_45457563_45457871	TESK2	C-term|canMet	0.35	-5.125769	0.0048761
chrX_123610917_123614189	THOC2	canSTOP|intMet	0.44	-4.633978	0.0114951
chr3_129827802_129832826	TMCC1	C-term|canMet	-0.72	-3.948013	0.0004381
chr7_66240324_66286709	TPST1	C-term|canMet|consStr	-1.47	-3.61222	6.44E-09
chr7_66240324_66241270	TPST1	C-term|canMet|consStr	-0.66	-3.88988	0.0048666
chr17_56901418_56904488	TRIM25	C-term|intMet	0.41	-4.467616	0.0205736
chr2_229858771_229880128	TRIP12	C-term|canMet	-0.58	-3.772907	0.0020531
chr3_12496517_12503784	TSEN2	C-term|intMet	-0.47	-4.872672	0.0025646
chr15_63529013_63537156	USP3	consStr	0.68	-4.541647	0.0002152
chr2_58084088_58089723	VRK2	lackDom	1.06	-2.749795	8.15E-06
chr10_28583398_28590832	WAC	canSTOP|intMet	0.53	-4.556368	0.0024167
chr10_1072115_1105267	WDR37	C-term|canMet|consStr	0.30	-5.107977	0.0220391
chr10_1072115_1080476	WDR37	C-term|canMet	1.08	-4.231871	2.30E-06
chr7_158911549_158918869	WDR60	C-term|intMet	-0.31	-4.850232	0.0377444
chr8_70674817_70707153	XKR9	C-term|canMet|consStr	-0.48	-5.042252	0.0120283
chr2_61498672_61533903	XPO1	canMet|consStr|premTerm	0.36	-4.964545	0.004739
chr2_61522610_61533903	XPO1	C-term|canMet|consStr	0.61	0.8583011	4.84E-05
chr11_114063210_114064568	ZBTB16	C-term|canMet|consStr	-0.94	-4.647651	2.43E-05
chr2_206279539_206297373	ZDBF2	C-term|canMet|consStr	-0.94	-2.891661	0.0042192
chr9_14639895_14680162	ZDHHC21	C-term|canMet|consStr	-0.51	-3.331943	0.0209867
chr3_44945167_44959460	ZDHHC3	C-term|canMet	0.31	-4.896015	0.0301248
chrY_2953908_2961646	ZFY	canMet|lackDom|premTerm	-1.73	-2.634374	0.0002095

chr20_47262287_47283648	ZMYND8	C-term|intMet|lackDom	0.44	-4.663643	0.0084119
chr2_218656149_218656463	ZNF142	C-term|canMet	0.43	-4.160057	0.0302275
chr3_125313307_125331238	ZNF148	C-term|canMet	-0.42	-1.495244	0.0086743
chr9_111527267_111534353	ZNF483	C-term|canMet|consStr	-1.30	-5.016455	2.71E-15
chr1_90937484_90982370	ZNF644	C-term|canMet|lackDom	0.81	-3.755868	0.0001164
chr15_66535932_66546705	ZWILCH	canSTOP|consStr|intMet	0.75	-4.506785	7.80E-06

Table 1.1: CircRNAs differentially expressed in pan-cancer dataset "MiOncoCirc". Benjamini Hochberg adjusted pvalue < 0.05. Abbreviations. logFC: log fold change; canMet: canonical methionine; canSTOP: canonical STOP; lackDom: lacking domain; consStr: conserved structure; premTerm: premature term; diffOrd: different order; intMet: intern methionine; insLackDom: inserted and lacking domains; novDomStr: novel Domain Structure. Color Legend: "green" rows indicated the circRNAs down-regulated in tumor samples than control while "red" rows indicated those over-expressed.

When reassessing the predicted protein sequence for the differentially expressed circRNAs, we determined that 121 of them had only changes in N- and/or C-terminal sequence/s, 9 displayed only novel domain content, 28 had both types of structural changes. Furthermore, 12 circRNAs started from an internal methionine (shorter N-terminal) and/or premature termination. The remaining part of circRNAs (n=13) conserved the structure domain of the linear counterparts.

The Figure 1.5 illustrates the candidate circRNA proteins (orange points) differentially and significantly expressed and also down or over expressed in cancer than control samples.

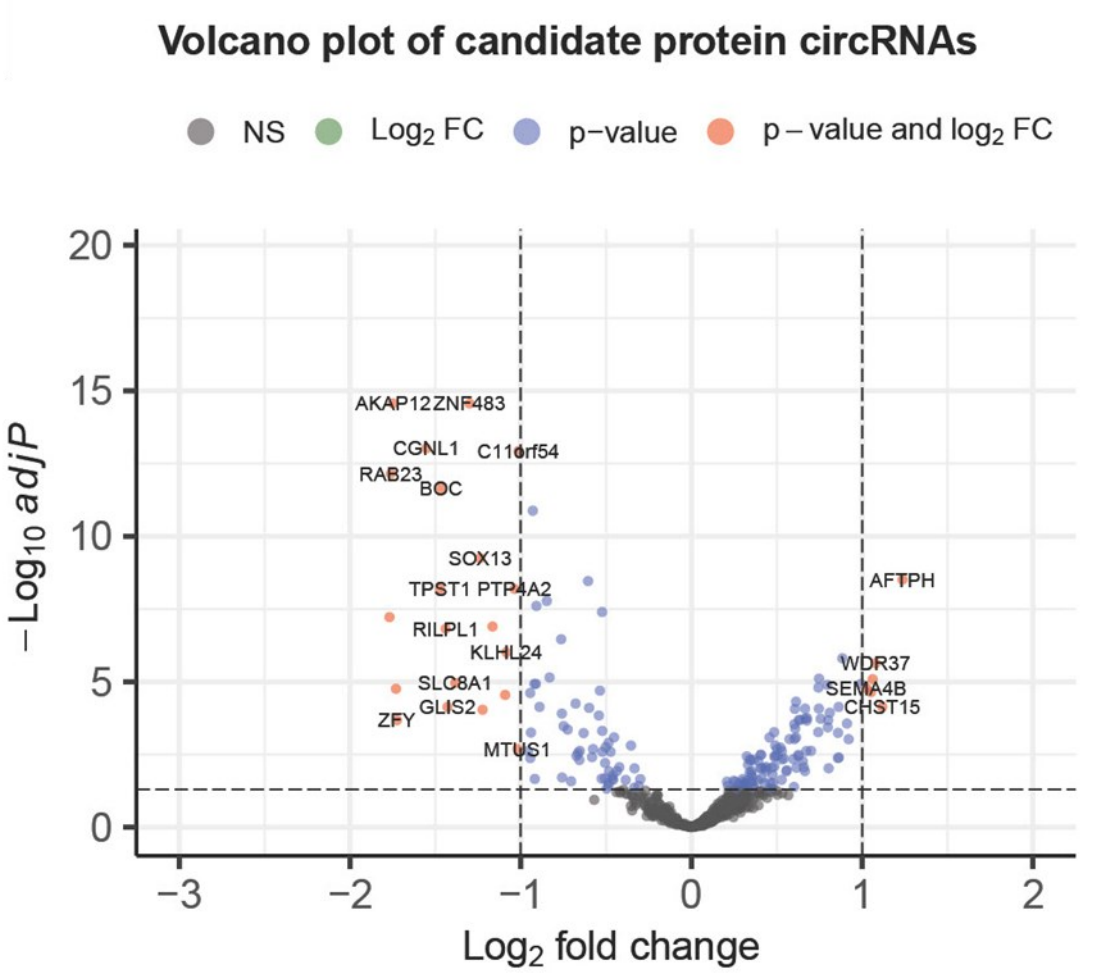

Table 1.6: The volcano plot shows the circRNA protein (orange point) differentially and significantly expressed(-Log$_{10}$ adjusted pvalue) and also down or over expressed in cancer than control samples (Log$_2$ fold change).

1.2.3 Expressed circRNAs with novel coding properties participate in cancer pathways

The circRNAs with coding potential for novel polypeptides could in principle bear novel functional roles. For example, a circular RNA protein missing a domain could act as dominant negative, or display altered cellular localization. Therefore, we studied the gene ontology and the molecular features of the genes bearing the forementioned characteristics. We focused on the 183 circRNAs that were regulated in cancer and normal samples. We interrogated PantherDB[48] to perform a statistical over-representation analysis of the circRNA genes (n=156). The results of this analysis (Table 1.1) showed a significant (BH corrected p<0.05) over-representation for reactome pathways, biological processes, molecular functions and cellular components.

GO categories	GO	obs	exp	fold	P-value	FDR
AKT phosphorylates targets in the nucleus	RP	3	0.08	38.85	1.19E-04	3.31E-02
Estrogen-dependent nuclear events	RP	4	0.19	21.58	5.89E-05	2.45E-02

downstream of ESR-membrane signaling						
Constitutive Signaling by AKT1 E17K in Cancer	RP	4	0.2	19.92	7.79E-05	2.77E-02
Heme signaling	RP	6	0.36	16.53	3.14E-06	2.61E-03
Regulation of TP53 Activity through Phosphorylation	RP	6	0.71	8.45	1.08E-04	3.38E-02
aryl hydrocarbon receptor binding	MF	3	0.07	43.16	9.23E-05	3.78E-02
protein serine kinase activity	MF	14	2.8	4.99	1.30E-06	2.13E-03
protein serine/threonine kinase activity	MF	14	3.34	4.2	9.06E-06	6.35E-03
protein serine/threonine/tyrosine kinase activity	MF	14	3.46	4.05	1.34E-05	7.33E-03
DNA binding	MF	39	19.3	2.02	1.57E-05	7.68E-03
rough endoplasmic reticulum	CC	5	0.63	7.9	5.53E-04	4.70E-02
transcription regulator complex	CC	15	3.91	3.84	1.20E-05	1.63E-03
nuclear speck	CC	11	3.19	3.45	4.41E-04	4.09E-02
centrosome	CC	14	4.87	2.87	4.57E-04	4.05E-02
cytosol	CC	65	42.04	1.55	9.16E-05	1.04E-02
mRNA transcription	BP	5	0.38	13.21	5.80E-05	3.49E-02
peptidyl-threonine phosphorylation	BP	6	0.58	10.36	3.72E-05	3.43E-02
peptidyl-serine phosphorylation	BP	9	1.42	6.33	1.85E-05	3.23E-02
negative regulation of RNA metabolic process	BP	28	11.02	2.54	5.46E-06	2.14E-02
organelle organization	BP	48	26.44	1.82	2.44E-05	3.19E-02
regulation of cell communication	BP	46	25.81	1.78	5.71E-05	3.58E-02
regulation of signaling	BP	46	25.91	1.78	8.60E-05	4.65E-02
regulation of response to stimulus	BP	53	30.9	1.72	4.71E-05	3.69E-02

Table 1.1 Gene Ontology analysis for circRNAs novel peptides in cancer. The table illustrates the GO category significantly mapped and over-represented by the coding circRNAs differentially expressed in cancer. We used PantherDB to perform a statistical over-representation GO analysis. The Fisher's exact test was applied to evaluate the significance of the observed/expected gene ratio for each GO category and the Benjamini-Hochberg method to adjust p-values (FDR<0.05). Abbreviations. MF: molecular function; BP: biological process; CC: cellular component; RP: Reactome Pathway; pol II: RNA polymerase II; obs: observed; exp: expected.

In particular, coding circRNAs were over-represented in several interesting reactome pathways and biological processes illustrated in Figure 1.6. Among the most significant reactome pathways associated to coding circRNAs: the regulation of TP53 activity through phosphorylation, the heme signaling and the constitutive signaling by AKT1 E17K mutation in cancer. While, the regulation of response to stimulus, of signalling and of cell communication, the organelle organization and peptydil phosphorylation were some of the most significant biological processes overrepresented by coding circRNAs

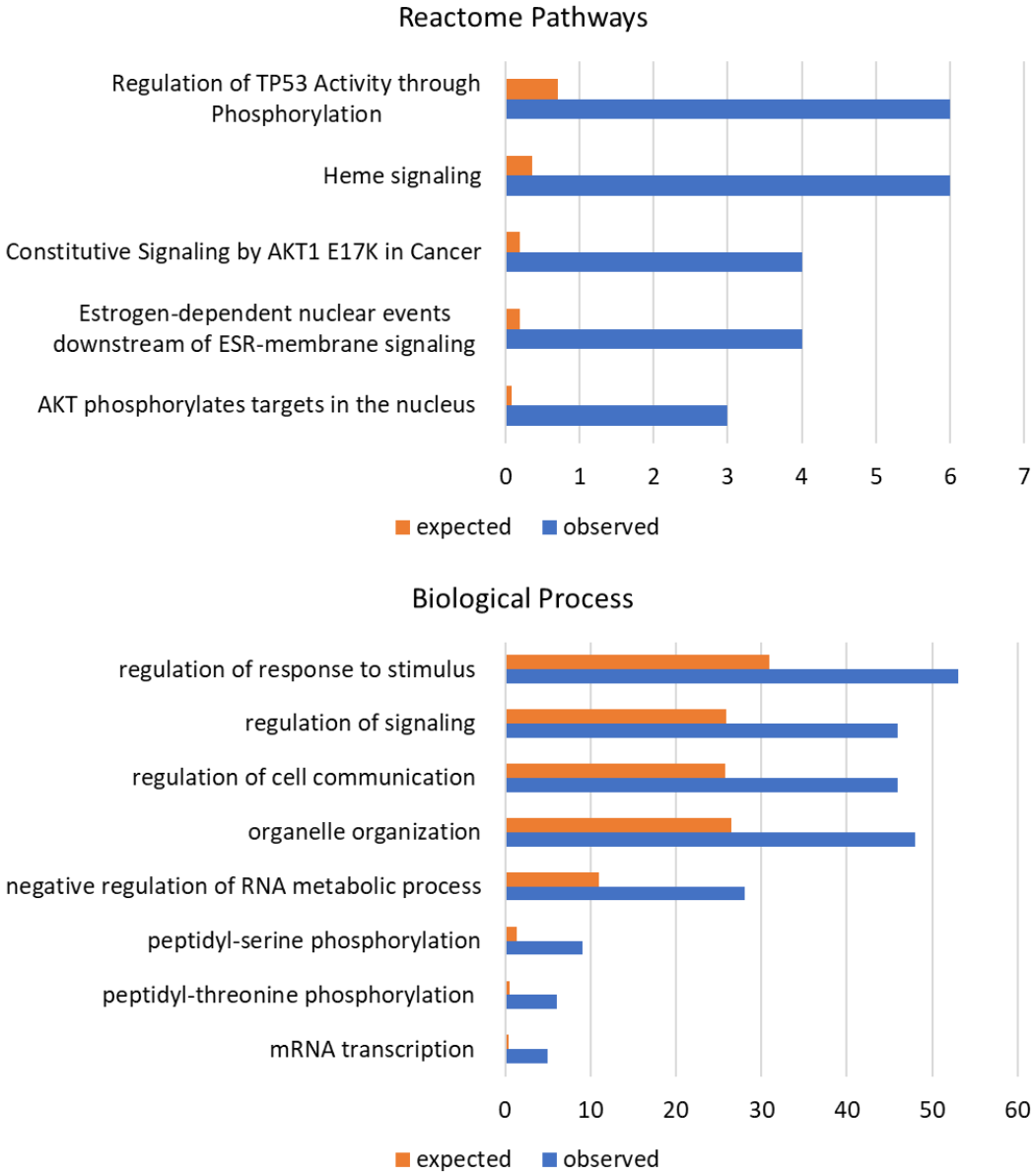

.

Figure 1.6 Gene Ontology analysis: Reactome pathways and biological process for circRNAs novel peptides in cancer. The figure shows the statistical over-representation of the reactome pathways and biological processes altered in cancer for the differentially expressed circRNAs with novel coding potential (n=197). The orange bars indicate the expected number of genes predicted for each category, while the blue bars show the

observed number of genes in each of them. P-values were adjusted using FDR correction (adjusted p-value<0.05).*

Also molecular functions such as protein kinase activity and DNA binding, and cellular components such as nuclear speck and rough endoplasmic reticulum were mapped by the circRNAs with coding potential.

1.2.4 The coding circRNAs and differentially expressed in cancer are also involved in cytogenetically normal acute myeloid leukemia (CN-AML).

We compared the circRNAs which can encode for unique protein and differentially expressed in the pan cancer dataset (MiOncoCirc) and those associated with prognosis in a cohort of 365 younger CN-AML patients[29]. Interestingly, 24 circRNAs relevant for prognosis in AML (Table 1.2) were also present in the pan cancer dataset, with 8 of them being differential expressed in cancer (adjusted p-value <0.05).

gene	chr	start	end	annotation
ABHD2	chr15	89113724	89116521	C-term|canonicalMet
ANKRD12	**chr18**	**9182381**	**9221999**	**C-term|canonicalMet|conservedStructure**
ARAP2	**chr4**	**36228581**	**36229645**	**C-term|canonicalMet|lackingDomain**
CLNS1A	chr11	77619605	77625818	canonicalSTOP|conservedStructure|internalMet
CPSF6	chr12	69251128	69262562	canonicalSTOP|conservedStructure|internalMet
CSNK1G3	chr5	123545416	123557564	C-term|canonicalMet
FBXW7	chr4	152411302	152412529	C-term|canonicalMet
HIPK3	**chr11**	**33286412**	**33287511**	**C-term|canonicalMet|conservedStructure**
KLHL8	chr4	87195323	87195690	C-term|canonicalMet
MGA	chr15	41668827	41669958	C-term|canonicalMet|lackingDomain
NCOA2	**chr8**	**70213902**	**70216764**	**C-term|canonicalMet|novelDomainStructure**
OMA1	chr1	58506059	58539310	C-term|canonicalMet|conservedStructure
PCMTD1	chr8	51860844	51861246	C-term|canonicalMet|conservedStructure
PDE3B	chr11	14771936	14789242	C-term|internalMet
RELL1	chr4	37631384	37638504	canonicalSTOP|internalMet
RNF13	**chr3**	**149846010**	**149921227**	**C-term|canonicalMet|conservedStructure**
RNF220	chr1	44411980	44412722	C-term|canonicalMet
RSRC1	chr3	158122102	158123991	C-term|canonicalMet
SATB1	**chr3**	**18378169**	**18420991**	**C-term|canonicalMet|lackingDomain**
SHOC2	chr10	110964124	110985765	lackingDomain
SLC38A1	chr12	46229152	46243314	C-term|canonicalMet|conservedStructure
SLC8A1	**chr2**	**40428472**	**40430304**	**C-term|canonicalMet|conservedStructure**
XPO1	**chr2**	**61522610**	**61533903**	**C-term|canonicalMet|conservedStructure**
ZBTB44	chr11	130260855	130261929	C-term|canonicalMet|lackingDomain

Table 1.2. Coding circRNAs associated with prognosis in cytogenetically normal AML. Legend: the differentially expressed circRNAs in pan-cancer dataset (adjusted p-value<0.05) are indicated in bold. Abbreviations. chr: chromosome

We performed a two tailed Fisher's test to demonstrate that the presence of 8 genes, encoding circRNAs with coding potential, in the intersection of the cancer

and CN-AML sets, far exceeds that expected by random association (p-value<0.001).

1.3 DISCUSSION

Since their discovery, circRNAs have been much debated with regards to their roles in the physiological and pathological processes. To date, an increasing number of reports have been confirming the differential expression of circRNAs in normal and tumor samples [49], their activity as microRNA 'sponges'[50, 51] or as protein decoys [52, 53]. Among many studies, some investigators also reported that circRNA can act as messenger RNAs and be used by ribosomes to translate proteins[54]. The aim of our study was to explore this latter avenue and systematically investigate the coding potential of more than 160,000 different circRNAs in cancer tissues. For this purpose, we leveraged on data from the "MiOncoCirc" pan-cancer compendium, produced by RNA-seq through a poly(A)-independent method and using gene-body targeting exome capture. Using a bioinformatics approach, we predicted all peptides longer than 50 residues arising from circRNA open reading frames. Then we focused on the predicted circular RNA proteins that, with respect to their gene linear isoforms, had novelty either: i) in their primary structure, or ii) domain structure. Critically, we further highlighted those circRNAs with predicted polypeptides starting at the same AUG of their linear mRNAs (canonical AUG), and therefore expected to be '*de facto*' translatable. In a different approach, other investigators considered an internal ribosome entry site (IRES) in the circRNAs sequence as necessary for efficient circRNA translation [55, 56]. Due to the overall majority of canonical AUG in the circRNA ORFs we identified (about 3/4 of the proteins were predicted to start at the canonical Met), we did not deem necessary to investigate further for an IRES presence. Overall, we identified 3723 circRNAs potentially encoding for novel peptides at carboxy or amino termini in absence of domain alterations, and 1179 such circRNAs encoding for proteins with novel domain structures.

To further pinpoint highly relevant circRNAs with coding potential in cancer, we performed a differential expression analysis in 1018 human cancer, cell line and control samples and identified 183 circRNAs. These circRNAs are associated with i) biological processes such as regulation of signalling and protein phosphorylation, ii) molecular functions such as DNA binding and protein serine kinase activities, iii) cellular components such as nuclear speck, iv) reactome pathways such as Constitutive Signaling by AKT1 E17K in Cancer and heme signaling. In confutation of our working hypothesis, we searched through the list of circRNAs with coding potential, for any circRNA already reported in the literature. Reassuringly, we successfully identified 24 such circRNAs (Table 1.2) associated with prognosis in CN-AML[29]. We further identified the ß-catenin-370aa isoform [57] which is annotated in our pan-cancer derived list, as a circORF with novel C-terminus (six extra amino acids not aligned to the linear isoforms). A second previously reported protein circRNA, FBXW7-185aa[35, 58], was present among our circORFs, with a novel C-terminal in cancer samples albeit not significant overall. To further support our study we interrogated Peptide Atlas database to find any

matches with peptides validated by mass spectrometry. Among the alignments, we identified an overlap between the carboxy-terminus of the analyzed circRNAs and peptides sourced from Peptide Atlas not referred to the linear counterparts. These results can further suggest an unexplored landscape of transcriptomics and proteomics regulators in human cancer.

CHAPTER 2: UC.183, UC.110, AND UC.84 ULTRA-CONSERVED RNAS ARE MUTUALLY EXCLUSIVE WITH MIR-221 AND ARE ENGAGED IN THE CELL CYCLE CIRCUITRY IN BREAST CANCER CELL LINES

Pineau et al. demonstrated that miR-221/miR-222, the most upregulated miRNA in hepatocarcinoma, dysregulated cell growth by targeting the CDK inhibitor p27 [59]. The same miR-221/miR-222 have a strong effect on cell cycle with the promotion of G1/S transition and contribute to aggressiveness of breast cancer (BC) [60].

In this study[61], we investigated the genome-wide expression of all UCRs, analyzing the T-UCRs levels in a very large dataset of human normal and cancer samples. Thus, we identified strong T-UCRs candidates for cell cycle regulation using the expression of miR-221 as a 'bait'. Then, we employed siRNAs against T-UCRs to evaluate their impact on cell cycle regulation, focusing on their interactions with miR-221 and on some other key effectors of cell cycle. With this aim, we further investigated the T-UCRs' expression upon treatments of BC cell lines using anticancer drugs, which led to the identification of an alternative modulation of miR-221 and T-UCR.

2.1 METHODS

Data Mining of miRNA and T-UCRs Expression Profiles. We studied the expression of T-UCRs and miRNAs in 6604 samples, derived from cancer and control tissues, using the Ohio State University Comprehensive Cancer Center (OSUCCC) custom microarray [8, 22]. Two sub-cohorts of identical size (each one consisting of 3302 samples), a test and a validation dataset, were generated by random selection. The interquartile range (IQR) was used as a threshold to remove T-UCRs and miRNAs with low variability. Linear correlation (Pearson) and mutual information content (MIC) [62] were used to assay co-regulation of miR-221 expression with T-UCRs and other miRNAs, and thus detect candidate alternatives/antagonists. Custom made scripts were coded using Python and R.

Cultures, Cell Cycle Synchronization, Silencing, and Drug Treatments. We used two breast cancer derived cell lines, MCF-7 and MDA-MB-231. MCF7 has a luminal A profile (ER+, PR+, HER2−) and wild type TP53, with a low proliferation rate and a low capacity of invasion. MDA-MB-231 belongs to the basal mesenchymal-like triple negative subtype presenting mutated TP53 with high proliferative and invasiveness potential [63, 64]. Cells were cultured in Dulbecco's modified Eagle's medium DMEM (GE-Healthcare) supplemented with 10% FBS, 2 mM L-Glutamine and 50 U/mL Penicillin and 50 µg/mL Streptomycin (Sigma-Aldrich, Milan, Italy).

The DNA content was evaluated to determine the percentage of cells in the different cell cycle stages. Fluorescence emitted from the propidium iodide–DNA complexes was quantified by the MUSE analyzer and the cell cycle kit (Luminex Corporation, Austin, TX, USA).

RNA interference experiments were carried out targeting selected T-UCRs, as reported in Table S1(https://www.mdpi.com/2073-4425/12/12/1978). The cells were transfected with 75 nM of a specific siRNA directed against the T-UCRs elements or against hsa-miR-221-3p (5′-AGCUACAUUGUCUGCUGGGUUUC-3′) [65]. Anti-miR-221 (5′-GAAACCCAGCAGACAAUGUAGCU-3′) [65] and a random pool of siRNAs were respectively used as positive or negative control [66] (Fidelity Systems Inc., Gaithersburg, USA). Approximately 100,000 cells/well were cultured in 6-well plates with complete medium 10% FBS and after 16 h the medium was replaced with 0.1% FBS-containing medium. Transfection with siRNA molecules was then performed using the siPORT transfection agent (Life Technologies, Monza, Italy) according to the manufacturer's instructions.

For cell cycle synchronization in G0/G1 phase, we used two different setups: double thymidine block [67] or serum starvation for 48 h [68]. For the double thymidine block, cells were treated 18 h with 2 mM thymidine (Sigma-Aldrich, Milan, Italy), then washed twice with complete medium and incubated for additional 8 h (to release them from the first thymidine block). Subsequently, cells were treated again with 2 mM thymidine for 15 h before the second release. Finally, the cells were collected at 2 different times, i.e., at the end of the block (T0, release) (cell arrested in G0/G1 phase) and 8 h later (T8). For serum starvation, cells were maintained in 0.1% FBS medium for 48 h and harvested 8 h after replacement with complete medium. The BC cell lines were treated using 14 different anticancer drugs (Chemietek, Indianapolis, IN, USA), selected to target the major dysregulated pathways in BC and used at half maximal inhibitory concentration (IC50), as reported by Baldassari et al. [69]. After 24 h of exposure to drugs, total RNA was collected using Trizol™ (Invitrogen, Monza, Italy).

Quantitative RT-PCRs. To analyze RNA expression, Reverse Transcription (RT) was performed using 400 ng of total RNA and oligo-dT plus random primers with the Superscript II enzyme (Invitrogen, Monza, Italy). Quantitative PCR (qPCR) was carried out using the power SYBR Green PCR master mix (Applied Biosystems,Foster City, CA) with the primer pairs listed in Table S2 (https://www.mdpi.com/2073-4425/12/12/1978). Reactions were first incubated at 50 °C for 2 min and then at 95 °C for 2 min, followed by 40 cycles, each at 95 °C for 15 s and at 60 °C for 1 min, on a Bio-Rad CFX thermal cycler. Each sample was analyzed in duplicate. β-actin was used as the endogenous reference gene. The RNA levels were assessed as relative expression values measured using ΔΔCq (Bio-Rad CFX Manager Software, version 3.1). The log2 fold changes ($2^{-\Delta\Delta Cq}$) were calculated and compared to control samples. MiR-221 RT-qPCRs were performed following the protocol described by Wang et al. [70].

Statistical Analysis. The qPCR data were normalized using mock transfections and analyzed applying two-tailed unpaired Student's *t*-test as calculated by Bio-Rad CFX Manager Software (version 3.1), with significant adjusted *p*-values < 0.05. As control for multiple testing in the drug treatments, we used the Benjamini–Hochberg correction (FDR < 0.05). Cell cycle results were obtained from at least three independent experiments and analyzed using the Mann–Whitney U test.

2.2 RESULTS

2.2.1 Identification of T-UCRs Alternatively Expressed with miR-221

We performed a genome-wide study of T-UCRs expression with the aim to identify novel ncRNAs involved in the human cell cycle. We used approaches from information theory and statistics, respectively Maximal Information Coefficient (MIC) [71] and Pearson correlation, to reveal any significant co-regulation between the expression of T-UCRs and miRNAs. The two data mining approaches we used were as distant as possible, although it has been previously reported that there still is a strong correlation between Pearson r and MIC [71]. We took advantage of a large dataset of T-UCRs and miRNA expression profiles, derived from 6604 human samples of cell lines, cancers and normal tissues [2], and randomly divided in two sub-sets representing a Test and a Validation cohort, each one containing 3302 samples. IQR was used to discard the ncRNAs with lowest variation. Finally, we retained the expression measures for 860 genome elements, either T-UCRs or miRNAs, expressed above background in at least 255 samples. We then proceeded to identify the strongest, positive, or negative, co-regulations in the Test cohort. A permutation analysis was used to simulate the noise in the procedure and generate confidence intervals. Depending on the role of the T-UCR, or its position in the transcriptional cascade, we would detect either a positive or a negative correlation score with miR-221. The scatter plot of all Pearson r and MIC score obtained in the test cohort (red points) and in the simulation (blue points) is shown in Figure 2.1.

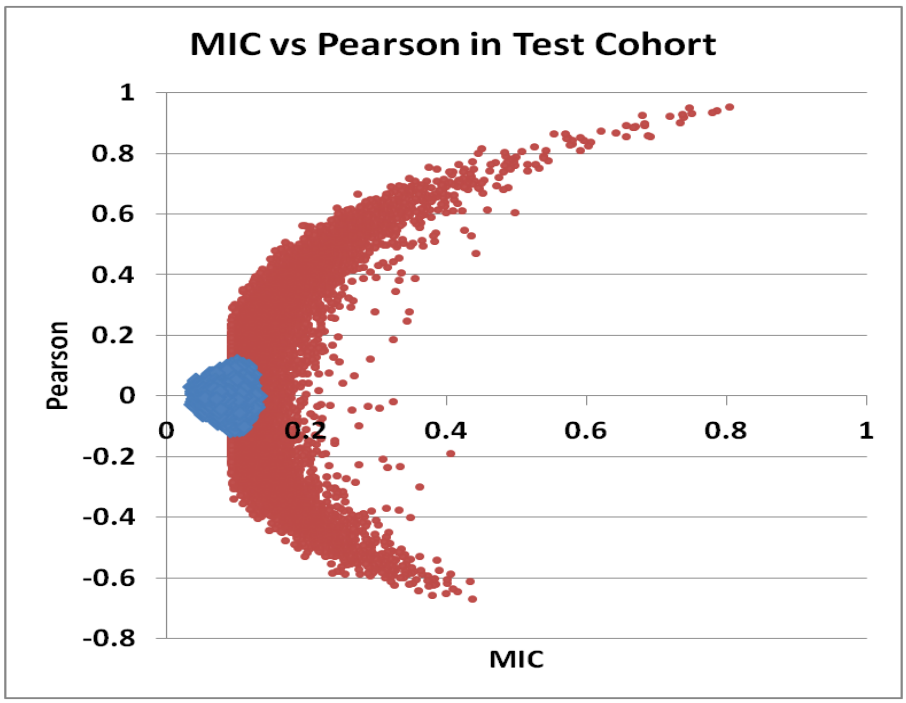

Figure 2.1. Scatter plot of Maximal Information Coefficient and Pearson correlation of ncRNAs in the Test cohort (n = 3302). The values for 40,486 pairs of ncRNAs (T-UCRs and miRs) are reported in red. In blue are also plotted the values for the simulation.

The same procedure was performed in the Validation cohort, essentially confirming the results of the Test cohort. Of note these measures provided a profile of the cellular steady-state, as basically no time courses were used but only tissues and cell cultures.

As expected from a structured genome geared towards maintaining homeostasis, most of the real-world interactions (red dots) between miRNA: miRNAs, miRNAs:T-UCR, and T-UCR:T-UCR are located away from the noise (blue dots). Additionally and reassuringly, miR-222 (co-localized with miR-221 at Xp11.3) was the ncRNA with the maximum positive r and MIC in conjunction with miR-221. The miR-221/miR-222 relation was plotted as a red point at the top and right-hand quadrant of Figure 2.1, together with other cell cycle and miR-221 co-regulated ncRNAs. Conversely, the values for alternative ncRNA associations are graphed as red points in the right-hand side and lower quadrant of the distribution. In the following step, we focused on ncRNAs which could act as cellular alternatives, or even antagonists, to miR-221. Thus, we selected the T-UCRs/miR-221 pairs with MIC larger than 0.2 and Pearson r lower than −0.4, as listed in Table 2.1.

Bait	OSU Chip Definition	ncRNA	Genomic Strand	MIC (Strength)	MAS (non-Monotonicity)	Pearson Correlation (r)	Type of Correlation
miR-221	MATURE	hsa-miR-222	+	0.42	0.03	0.70	direct
miR-221	ULTRACONS	uc.84	–	0.32	0.03	−0.55	inverse
miR-221	MATURE	hsa-miR-634	+	0.28	0.01	−0.52	inverse
miR-221	ULTRACONS	uc.340	+	0.26	0.04	−0.49	inverse
miR-221	ULTRACONS	uc.478	–	0.26	0.01	−0.49	inverse
miR-221	ULTRACONS	uc.167	+	0.25	0.02	−0.50	inverse
miR-221	MATURE	hsa-miR-497	+	0.25	0.02	−0.43	inverse
miR-221	MATURE	hsa-miR-26b	+	0.24	0.04	0.43	direct
miR-221	MATURE	hsa-miR-26a	+	0.24	0.06	0.40	direct
miR-221	ULTRACONS	uc.110	–	0.24	0.04	−0.45	inverse
miR-221	MATURE	hsa-miR-602	+	0.24	0.04	−0.45	inverse
miR-221	ULTRACONS	uc.31	+	0.24	0.02	−0.43	inverse
miR-221	MATURE	hsa-miR-320	+	0.23	0.01	0.45	direct
miR-221	ULTRACONS	uc.10	–	0.23	0.01	−0.47	inverse
miR-221	ULTRACONS	uc.48	–	0.23	0.02	−0.48	inverse
miR-221	ULTRACONS	uc.78	+	0.23	0.01	−0.44	inverse
miR-221	MATURE	hsa-miR-361-5p	+	0.23	0.02	0.45	direct
miR-221	ULTRACONS	uc.183	+	0.22	0.04	−0.43	inverse
miR-221	ULTRACONS	uc.96	+	0.22	0.03	−0.41	inverse
miR-221	ULTRACONS	uc.309	–	0.21	0.01	−0.47	inverse
miR-221	MATURE	hsa-miR-30a	+	0.20	0.02	0.43	direct
miR-221	ULTRACONS	uc.177	–	0.20	0.01	−0.43	inverse

Table 2.1. Data mining results for co-regulations of T-UCRs and miR-221. The name and genomic strand of both miRs (MATURE) and T-UCRs (ULTRACONS) correlated with miR-221 (bait) are reported, after selection of those with MAS ≥ 0.01, MIC ≥ 0.2, and abs(r) ≥ 0.4 threshold. The OSU microarray chip has probes for mature miRNAs (which tend to be conserved in the genomic sequences) and ultraconserved UCRs.

The most relevant T-UCRs, candidate as miR-221 alternatives/antagonists, are listed in Table 2.2.

T-UCR	Strand	Chromosome Coordinates (hg19)	Chromosome Coordinates (hg38)	Length (nt)	Type	Annotations
uc.84	–	chr2:157194706-157194914	chr2:156338194-156338402	209	exonic/ intronic	AK128708/intron of NR4A2; possible coding exon (42 amino acids starting with MET)—no known homology—Immediate-early response gene of the steroid-thyroid hormone-retinoid receptor superfamily [72]
uc.340	+	chr12:54090832-54091090	chr12:53697048-53697306	259	intergenic	partially overlaps with TCONS_00020432 lincRNA
uc.478	–	chrX:122599457-122599708	chrX:123465606-123465857	252	exonic	antisense of GRIA3
uc.167	+	chr5:88179624-88179824	chr5:88883807-88884007	201	intronic	antisense of MEF2C
uc.110	–	chr2:237071382-237071624	chr2:236162738-236162980	243	intergenic	enhancer and overlaps with the transmap of GBX2, an embryonal transcription factor [73]
uc.31	+	chr1:88928018-88928270	chr1:88462335-88462587	253	intergenic	BC045705 upstream of TCONS_00001016/TCONS_00001015
uc.10	–	chr1:10965574-10965848	chr1:10905517-10905791	275	intergenic	none
uc.48	–	chr2:20478333-20478630	chr2:20278572-20278869	298	exonic	overlaps with sense PUM2
uc.78	+	chr2:145188354-145188601	chr2:144430787-144431034	248	intronic	antisense of ZEB2
uc.183	+	chr5:171384520-171384755	chr5:171957516-171957751	236	exonic	antisense of FBXW11 [74–77]
uc.96	+	chr2:172820674-172820934	chr2:171964152-171964412	261	intronic	intron of HAT1—possible novel exon-homology to a non-human HAT [78–81]
uc.309	–	chr10:103267031-103267298	chr10:101507274-101507541	268	intronic	antisense of BTRC
uc.177	–	chr5:170417629-170417885	chr5:170990625-170990881	257	intronic	antisense of RANBP17

Table 2.2. Genomic coordinates and characteristics of T-UCRs, candidate alternatives/antagonists of miR-221.

Finally, we used the miRDB [82] online tool to verify whether any of these T-UCR sequences could bear predicted targeting sites for miR-221, or miR-222. We further extended this investigation applying the RNA22 [83] and PITA [84] algorithms, but no targets for miR-221 or miR-222 were detected, suggesting that the microRNA and the T-UCRs could be indirectly linked, perhaps through an indirect transcriptional control.

2.2.2 Analysis of T-UCRs Involvement in the Cell Cycle of BC Cells

We performed in vitro experiments to evaluate the possible role of the T-UCRs associated with negative co-regulation of miR-221, in relation to cell cycle and to quantify their levels in different cell cycle phases. We designed specific siRNA molecules against T-UCRs, one pair for each strand, as reported in Table 2, and assayed their silencing potential on MCF-7 and MDA-MB-231 cells. Since miR-221 strongly affects cell cycle promoting G1/S transition, we investigated whether these siRNAs showed comparable activity. We performed a primary screen of these thirteen candidate T-UCRs using siRNA pools (Figure S1-S3; https://www.mdpi.com/2073-4425/12/12/1978), and chose uc.183, uc.110, uc.96, and uc.84 (Appendix A, Figure SA1-SA4; https://www.mdpi.com/2073-4425/12/12/1978) for further validation. Their expression was quantified in unsynchronized MCF-7 and MDA-MB-231 cells (basal levels reported in Figure S4; https://www.mdpi.com/2073-4425/12/12/1978), as well as upon double thymidine block or serum starvation (Table S3; https://www.mdpi.com/2073-4425/12/12/1978). The results confirmed that miR-221 transcription was abundant in MDA-MB-231, as previously reported [60]. Consistently, the levels of both pre-miR-221 and miR-221 were increased at T8 (8 h from block release) in synchronized MCF-7 and MDA-MB-231 cells, while the levels of uc.183, uc.110, and uc.96 were decreased when cell cycle was blocked using double thymidine or serum starvation. Such pattern was thus in agreement with the inverse correlation between these T-UCRs and miR-221 expression detected in the Test cohort.

Focusing our attention on the relationship between T-UCRs and miR-221, we carried out experiments of silencing in each synchronized cell line, and assaying cell cycle phases using the MUSE cell analyzer. If a siRNA against T-UCRs was effective, it would show an effect similar to that observed with miR-221. As described in Figure 2.2, uc.183 and uc.96 both revealed such a miR-221-like activity, leading to significant increase of MDA-MB-231 cells in the S phase.

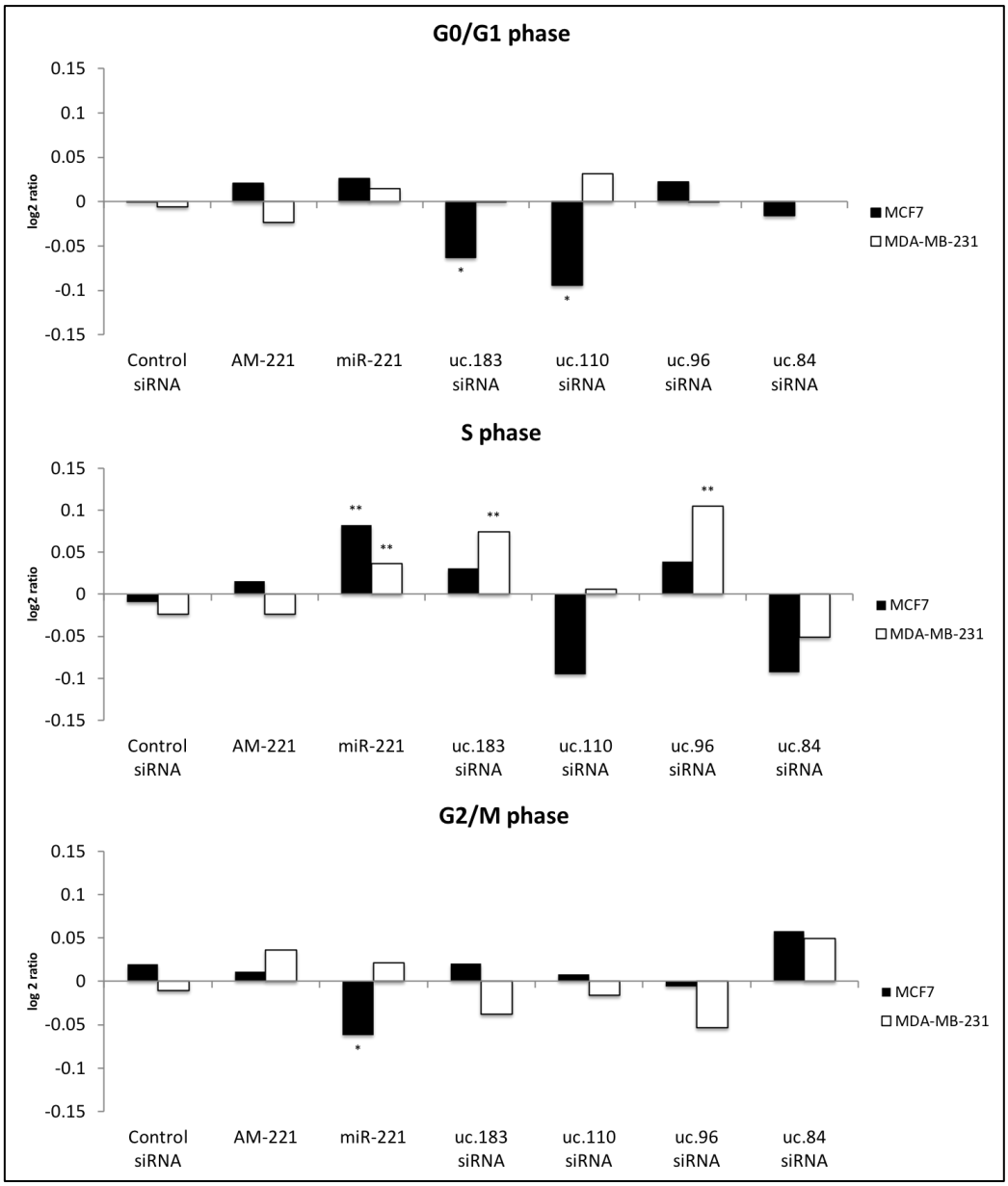

Figure 2.2. RNA interference of uc.84, uc.96, uc.110, and uc.183 on cell cycle in BC synchronized cell lines. Cell cycle was analyzed after transfections with siRNAs against the selected T-UCR, with miR-221 or anti-miR-221 (AM-221). Quantification was plotted as log2 ratio (median). Statistical significance was calculated, and the result compared to control random siRNA by 2-tailed Mann–Whitney test. p-values < 0.05 (*), p-values < 0.01 (**).

By analogy, the same trend of uc.183 and uc.96 was detected in MCF-7 cells; however, the data were not significant, maybe depending on the higher basal levels in this kind of cells as occurred in the case of treatment with anti-miR-221 (see Figure 2.2, phase S). The effects on cell cycle by uc.183 and uc.110 siRNAs, and by miR-221 transfection were confirmed when considering all data independently from the cell line ($p < 0.05$). We also provide a representation of the mean fold change of cell cycle data ± SEM in Figure S5 (https://www.mdpi.com/2073-4425/12/12/1978).

For this reason, we further studied the possible relationship between T-UCRs and miR-221, in synchronized MCF-7 cells using another approach, i.e., evaluating the expression of T-UCRs upon transfection with synthetic miR-221. Indeed, uc.183, uc.110, and uc.84 decreased at very low levels after treatment with the miR-221 mimic molecule (Figure 2.3A).

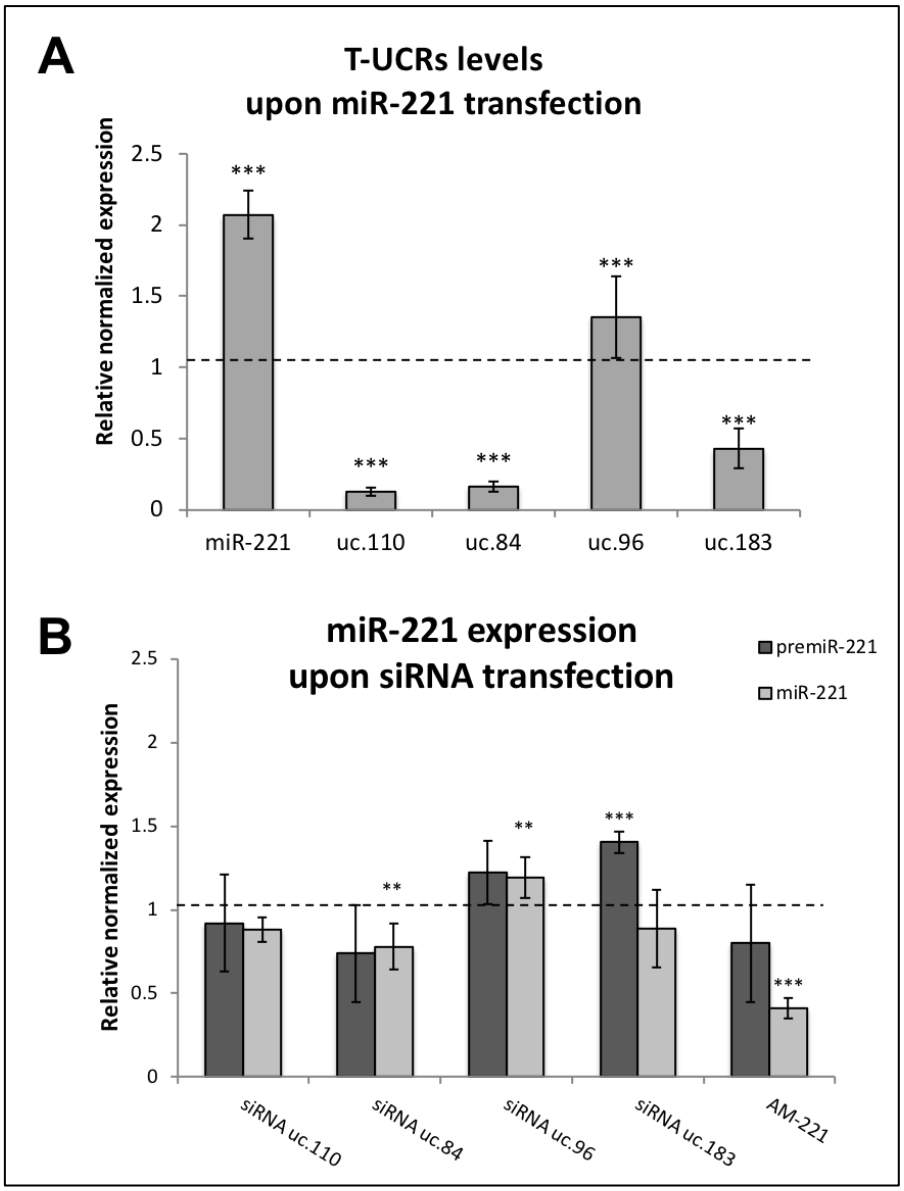

Figure 2.3. Effects of downregulation of T-UCRs or miR-221 in MCF-7 cells. RT-qPCR analysis of T-UCRs and miR-221 levels. (A), transfection using miR-221 mimic molecule and evaluation of T-UCRs expression; (B), transfection using T-UCR siRNAs and evaluation of pre-miR-221 and miR-221. The relative expression was normalized on the mock transfection and calculated as $2^{-\Delta\Delta Cq}$*. Values reported are the means of 4 experiments ± SEM. Statistical significance was determined by unpaired two tailed Student t-test. p-values: < 0.05 (*), p-values< 0.01 (**), p-values < 0.001 (***).*

Conversely, we also evaluated the levels of both pre-miR-221 and miR-221 following MCF-7 transfection with T-UCRs' siRNAs. As shown in Figure 2.3B, miR-221 displayed increase levels after treatment with uc.183 and uc.96 siRNAs.

Summarizing the data obtained considering these T-UCRs, the uc.183 was the only effective in all the investigated systems and seems to be the best candidate to interfere with miR-221 expression in inverse manner and dependently of S phase of cell cycle. Other T-UCR, namely uc.84 and uc.110, were also modulated during the cell cycle and showed a negative response in vitro to miR-221 up-regulation. However, unlike uc.183, these two T-UCR could not reciprocate and appeared as simply downstream of miR-221.

2.2.3 Downstream Effectors of T-UCR Inhibition

Since uc.183 is localized on a *FBXW11* coding exon (Table 2, Figure S1; https://www.mdpi.com/2073-4425/12/12/1978), we investigated *FBXW11* mRNA expression in synchronized MDA-MB-231 cells (either at T0 or T8), and any effect determined by T-UCR siRNAs. *FBXW11* levels were apparent at T8 (Figure 2.4A), thus siRNA treatment was performed in this cell culture condition.

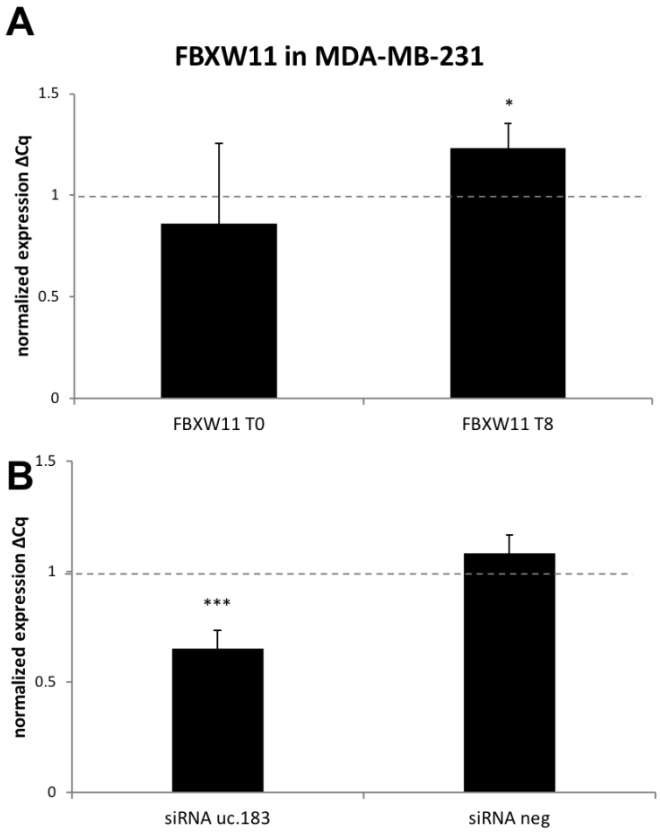

Figure 2.4. RT-qPCR analysis of FBXW11 mRNA in synchronized MDA-MB-231 cells. (A) FBXW11 mRNA levels evaluated at T0 (release from double thymidine block) and T8 (8 h after release). (B) FBXW11 mRNA levels analyzed in silenced cells with siRNA against uc.183 or siRNA negative control. The values were expressed as log2 fold changes quantified using $2^{-\Delta Cq}$ formula with respect to control. Statistical significance was determined by standard two-tailed Student t-test, p-value < 0.05 (*),p-value < 0.001 (***), derived from n = 4 independent replicates.

As displayed in Figure 2.4B, transfection with siRNAs against uc.183 led to down-regulation of *FBXW11* expression at T8 suggesting an involvement also of the protein-coding gene in the network under miR-221/uc.183 control [85].

Therefore, we enlarge our study investigating the effects of T-UCR perturbation, to include some genes known to be associated with the cell cycle and miR-221, e.g., *CDKN1B*, *TP53* and *E2F1* (known to be regulated by miR-221 [86–88]), as well as *CCNB1* and *CDKN1A* (Figure 2.5).

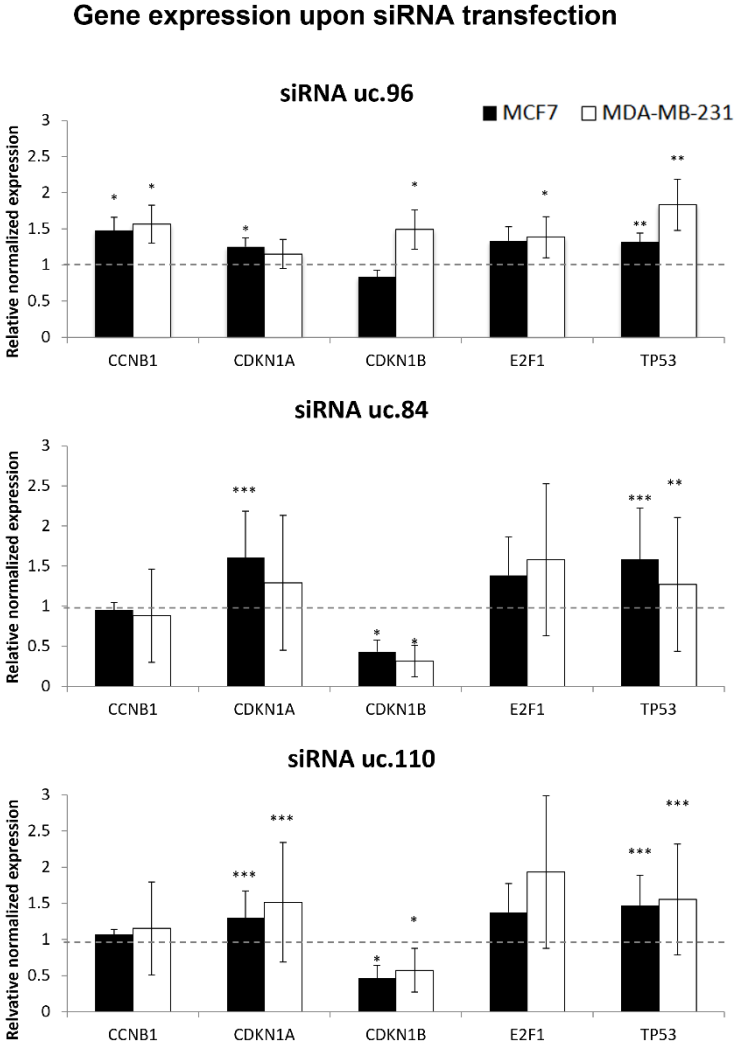

Figure 2.5. Quantitative analysis of miR-221 targets and cell cycle genes upon T-UCR siRNA transfection. Quantification by RT-qPCR demonstrated modulation of gene expression after treatment, calculated with respect to mock transfections. The dashed line parallel to the X axis indicates control relative expression of 1. Histograms represent the means of 8 independent experiments ± SEM. Statistical significance was determined by unpaired two tailed Student's t-test; p-value < 0.05 (*), p-value <0.01 (**), p-value <0.001 (***).

Analyzing the levels of these transcripts, we observed that uc.110, uc.96, and uc.84 siRNAs significantly up-regulated *TP53*, *E2F1*, and *CDK1A* in at least one cell line, while the uc.96 siRNA was effective on the rise of *CCNB1*. The effects of uc.110 and uc.84 were consistent with their interference in cell cycle; indeed, they caused also a strong down-regulation of *CDKN1B*, a known target of miR-221 [59].

2.2.4 Modulation of T-UCR Levels by Anticancer Drugs

Since anticancer drugs often affect pathways related with the cell cycle, we investigated their possible action as modulators of T-UCRs. We used 14 drugs targeting the most frequently activated pathways in BC. We focused on the T-UCRs which were shown here to be experimentally involved in miR-221 activity or in the cell cycle. Therefore, we selected uc.183, which seemed to be entangled with miR-221 in a sort of negative loop, and uc.110 and uc.84 that seemed to succeed in the modulation of some cell cycle genes. We hypothesized a rise of these T-UCRs following the inhibitory activity of cancer drugs on cell cycle. Figure 2.6 shows an increase in expression of all tested T-UCRs (uc.183, uc.110, uc.84), in at least one cell line, upon treatment with the PI3K pathway inhibitors, AZD5363 (capivasertib) and BYL719 (alpelisib) that leave miR-221 completely unaffected (significant increase above 2-fold changes compared with untreated cells).

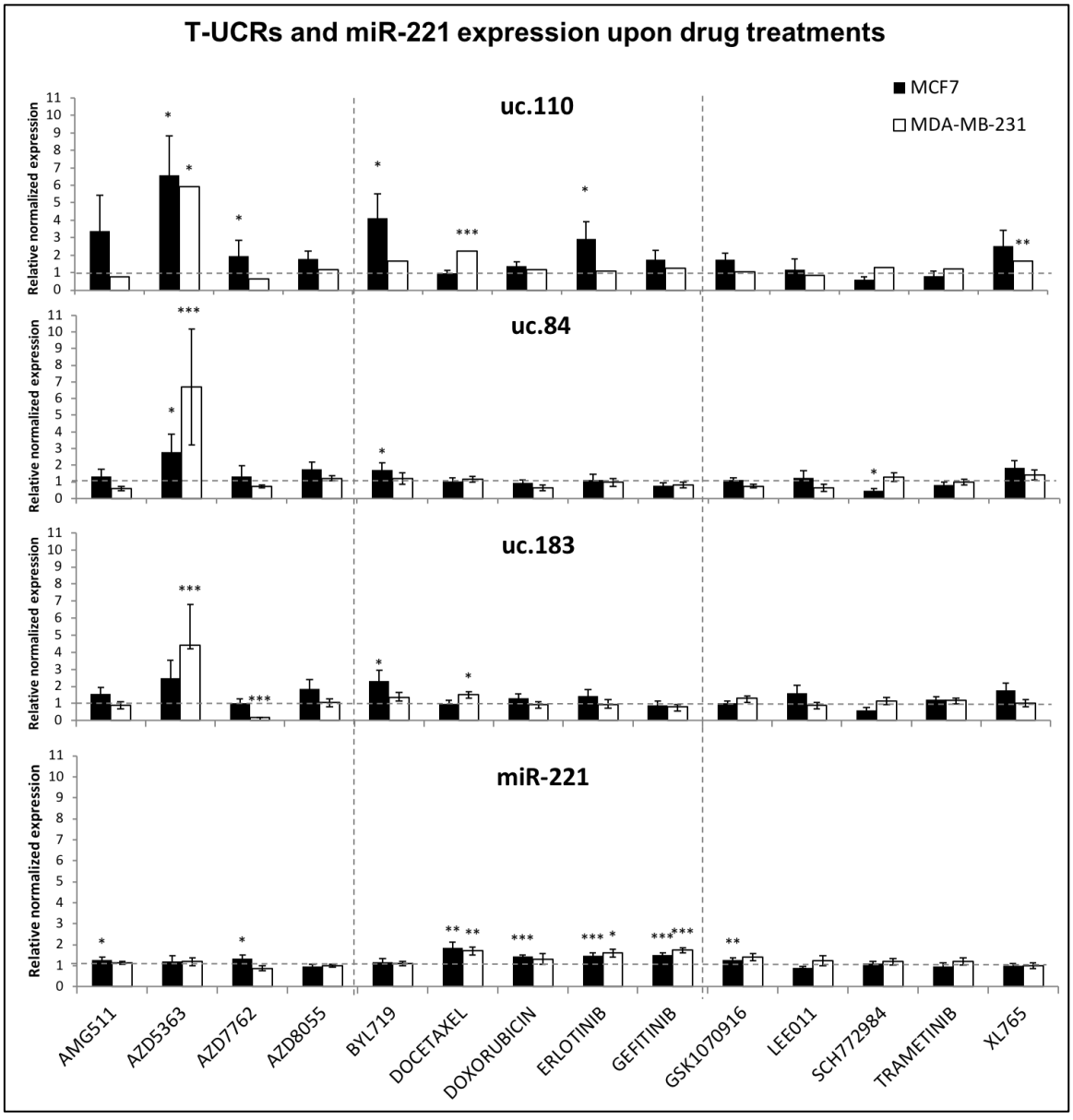

Figure 2.6. Gene expression analysis of T-UCRs and miR-221 upon treatment with anticancer drugs. Histograms describe the expression of uc.110, uc.84, and uc.183

detected by RT-qPCR and quantified by comparison with untreated cells using $2^{-\Delta\Delta Cq}$ formula. Values are mean of 5 experiments ± SEM. For statistical analysis, unpaired and two tailed Student's t test has been used; adjusted p-values: < 0.05 (*), p-value< 0.01 (**), p-value< 0.001 (***). Benjamini–Hochberg correction (FDR< 0.05) (Table S4; https://www.mdpi.com/2073-4425/12/12/1978). The dashed line parallel to the X axis indicates control relative expression of 1.

The *p*-values were adjusted according to Benjamini and Hochberg, for correction of multiple testing (FDR = 0.05) (Table S4; https://www.mdpi.com/2073-4425/12/12/1978).

Interestingly, the expression of miR-221 was upregulated by a range of other compounds, including doxorubicin and gefitinib, which instead did not up-regulate the T-UCRs. Thus, the treatments which affected the T-UCR expression did no alter the miR-221 levels and vice versa. Thus, with the small molecules inhibitors, we could show a completely differential response by miR-221 and T-UCRs, confirming the mutual exclusion detected in the initial data mining study.

In general, the accumulation of T-UCR occurred mostly in MCF7, excluding docetaxel and XL765, which acted selectively on uc.110 and uc.183 in MDA-MB-231. The Chk inhibitor, AZD7762 and ERK1/2 inhibitor, SCH772984 were the only compounds leading to high down-regulation of a T-UCR, respectively uc.183 in MDA-MB-231 and uc.84 in MCF7.

2.3 Discussion

Notably, ncRNAs, such as T-UCRs are linked to cancer [89, 90] via various mechanisms such as miRNA regulation [91]. In this context, miR-221 is one of the most relevant miRNAs in association with tumorigenesis [59], cell proliferation, invasion [60] malignancy, and metastasis [92]. In addition, miR-221 plays a pivotal role in cell cycle control [60] driving G1/S transition by targeting cyclin-dependent kinase inhibitors, p27 and p57 [59]. The aim of this work was to discover ncRNAs involved in the regulation of miR-221 and cell cycle. To identify candidate RNAs, we studied a very large dataset of tumors and normal RNA profiles, including data from over 1000 T-UCRs and miRNAs. Amongst them, 13 T-UCRs displayed inverse co-regulation with miR-221, e.g., were strongly expressed in the absence of miR-221 and vice versa. For the purposes of our research, we focused only on uc.183, uc.110, uc.96, and uc.84, the most effective in modulating cell cycle phases with their respective siRNA. Our observation on T-UCRs are novel, as there are no other reports in the literature, not only in breast cancer, but also for other cancer types. We further investigated the relationship between these selected T-UCRs and miR-221, analyzing RNA interference of uc.84, uc.96, uc.110, and uc.183 on the cell cycle in synchronized BC cell lines. The results confirmed the mutually exclusive roles for miR-221 and the T-UCRs. In fact, the treatment with siRNAs against uc.183 and uc.96 increased cells in the S phase, just like miR-221 mimics. Additionally, miR-221 reduced the expression of uc.183, uc.110, and uc.84, and conversely, siRNAs against uc.183 and uc.96 increased pre-miR-221 and miR-221. By investigating the role of T-UCRs in the control of cell cycle, we demonstrated that siRNAs against uc.110, uc.96, and uc.84 up-

regulated *TP53*, *E2F1*, and *CDK1A*, whilst uc.110 and uc.84 siRNAs led to reduction of levels of *CDKN1B*, one of the most important targets for miR-221 [59]. Moreover, siRNA against uc.183 is associated with a downregulation of *FBXW11*. Lastly, the siRNAs against uc.96 solely up-regulated *CCKNB1*. Thus, T-UCRs appeared to be involved in the regulation of some key cell cycle genes, and, in particular, uc.110 and uc.84 to be engaged with CDKN1B.We further dissected the miR-221 and T-UCR response in vitro, using a set of cancer drugs. The drugs targeting PI3K (AZD5363, AZD7762, AZD8055) and mTOR pathway (XL765) [93] determined an over-expression of T-UCRs that was predominant in MDA-MB-231 cells, while BYL719, which directly targets PIK3CA, was borderline effective only in MCF-7 cells, possibly because the mutations of PIK3CA (E542K and E545K) are not present in MDA-MB-231 cells [94].

CHAPTER 3: THE NETWORK OF NON-CODING RNAS AND THEIR MOLECULAR TARGETS IN BREAST CANCER

The studies on non-coding RNAs and breast cancer (BC) prevalently investigate one or few RNAs that have been selected from clinical genomics. Typically, such works analyze the BC transcriptomes from retrospective cohort studies.

We decided to apply a data-driven study selection rather than use only our human and scientific sensitivity[95]. Firstly, we performed two queries to isolate from PubMed all the articles on ncRNAs and miRNAs published in the last 5 years on BC (Table 3). To triage the studies considered for this review we then selected the journals based on their impact factors. A different, and probably fairer, criterion would have been the citation number, but this is impractical for articles with recent publication time, such as those we wanted to consider here. Furthermore, we let the skeleton of our work to self-assemble using the data themselves. We explored this procedure in our earlier organized view of the role of non-coding RNAs in drug resistance. Using an approach where the nodes are the non-coding RNAs, or their target genes and the edges (connections) are the PMIDs of their relative articles, we obtained a network that was used to organize this review. Separate groups of RNAs and genes that were not linked will be discussed as separate entities or 'sub-networks'. A statistical analysis of the network helped to identify nodes (RNAs or genes) with particular properties (i.e. degree, or number of interacting RNA/genes) and ultimately for prioritization. The number of citation of an RNA/gene depends both on its 'real' importance as determined by the experimental method, or on its 'perceived' importance, making it an element of choice by the investigators. The network of non-coding RNAs (ncRNAs) and their targets in BC, defined using this approach is shown in Figure 3.1.

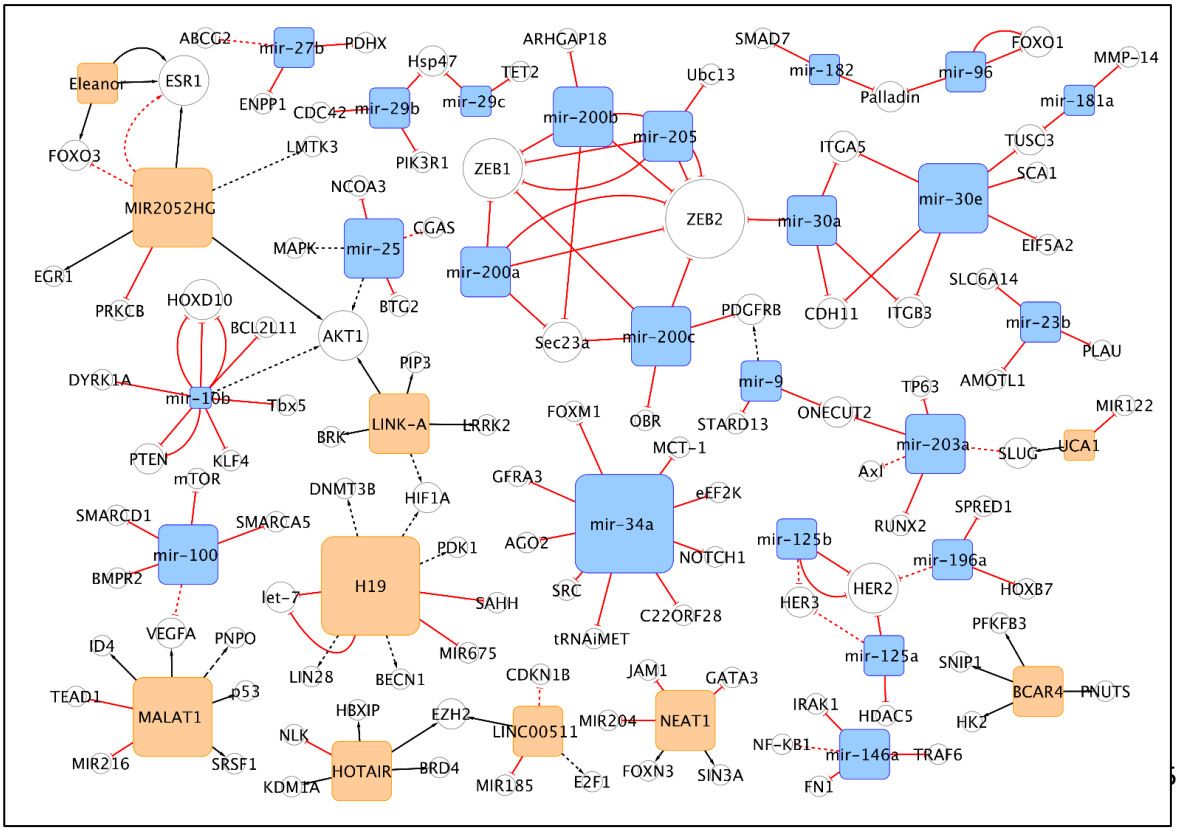

Figure 3.1. The network of non-coding RNAs and its targets in breast cancer. The graph shows the non-coding RNAs (in the square nodes) cited in at least 2 different sources from literature. Empty circles correspond to the coding genes. Each connecting line (or edge) indicates a publication (PMID) from PubMed. When multiple edges connect the same two RNAs in the network, then multiple publications described this interaction. The edges aredirected (i.e. from the non-coding RNA to its target, being either coding or non-coding). In red are depicted the links indicating a repressive action (flat arrowhead), while in black are those showing activation (with traditional arrowhead). Dashed lines correspond to edges indicating indirect effects. The network is the essential core showing what remains after filtering the nodes (non-coding RNAs, in orange, and miRNAs, in light blue) based on their degrees (i.e. the number of connections to targets or other non-coding RNAs). The network's details are reported in the Table 2.

The graph shows the non-coding RNAs, and their targets, validated in at least two independent sources from literature. The edges are directed (i.e. from the non-coding RNA to its target). In red are depicted the links indicating a repressive action (flat arrowhead), while in black are those showing activation (with traditional arrowhead). Dashed lines correspond to edges indicating indirect effects. The network in Figure 1 is the essential core showing what remains after filtering the nodes (non-coding RNAs) based on their degrees (i.e. the number of connections to targets). The filtered out nodes, basically un-replicated findings, are shown in Table1. They are still worthy of consideration, but were strictly left out of the major network. We will discuss here the most prominent sub-networks and their single components and interactions, with the goal of understanding the involvement and roles of non-coding RNAs in BC.

3.1 THE MIR-200/205 ZEB2 SUB-NETWORK

Figure 3.2 shows that ZEB2 is a pivotal actor in this sub-network, interconnecting the cluster composed by miR-200a/b/c and miR-205 with that of miR-30a/e and miR-181. Several research groups independently asserted that miR-200a/b/c are down-regulated in triple negative breast cancer (TNBC) and function as metastasis suppressor reducing epithelial mesenchymal transition (EMT), tumour invasion and drug resistance[96].

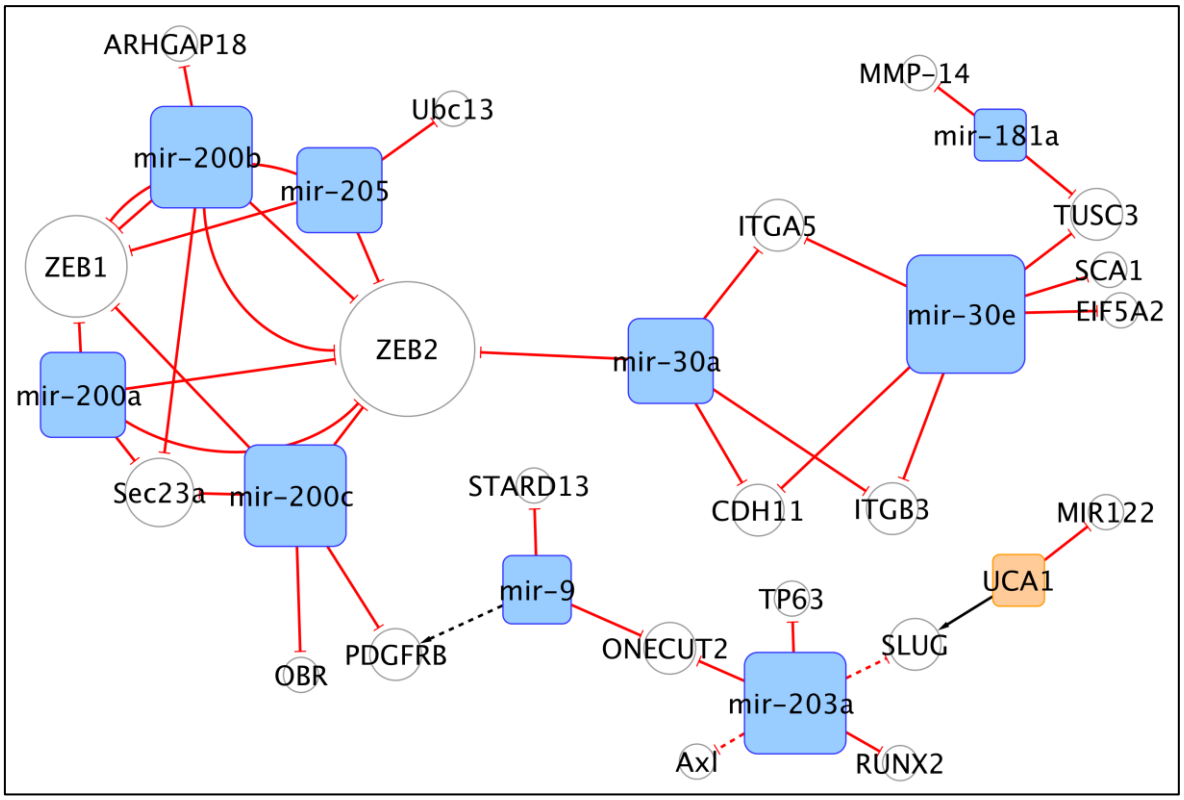

Figure 3.2. The miR-200s/ZEB2 cliche

MiR-200 family's components target other genes that antagonize malignant processes, among them Rho GTPase-activating protein 18 (ARHGAP18), an important regulator of cell shape, spreading, migration, and angiogenesis[97] and the leptin receptor (OBR), which promotes the formation of cancer stem-like cells (CSCs) and up-regulates the obesity-associated adipokine itself associated to BC[98]. Furthermore, in this subnetwork miR-205 is involved in the modulation of basal-like BC motility mediated by the ΔNp63α pathway, by preserving the epithelial cells characters[99]. Mir-205 also is negatively correlated with DNA damage repair, promoting radio-sensitivity in TNBC, by targeting the ubiquitin conjugating enzyme E2N (UBC13) [100]. In contrast, Le et al. demonstrated that delivery of miR-200 family (miR-200a/b/c) by extracellular vesicles, through the circulatory system from highly metastatic tumour cells to poorly metastatic cells, in which ZEB2 and SEC23A were down-regulated, induced EMT and conferred the ability to colonize distant tissues[101]. Further considerations on opposite effects of ncRNAs could be drawn by the second cluster, where the miR-30's family members suppressed cell invasion *in vitro* and bone metastasis *in vivo* by targeting genes implicated in invasiveness (ITGA5, ITGB3) and osteo-mimicry (CDH11) in TNBC[102]. Consistently, miR-30a was involved in EMT regulation, upon TP53 stimulation, by targeting ZEB2 [103], while miR-30e displayed an onco-suppressor role through the modulation of ataxin 1 (SCA1) and EIF5A2, two disruptors of the BC acini morphogenesis promoted by laminin111 (LN1)[104]. MiR-181a could also lead to a reduction in the activation of pro-MMP-2, cell migration and invasion of BC cells through matrix-metalloproteinase MMP-14[105]. In an apparently opposed fashion, Kuancan et al. demonstrated that miR-181a and miR-

30e, once stimulated by SOX2 activation, could promote migration and metastasis dissemination in Basal and Luminal BC via silencing of Tumour Suppressor Candidate 3 (TUSC3)[106]. This subnetwork includes another crucial connection between miR-200c and miR-9, as antagonistic modulators of PDGFR ß-mediated vasculogenesis in TNBC. High levels of miR-9 exerted pro-metastatic function and mediated the acquisition of a mesenchymal and aggressive phenotype. In addition, miR-9 enhanced the generation of vascular lacunae both *in vitro* and *in vivo*, in part by direct repression of STARD13, and was also required for PDGFRß-mediated activity. On the other hand, miR-200c in TNBC models strongly inhibited tumour growth and impaired tumour cell–mediated vascularization, by inhibiting PDGFRß activity in vascular lacunae and acting on ZEB1, one of the main transcriptional factors in EMT induction [107]. Furthermore, miR-9 in collaboration with miR-203a could lead to a CSC phenotype and to drug resistance after their release from exosomal vesicles (EV), upon treatment with chemotherapeutic agents. These miRNAs target the transcription factor One Cut Homeobox 2 (ONECUT2), whose reduction induces the expression of a variety of stemness-associated genes, including NOTCH1, SOX9, NANOG, OCT4, and SOX2[108]. Blocking the EV miRNA-ONECUT2 axis could constitute a potential strategy to maximize the anticancer effects of chemotherapy, as well as to reduce chemoresistance. MiR-203a can collaborate with miR-135 (not showed in this subnetwork) to inhibit cell growth, migration and invasion, by the down-regulation of Runx2 and IL11, MMP-13 and PTHrP targets. Indeed, an aberrant expression of Runx2, which promotes tumour growth and bone metastasis formation, was detected in BC[109]. This subnetwork highlights another connection of miR-203a, occurring with the long non coding UCA1 which affects directly and indirectly the snail family transcriptional repressor 2 (SLUG). MiR-203 prevents the induction of motility in luminal BC cells, through down-regulation of ΔNp63α activity, and the inhibition of its SLUG and AXL targets[99]. Of interest, UCA1 expression in BC cells correlated with TGF-β-induced EMT and tumour metastasis. Mechanistically UCA1 is up-regulated by TGF-β and cooperates with the LINC02599 (AC026904.1) in order to promote SLUG activation and maintenance[110]. Furthermore, UCA1 was proposed to act as a competing endogenous RNA (ceRNA) to sequester miR-122, thus promoting BC invasion. Interestingly, a mechanism mediated by insulin-like growth factor 2 messenger RNA binding protein (IMP1) and repressing invasion has also been hypothesized, via UCA1 decay through the recruitment of the CCR4-NOT1 deadenylase complex. According to this model, IMP1 could compete with UCA1 for binding to miR-122 and restore miRNA targets to inhibit cell invasion[111].

3.2 THE LINC0511-HOTAIR SUBNETWORK

The intergenic non-protein coding RNA 00511 (LINC00511) participates in a subnetwork with HOTAIR (HOX transcript antisense RNA), which is linked to the methyltransferase EZH2 and causes impaired cell proliferation and inhibition of apoptosis in estrogen receptor (ER) negative BC cells[112]; indeed, LINC00511 promotes metastasis dissemination by silencing NLK [113]. In this subnetwork LINC00511 was proposed to function as a competitive endogenous RNA,

sequestering miR-185, with the effect of inducing E2F1 expression, ultimately leading to stemness and tumorigenesis in all BC subtypes[114]. The other subnetwork member HOTAIR, can act as a scaffold for the late endosomal/lysosomal adaptor, MAPK and MTOR activator 5 (HBXIP), which promotes the expression of three MYC targets, i.e. CCNA1, EIF4E and LDHA, as well as of the lysine demethylase 1A (LSD1), recruited by HBXIP itself [115]. A novel isoform of HOTAIR, named HOTAIR-N, was observed in association with an increase of invasion and metastasis in laminin-rich extracellular matrix-based three-dimensional organotypic cultures (lrECM 3D), compared with traditional "Claudin-low" culture. HOTAIR-N, once cells are attached to extracellular matrix, binds BRD4, a reader of histone markers that recognizes trimethylation on histone H3 lysine 4[116].

3.3 The H19/LINK-A/MIR2052HG/miR-25/miR-10b/Eleanor sub-network

This relatively large sub-network is depicted in Figure 3.3.

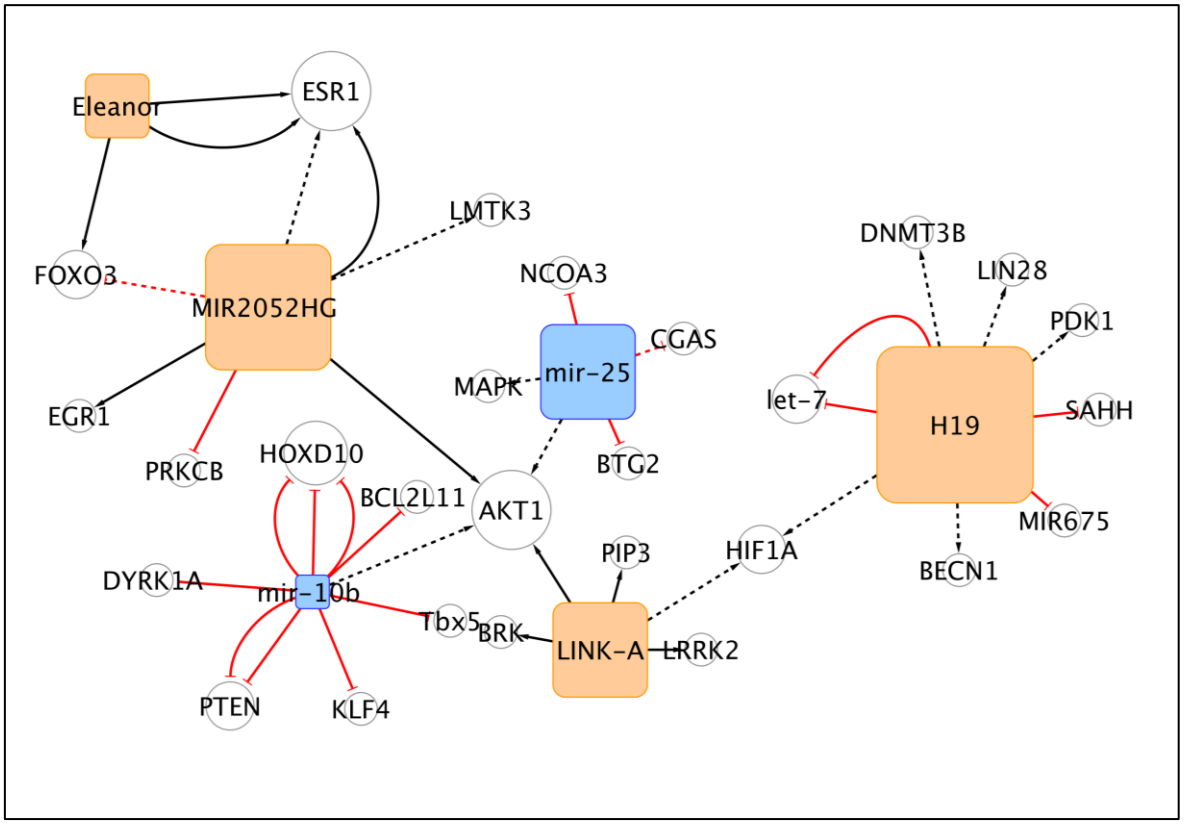

Figure 3.3. The H19/LINK-A/MIR2052HG/miR-25/miR-10b/Eleanor sub-network

Lnc-H19 and Long intergenic non-coding RNA for kinase activation 01139 (LINK-A) are both indirectly involved in the regulation of the expression of HIF1A. In particular, H19 could induce CSC properties and tumorigenesis possibly via LIN28 by acting as a competitive endogenous RNA towards let-7 miRNA. Furthermore, H19 can indirectly stimulate the expression of HIF1A and PDK1, thus promoting the glycolysis pathway, a crucial step in CSC reprogramming.

H19 and PDK1 therefore may represent possible therapeutic targets, to contrast glycolysis and cancer stem-like properties[117],[118]. Consistently, LINK-A is involved in the normoxic HIF1A stabilization pathway, through the recruitment of the protein tyrosine kinase 6 (BRK) and of LRRK2, that phosphorylate and activate HIF1A itself. From a functional point of view, LINK-A is associated with glycolysis reprogramming in TNBC and promotes tumorigenesis[119]. H19 promotes tamoxifen resistance and autophagy in MCF7 cells, by down-regulating Beclin-1 methylation via epigenetic mechanisms. In details, H19 inhibits adenosylhomocysteinase (SAHH), with subsequent acyl-CoA synthetase medium chain family member 3 (SAH) accumulation, which in turn inhibits Beclin-1 promoter methylation by DNMT3B. Therefore the H19/SAHH/DNMT3B axis was proposed as a therapeutic target against tamoxifen resistance[120]. LINK-A is further connected with MIR2052HG, miR-25 and miR-10b, all known activators of AKT1. In this sub-network a single nucleotide polymorphism (SNP), rs12095274: A>G, in LINK-A affects the phosphorylation status of AKT1 and is associated with AKT inhibitor-resistance by AKT-PREX1 interactions, which results in a worse prognosis for patients[121]. Also MIR2052HG presents a SNP (rs13260300), which have been associated with a higher recurrence of BC and resistance to aromatase inhibitors. MIR2052HG positively regulates estrogen receptor alpha (ERα) via the AKT/FOXO3 pathway, and limiting ERα ubiquitination[122]. MIR2052HG has shown to regulate ERα expression by: *i)* promoting the recruitment of EGR1 on LMTK3 promoter with reduction of PKC activity, indirectly enhancing ERα protein levels; *ii)* limiting ERα ubiquitination via PKC/MEK/ERK/RSK1 pathway. Both mechanisms have been identified as active in the presence of the MIR2052HG SNP rs13260300 and of aromatase inhibitors in ERα-positive BC[123]. MiR-25 can promote cell proliferation in TNBC by silencing B-cell translocation gene 2 (BTG2) and, indirectly, by the activation of AKT and ERK-MAPK pathways[124]. Additionally it has been reported that miR-25 interacts with miR-93 (not present in this network), to down-regulate CGAS, by targeting NCOA3 at its promoter. Hence, it could determine immune evasion and accelerated cell cycle progression under hypoxia in Luminal A cells[125].

The other microRNA engaged in this network is miR-10b which targets HOXD10 and KLF4 to play a pro-oncogenic role. It can promote cell invasion and metastasis formation in the TNBC subtype through its secretion via exosomal vesicles, mediated by neutral sphingomyelin phosphodiesterase 2 (nSMase) indeed and it is capable of transforming non malignant HMLE cells into cells with invasion-ability[126]. Metastasis generation and self-renewal of CSCs driven by miR-10b are the results of the directly inhibition of miRNA target, PTEN, and the indirectly increase of the expression of AKT[127], as well as that of HOXD10 and BCL2 like 11(BIM) [128].

For this reason, miR-10b has been proposed as a “metastamiR”, re-asserted by Kim and co-workers who focused on its targets onco-suppressors Tbx, PTEN, DYRK1A and the anti-metastatic gene HOXD10[129]. Finally, Eleanor also plays a role in the cluster of non-coding RNAs, cis-activating both ESR1 and FOXO3[130]. The inhibition of Eleanor could represent a key to switch off topologically

associating domain (TAD) containing proteins and to target cells resistant to endocrine therapy[131].

3.4 THE MALAT1/MIR-100 PARTNERSHIP

The sub-network shown in Figure 3.4 evidences long non-coding MALAT1 and miR-100. These non-coding RNAs are indirectly interconnected by VEGFA.

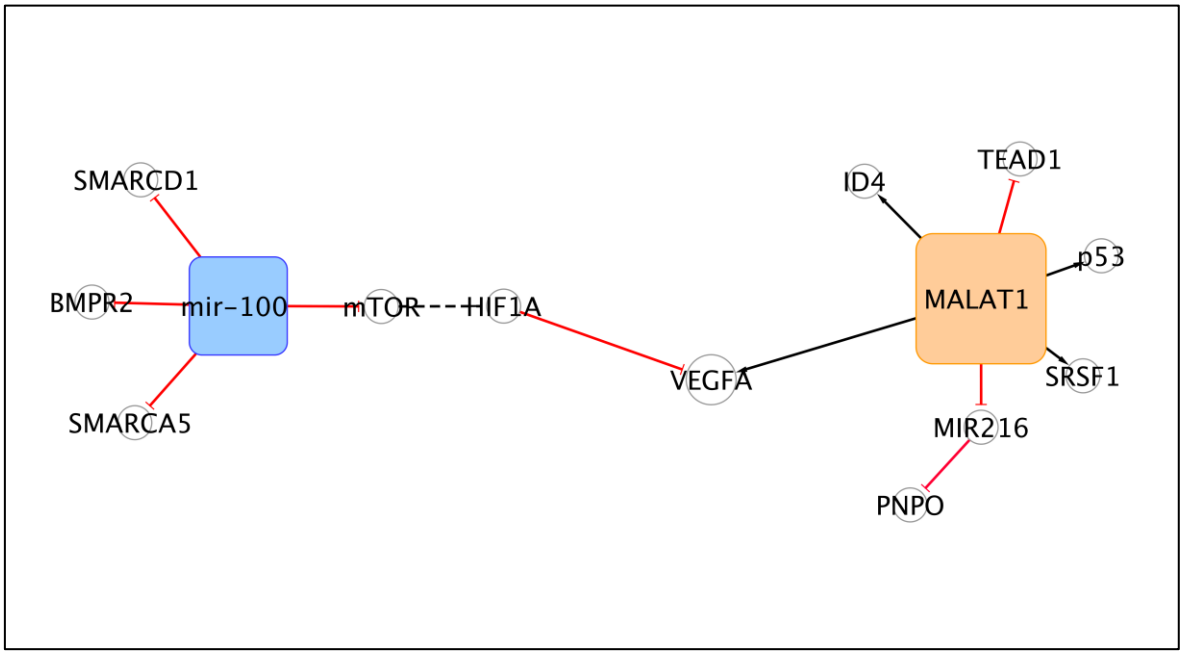

Figure 3.4. The MALAT1/miR-100 sub-network

MALAT1 modulates VEGFA isoforms expression enhancing TP53 mutations in basal-like BC subtype (BLBC). The interaction between MALAT1 and mutant TP53/ID4 is mediated by SRSF1 splicing factor and promotes MALAT1 delocalization from nuclear speckles and its recruitment on VEGFA pre-mRNA. [132]. In addition, MALAT1 acts as competitive endogenous RNA to sponge miR-216b, thus restoring the expression of PNPO, which is associated with promoted cell proliferation, migration and invasion in invasive ductal carcinoma (IDC). MALAT1/miR-216/PNPO pro-metastatic axis represents a target for molecular therapy, as validated in Luminal A and TNBC subtypes[133]. However the role of MALAT1 is still debated. Other studies reported that MALAT1 inhibits the transcription of the pro-metastatic factor TEAD, hindering the interaction between the YAP1 at the TEAD promoters; suggesting MALAT1 as a metastasis-suppressing factor in BLBC[134]. The transfer of miR-100 via MSC-derived exosomes in cancer cells determines the down-regulation of VEGFA secretion by directly targeting mammalian target of rapamycin (mTOR) and modulating mTOR/HIF-1α axis, in fact the miR-100 up-regulation could inhibit angiogenesis and endothelial cell proliferation in the BC microenvironment[135].

Furthermore, mir-100 is negatively correlated with CSC-like self-renewal by inhibiting the SMARCA5, SMARCD1 and BMPR2 regulatory genes in TNBC and

Luminal A subtypes. The miR-100 involvement in the inhibition of metastasis has also been validated *in vivo*[136].

3.5 The miR-125a/b-miR196 sub-network

Figure 3.5 shows the miR-125/HER2 subnetwork.

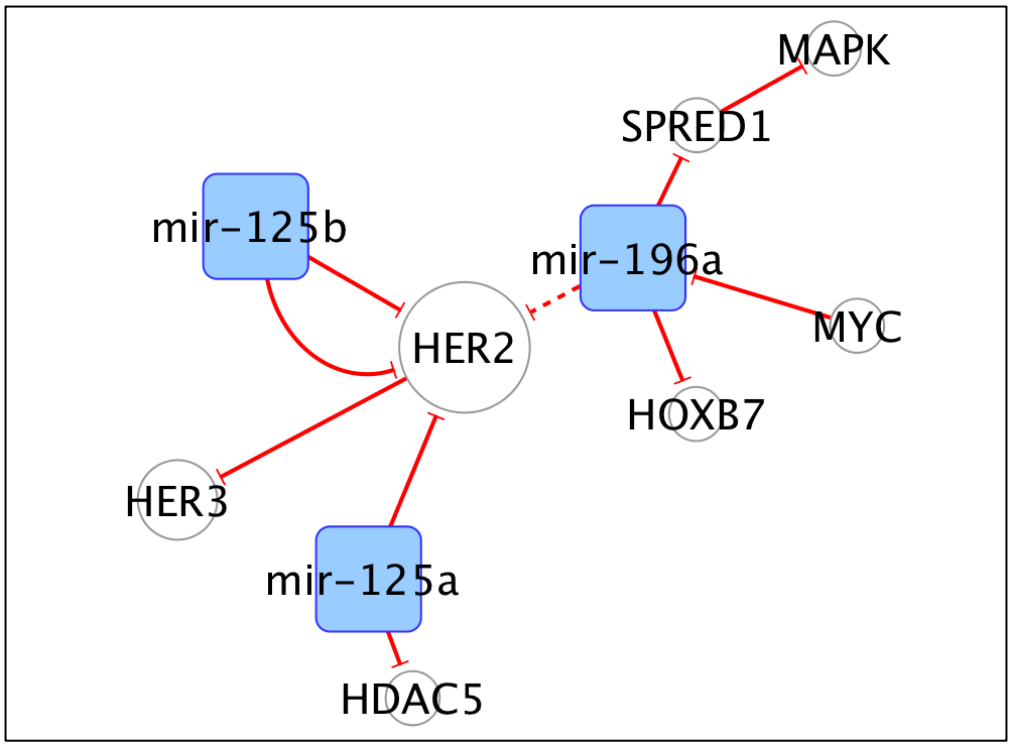

Figure 3.5. The miR125/HER2 subnetwork

MiR-125a/b target the 3'UTR region of both HER2 which elevates HER3 expression levels, thus reducing HER2 mRNA levels and consequently their oncogenic effects in cellular models, including increase of tumour growth rates and trastuzumab resistance [137]. Consistently, the loss of miR-125b promotes HER2 signalling, and is associated with poor prognosis in patients with Luminal A tumours[138]. MiR-125a exerts also a crucial role in the regulation of apoptosis by silencing of HDAC5, upon stimulation of the RUNX3/p300 pathway, representing a novel anticancer strategy able to activate caspase 3/9[139]. Indirectly, also miR-196 contributes to inhibit HER2 expression, by altering HOXB7 and HOXB7-ERα interaction. Nevertheless, miR-196 is down-regulated by MYC, which restores HOXB7 and promotes Luminal A breast cancer tumorigenesis and tamoxifen resistance[140]. On the contrary, Jiang et al. demonstrated that miR-196a, upon stimulation by ER-α interaction, promotes growth of Luminal A breast cancer inhibiting SPRED1, a negative regulator of the RAS/RAF/MAPK signalling, indirectly activated by miR-196[141].

3.6 The miR-182 and miR-96 microRNAs

A study by Yu et al. focuses on the pro-metastatic miR-182, which is associated with EMT, invasion, as well as distant metastasis formation. MiR-182 inhibits the

expression of SMAD7, which is both a transcriptional target of TGFβ and a negative regulator of TGFβ signalling[142]. Also, miR-96 modulates the pro-apoptotic FOXO1, a relevant target for precision therapies, and inspired the rational design of TargaprimiR-96[143]. As a proof of concept, the development of a conjugate small molecule that selectively binds the oncogenic miR-96 hairpin precursor (RIBOTACs), is able to recruit a latent endogenous ribonuclease (RNase L) to FOXO1 transcript, inducing its cleavage. Functionally the silencing of miR-96 de-repressed FOXO1 and induced apoptosis exclusively in TNBC[144]. Other articles highlight an opposite role for these two miRNAs. MiR-96 and miR-182 both target the 3'-UTR region of the PALLD gene. Down-modulation of Palladin transcript expression leads both to decreased migration and invasion of Luminal A breast tumour cells. However, when it is present rs1071738 SNP, a common functional variant of PALLD gene, at the miR-96/miR-182-binding site, the 3'UTR fails to bind the target microRNAs, compromising cell invasion, as verified in *in vitro* experiments[145].

3.7 miR29b and miR-29c

MiR-29b and miR-29c both target chaperone Hsp47, a modulator of the extracellular matrix (ECM) and promoter of BC development; their indirect regulation of ECM genes reduces collagen and fibronectin deposition[146].

In addition, miR-29c targets TET2, thus inhibiting the metastatic phenotype and the genome instability induced by the conversion of 5-methylcitosine(5-mC) to 5-hydroxymethylcytosine (5-hmC). Nevertheless, in TNBC this condition is antagonized by the lymphoid specific helicase (LSH), which induces miR-29c silencing[147].

Interestingly, miR-29b can act as both inhibitor and promoter of cell proliferation, in Luminal A and TNBC subtypes respectively, based on differential regulation of activation of NFkB and TP53 pathway, mediated by S100A7. In MCF7 cells, S100A7 inhibits NFKB signalling with a consequent upregulation of miR-29b that in turn targets CDC42 and PIK3R1 and indirectly activates TP53 leading to the activation of anti-proliferative pathways. In contrast, in MDA-MB-231 cells, miR-29b which has a lower expression than in MCF7 cells, is suppressed by NFkB with consequent repression of TP53 and promotion of metastasis dissemination[148].

3.8 Other non-coding RNAs relevant in breast cancer

In Figure 1 we showed all sub-networks, whose ncRNAs have been described in at least two different sources from literature.

One of these ncRNAs is the estrogen-inducible long non-coding NEAT1, which has been proposed to act as ceRNA and 'sponge' miR-204. MiR-204 inhibition in turn induced impaired cell proliferation and inhibition of apoptosis. These two processes were supported by the H19 lncRNA [149], to promote para-speckle formation under hypoxia condition, mediated by sequestration of HIF2A and F11 receptor (JAM1) [150]. NEAT1 was also involved in the promotion of invasion, EMT and metastasis dissemination in Luminal A cells by interfering with FOXN3/SIN3A

interactions and leading to the repression of GATA3, a crucial regulator of EMT[151].

Another miRNA, miR-27b negatively regulates the acquisition of drug resistance, and is able to induce tumour seeding, two critical properties of CSCs. These effects are mediated by the targeting of ENPP1 and by indirect prevention of the over-expression of ABCG2 transporter. This function was supported by anti-type II diabetes (T2D) drug metformin, that counteracted the generation of CSCs[152]. MiR-27b was also shown to promote the Warburg effect, by inhibiting the PDHX with subsequent dysregulation of the levels of pyruvate, lactate and citrate that increase cell proliferation in the Luminal A and TNBC subtypes[153].

MiR23b has also been subject of recent researches, and itself a notable ncRNA in BC. Its exosome-mediated delivery promoted by Docosahexaenoic acid, an anti-angiogenesis compound, was able to suppress the pro-angiogenic targets PLAU and AMOTL1 in Luminal A and TNBC [154]. Furthermore, in ER-positive endocrine therapy resistant cells, miR-23b was involved in the reprogramming of aminoacid metabolism occurring in association with the down-regulation of SLC6A14 aminoacid transporter, the stimulation of autophagy and the import of aspartate and glutamate by SLC1A2 transporter[155].

The lncRNA breast cancer anti-estrogen resistance 4 (BCAR4) is associated with advanced BC and metastasis. In response to CCL21 chemokine, BCAR4 binds SNIP1 and protein phosphatase 1 regulatory subunit 10 (PNUTS) activating the non-canonical Hedgehog/GLI2 transcriptional program and promoting cell migration[156]. It has been demonstrated that BCAR4 is also involved in the reprogramming of glucose metabolism mediated by YAP1 and favours the transcription of glycolysis promoters HK2 and PFKFB3 via Hedgehog-signalling. The activation of YAP1-BCAR4-glycolisis axis is linked with poor prognosis, and represents an interesting therapeutic target for locked nucleic acids (LNA) delivery, as shown by Zheng *et al.*[157]

In our review, miR-34a appears as the most discussed non-coding RNA, and several independent research groups all pointed it out as an oncosuppressor. MiR-34a, poorly-expressed in TNBC, revealed its anti-tumorigenic nature by direct targeting of c-SRC[158], GFRA3[159], and the MCTS1 re-initiation and release factor (MCT-1). Mir-34a also indirectly modulates IL-6, an interleukine associated with breast epithelial acini morphogenesis, and with EMT stimulation in TNBC[160]. Consistently, miR-34a inhibits cancer stem cell properties and promotes doxorubicin sensitivity in MCF7 cells, by targeting NOTCH1. In MCF7 doxorubicin resistant (MCF7/ADR) cells, miR-34a is expressed at low level, possibly due to TP53 mutations[161]. Other effects promoted by miR-34a are the cell-cycle arrest and the apoptosis of TNBC by targeting $tRNA_i^{Met}$ and AGO2 [162]. Furthermore, miR-34a negatively regulates the EEF2K and FOXM1 proto-oncogenes, both associated with short-term patient survival[163].

The tumour suppressor miR146a, (and its relative miR-146b) is up-regulated by FOXP3 and targets IRAK1 and TRAF6 causing NF-kB inactivation in the Luminal

A subtype. The FOXP3/miR-146/NF-kB axis limits tumour growth and could be a valuable target for therapy[164]. The role of miR-146a includes the reduction of fibronectin and opposing to the epithelial phenotype in TNBC subtype with a pro-metastatic activity supported via the oncosuppressor WWOX, that antagonizes MYC functions[165].

3.9 Discussion

The roles of non-coding RNAs in the establishment and evolution of breast cancer are still under scrutiny by many investigators currently active in the field. In this review we performed an unsupervised and large study of the recent literature in the last quinquennium (2014-2019). We used a data-driven approach in order to produce the most unbiased outcome. Orthogonally, we enforced a strict human based curation of each article selection by the PubMed queries. Only papers that clearly applied mechanistic approaches by using *in vitro* or *in vivo* methods were included in this review. Thus, we excluded, and did not report, papers with pure correlative analyses, which albeit revealing would not distinguish a causative action of the non-coding RNAs under scrutiny. All steps of our approach are synthesized in Fig. 3.6

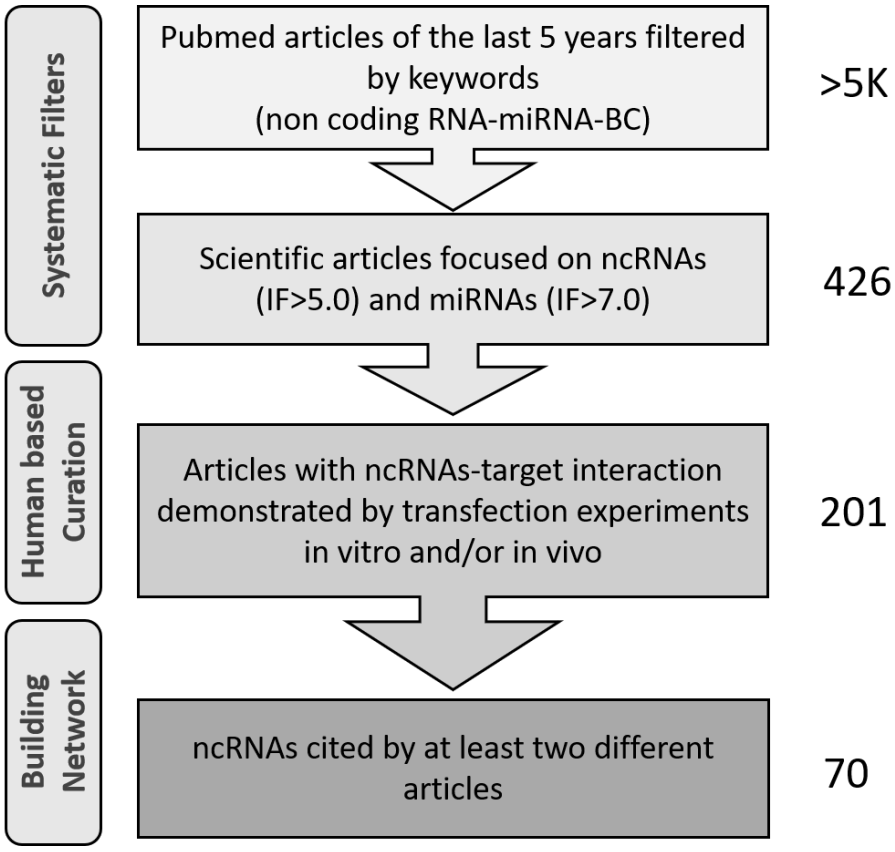

Figure 3.6. Synthesis of data-approach used to build the network ncRNAs-target

CHAPTER 4: THE CURATED NETWORKS OF MIRNAS AND THEIR TARGETS IN COLON CANCER DRUG RESISTANCE

In our previous works, we dissected the relations between long non-coding RNAs (lncRNAs), or microRNAs (miRNAs), and drug resistance in various types of carcinomas[166]; successively, we focused on non-coding RNAs and their targets in breast cancer[95]. Here[167], we merged these two approaches to systematically review the recent literature. Overall, our effort was aimed at the identification of the crucial central miRNAs and their targets in the pathways involved in the drug resistance of colon carcinoma. We restricted our study to 499 research articles listed in PubMed-NCBI and published after 2012 (Table 4.1).

Query for the article selection from Pubmed	Number of articles
((("Colonic Neoplasms"[MeSH Terms] OR "colon carcinoma" OR "colon cancer" OR "colon neoplasm" OR "colonic cancer" OR "colorectal Neoplasms"[MeSH Terms] OR "colorectal tumor" OR "colorectal tumors" OR "colorectal cancer" OR "colorectal cancers" OR "colorectal carcinoma" OR "colorectal carcinomas")) AND (((microRNA* OR miRNA* or microRNAs OR miRNAs OR ("MicroRNAs"[nm]) AND "last 5 years"[PDat])))) AND ("Drug Resistance, Neoplasm"[MAJR] or 'drug resistance' or chemoresistance) Filters: from 2013 - 2021	499

Table 4.1. Query composed by keywords and timing filter for the article selection from Pubmed.

The query we used for selection of the manuscripts on microRNA and drug resistance in colon cancer is reported in the Supplementary Information. Among those, we selected 102 research articles (not reviews or metagenomics studies) based solely on the journal impact factor (at least 5.0). We preferred the impact factor rather than the number of citations, since the latter is largely influenced by the publication age and might not be a fair criterium for papers published recently. Then, we carried out a fundamental task, that of human curation. This step allowed us to perform a quality control of the manuscripts to identify those describing validated and mechanistic models of interactions between miRNAs and protein targets. Thus, we excluded the miRNA/target associations when not validated by overexpression, silencing or genetic mutations. Finally, the manual curation allowed us to correctly standardize the gene naming, which so often diverges in the scientific literature. This final manual data standardization was necessary for the proper execution of the machine learning procedures and creation of networks. This procedure left us with a distilled set of 68 papers that we analyzed and whose results are included in this review. Cytoscape (v. 3.7.2) was used to create and visualize the networks describing the information obtained from the literature. With the aim of reporting robust findings, we start here by focusing on the miRNAs or drugs studied in at least two different scientific articles (Figure 4.1).

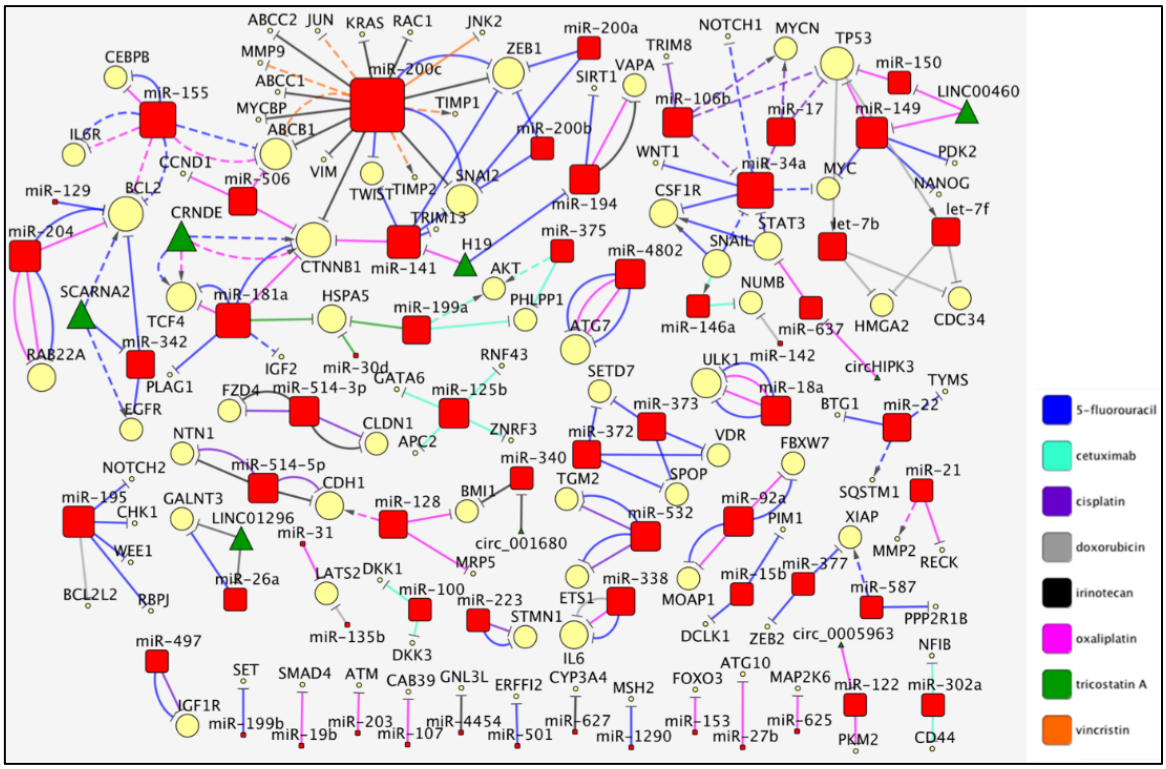

Figure 4.1. The molecular networks of miRNAs and their targets in colon cancer drug resistance. Each network shows the miRNAs/targets (nodes), or drug resistances (edges) described in at least two articles. MiRNAs are identified with red, rounded squares and the targets with yellow circles. The connecting edges corresponds to the drug resistance (color-coding for the drugs is reported in the legend). We used continuous lines for pairwise (first order) interactions and dashed for secondary (higher order) ones. Flat arrows indicate repression, while pointed arrowheads indicate activation. The map size of the miRNAs (red squares), targets (yellow circles) and non-coding RNA upstream regulators (green triangle) depends on the node degree.

The coding genes' nomenclature was standardized by using the HUGO Gene Nomenclature Committee (HGNC). In the network, we used a shape code to graphically highlight miRNAs (red square), their targets (yellow circle), miRNA upstream regulators (green triangle) and each type of drug (connection) with a specific color, as indicated in the legend of Figure 1. Each connecting edge corresponds to a single publication; thus, different lines of the same color indicate a different paper. To better visualize the most connected miRNAs, the node size is proportional to its degree (the number of links between a miRNA and its targets or vice versa); we assigned to lower degrees of value a smaller size. In the following paragraphs, we will describe the most prominent miRNA/target interactions within the context of drug resistance in colorectal cancer (CRC).

4.1 The MiR-200/MiR-181/MiR-155 CTNNB1 BCL2 Network

The members of the miR-200 family (miR-200a/b/c and miR-141) and miR-181a play a pivotal role in the multidrug resistance of colorectal carcinoma. These miRNAs were considered as suppressors of cancer growth and metastasis through the regulation of different molecular pathways. MiR-200c and miR-181a

are the most-connected miRNAs participating in this network, and both inhibit catenin beta 1 (CTNNB1) expression, a key target associated with three different drug resistances (Figure 4.2).

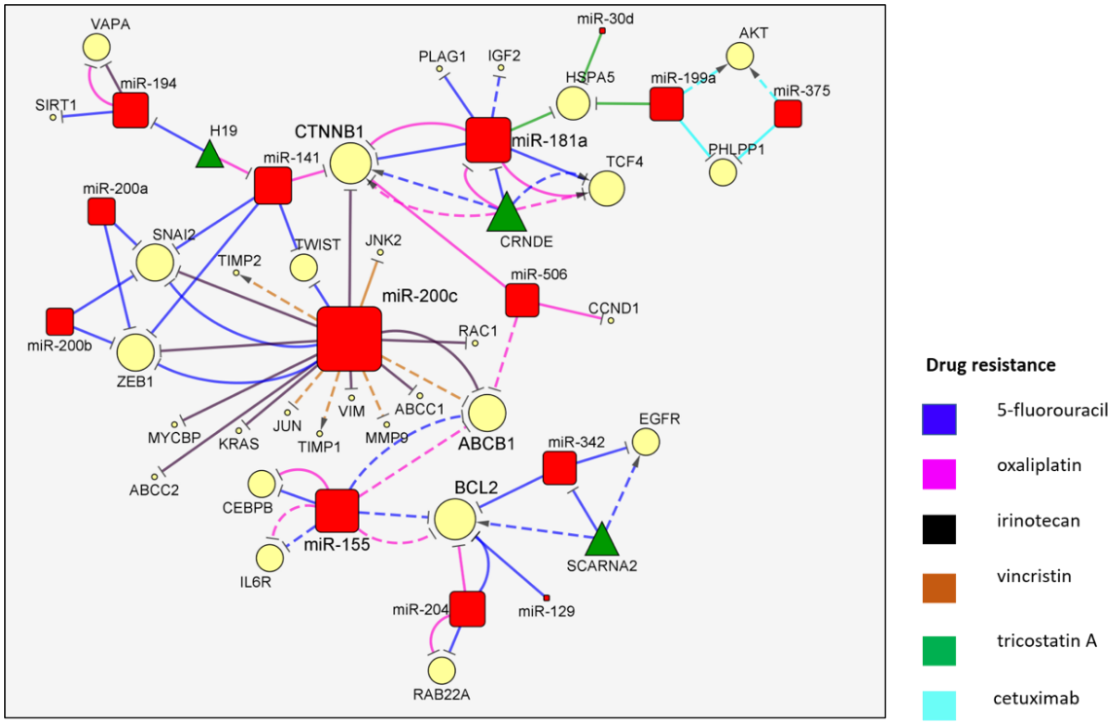

Figure 4.2. MiR-200s/miR-181a and their targets in CRC drug resistance.

The miRNAs in the network are connected with a number of targets (direct or indirect) and are involved in the resistance to vincristine (VCR), irinotecan (CPT11), 5-fluorouracil (5-FU), oxaliplatin (L-OHP), trichostatin A (TSA) and cetuximab (CET). In detail, the overexpression of miR-200c leads to the direct suppression of c-Jun N-terminal kinase 2 (*JNK2*) and indirectly to that of *JUN*, ATP-binding cassette subfamily B member 1 (*ABCB1*) and matrix metallopeptidase 9 (*MMP9*), leading, in turn, to the overexpression of TIMP metallopeptidase inhibitor 1 (*TIMP1*) and *TIMP2* in HCT8 cells treated with VCR[168]. The ABCB1 molecular transporter is also an indirect target of miR-506, a negative regulator of CTNNB1 and cyclin D1 (*CCND1*), and promotes L-OHP sensitivity in colon cancer after forced expression[169]. Juang *et al.* confirmed that miR-200c acted as promoter of CPT11 sensitivity in CRC cells after encapsulation in solid liposomes by suppressing the RAS/CTNNB1/ZEB pathway[170]. Consistently, the loss of miR-200 and miR-141 were related to the overexpression of the zinc finger E-box-binding homeobox 1 (*ZEB1)* and snail family transcriptional repressor 2 (*SNAI2*) (targeted by miR-200a, miR-200b and miR-141) and twist family bHLH transcription factors (*TWIST*) (targeted by miR-200c and miR-141), all contributing to the epithelial–mesenchymal transition (EMT) in 5-FU-resistant CRC[171]. Moon *et al.* investigated the direct correlation between the overexpression of miR-141 and the decrease of the tripartite motif containing 13 (*TRIM13*) expression in the 5-FU sensitivity of CRC and the consequent activation of apoptotic pathways[172]. Ren *et al.* focused their study on the antagonism

between miR-141, which inhibited cancer stemness by the suppression of *CTNNB1*, and H19 lncRNA, which promoted cancer growth and L-OHP resistance acting as sponge for miR-141[173]. Furthermore, miR-194 was reported to be 'sponged' by H19 lncRNA, albeit, as in most of these kinds of experiments, the stoichiometry was not reported; the restoration of the miR-194 levels led to the downregulation of sirtuin 1 (*SIRT1*), resulting in a decrease of H19/SIRT1-mediated autophagy and in an increase of 5-FU sensitivity[174].

CTNN1B, one of the most connected proteins of this network, alongside BCL2, was also targeted by miR-181 and CRNDE lncRNA. The repression of miR-181 by CRNDE determined the higher expression of CTNNB1 and transcription factor 4 (*TCF4*) miR targets with a promotion of cancer cell growth, 5-FU and L-OHP resistance in CRC cells[175]. MiR-181a also inhibited the 5-FU resistance directly targeting transcription factor 4 (*PLAG1*) and, indirectly, insulin-like growth factor 2 (*IGF2*)[176]. Furthermore, miR-181a cooperated with miR-199a and miR-30d (normally downregulated in colon cancer) to downregulate the endoplasmic reticulum chaperone heat shock protein family A (Hsp70) member 5 (*HSPA5*) and increase the TSA sensitivity in CRC cells[177]. On the other hand, miR-199a, in addition to miR-375, is one of the miRNAs that strengthen the resistance to CET. In details, miR-199a and miR-375 silenced the common target PH domain and leucine-rich repeat protein phosphatase 1 (*PHLPP1*), leading to activation of the AKT pathway and increase in CET resistance[178]. The involvement of miR-199a is the opposite for CET and TSA, since it promotes a resistance to the former (by targeting *PHLPP1* together with miR-375) while it inhibits that to the latter (by targeting *HSPA5* with miR-181a and miR-30d).

The miR-200c/*ZEB1* and miR-200c/*ABCB1* relations are confirmed in two different papers, with the first couple involved in 5-FU resistance[170, 171] and the second one involved directly with CPT11 and indirectly with VCR[168, 170]. Furthermore, the influence of CTNNB1 on L-OHP is confirmed by two different papers, although via different miRNAs: miR-141 or miR-181a[173, 175]. Finally, *PHLPP1*, *HSPA5* and *CTNN1B* are first-order targets of several miRNA families in the context of drugs resistance. The lower and left portions of this network have genes and miRNAs that likely arise from the tumor microenvironment and are not expressed in the cancer cells themselves. MiR-204 and miR-129, acting as onco-suppressors, directly affect 5-FU resistance by targeting *BCL2*, an antiapoptotic oncoprotein, which was also downregulated by miR-204/miR-155 in L-OHP resistance. MiR-204 and miR-155 were both downregulated in tumor-associated macrophages (TAMs), due to the inhibitory role of the activated interleukin 6 (IL6)/signal transducer and activator of the transcription 3 (STAT3) pathway, with a consequent upregulation of CCAAT enhancer-binding protein beta (*CEBPB*), IL6 receptor (*IL6R*), *ABCB1* (by miR-155), *RAB22A* (by miR-204) and the shared *BCL2* target[179]. This molecular mechanism, possibly involving exosomes and validated by a coculture of TAMs and CRC cells *in vitro*, conferred L-OHP and 5-FU resistance to CRCs. The miR-204 activity on RAB22A, a member of the RAS oncogene family, and the promotion of chemosensitivity after miRNA's ectopic expression was confirmed in L-OHP-resistant CRCs[180]. The resistance to 5-FU was also associated with a low

expression of miR-129. After an ectopic expression of miR-129 and the consequent targeting of *BCL2*, CRC apoptosis and 5-FU sensitivity were, in fact, promoted[181]. Furthermore, miR-342 was competitively bound by SCARNA2, a non-coding RNA highly expressed in CRC tissues, thus leading to a secondary upregulation of both the epidermal growth factor receptor (EGFR) and BCL2 oncoproteins and to a sustained 5-FU resistance[182]. BCL2 is one of the most-connected proteins (together with CTNNB1) and one of the most affected by miRNA activity, as reported by a number of studies on 5-FU resistance. Nevertheless, the implications of miR-204/RAB22A on the resistance to L-OHP were reported by two independent research groups[179, 180]. To understand the functional involvement of the genes in this network, we looked for the most-represented cellular pathways using Fisher's exact test (Table 4.2).

PANTHER Pathways	observed	expected	Fold Enrichment	raw P value	FDR
Ras Pathway	3	0.1	30.23	1.47E-04	6.16E-03
CCKR signaling map	7	0.23	29.93	3.35E-09	5.59E-07
p53 pathway feedback loops 2	2	0.07	28.84	2.35E-03	4.35E-02
Oxidative stress response	2	0.08	26.27	2.80E-03	4.68E-02
PI3 kinase pathway	2	0.08	25.81	2.90E-03	4.40E-02
Apoptosis signaling pathway	3	0.16	18.7	5.80E-04	1.94E-02
Gonadotropin-releasing hormone receptor pathway	5	0.31	15.92	1.49E-05	8.30E-04
EGF receptor signaling pathway	3	0.19	15.65	9.61E-04	2.67E-02
PDGF signaling pathway	3	0.2	15.01	1.08E-03	2.58E-02
Angiogenesis	3	0.24	12.61	1.77E-03	3.69E-02

Table 4.2. The cellular pathways over-represented by the genes included in the network composed by miR-200s/miR-181a and their targets in CRC drug resistance.

The false detection rate was additionally computed to control for multiple testing[183]. As expected, RAS and PI3K are among the most-represented pathways (FDR <0.05), although the signaling by the cholecystokinin (CCK) receptor is the one spanning the most members (n = 7) in the network (fold enrichment of 29.9 and FDR 5.6×10^{-7}). In both gastric and colon cancer cells transfected with the cholecystokinin 2 receptor (*CCK2R*), gastrin has been shown to enhance cyclooxygenase-2 (*COX-2*) gene expression. This key enzyme is known to play an important role in inflammation and carcinogenesis. COX-2 has been involved in hyperproliferation, transformation, invasion, and angiogenesis. In CRC, the extracellular signal-regulated kinase 1/2 (ERK1/2) and PI3-kinase pathways are also involved in gastrin-induced COX-2 expression[184].

4.2 The TP53/miR-34a Network

In the second network we describe, miR-34a and TP53 are, respectively, the miRNA and the protein node with the highest degree. MiR-34a was involved in the regulation of resistance to 5-FU and cisplatin (CDDP) (Figure 4.3).

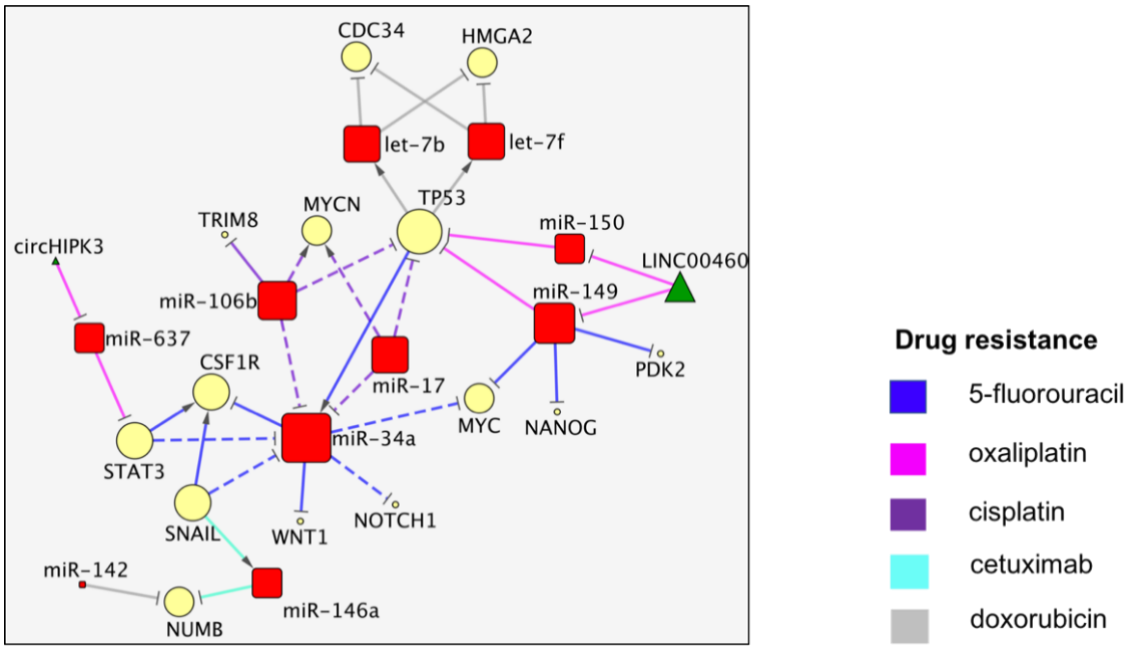

Figure 4.3. The miR-34a/TP53 network.

The loss of miR-34a expression by CpG methylation or mutation in the *TP53* gene can determine an increase of the colony stimulating factor 1 receptor (*CSF1R*), a direct target of miR-34a and a mediator of EMT, metastasis and 5-FU in CRC[183]. CSF1R was also positively regulated by SNAIL and STAT3 levels, which negatively regulate the miR-34a. The restoration of the miR-34a levels in 5-FU-resistant CRC through the treatment with regorafenib induced the decrease of *WNT1* and, indirectly, of *MYC* and *NOTCH1* expression, leading to an inhibition of the stemness[185]. MiR-34a action was also indirectly inhibited by miR-106b and miR-17, two miRNAs that promoted both cell proliferation and CDDP resistance by silencing *TRIM8* and by the indirect regulation of MYCN signaling[186]. *MYC* and *TP53* are also two of the direct targets of miR-149 involved, respectively, in L-OHP and 5-FU action. The replacement of miR-149, normally suppressed by SNAIL2 in colon carcinoma, was associated with an inhibition of EMT and 5-FU chemo-resistance upon the targeting of *MYC* and nanog homeobox (*NANOG)*[187] and with a reduction in glucose metabolism after pyruvate dehydrogenase kinase 2 (PDK2) inhibition[188]. MiR-149 was also implicated in the L-OHP resistance regulated by a LINC00460 feedback loop in p53-mutated CRC cells (SW480/OxR), which, in turn, promoted the suppression of miR-149 and miR-150 and, thus, the overexpression of *TP53*[189]. Let-7b/f were proposed as tumor suppressor miRNAs, due to their negative regulation of the cell division cycle 34 (*CDC34*) and high mobility group AT-hook 2 (*HMGA2*) oncogenes[190]. In this article, it was demonstrated that the levels of both let-7b and let-7f were upregulated by doxorubicin (DOXO) in a wild-type p53-dependent fashion, which led to the slowing of cancer cell proliferation. The Snail-dependent upregulation of miR-146a and the silencing of the NUMB endocytic adaptor protein (*NUMB*) were associated with asymmetrical cell division in colorectal CSCs and the promotion of resistance to CET[191]. The downregulation of *NUMB* by miR-142 was also correlated with DOXO resistance in CRC cells. The miRNA-induced activation of Notch signaling determined an

increase in the stemness and drug resistance[192]. It is interesting to note the bivalent position of miR-34a in two different contexts, the resistance to CDDP and 5-FU. MiR-34a can act as an inhibitor of *CSF1R*, *WNT1*, *MYC* and *NOTCH1* in 5-FU-resistant cells and promotes chemosensitivity, while it is downregulated by miR-106b and miR-17, which promote CDDP resistance. MiR-637 increased the L-OHP sensitivity by repressing *STAT3*, normally highly expressed in colon cancer. The circular RNA encoded by the homeodomain-interacting protein kinase 3 gene (circHIPK3) can compete with miR-637 in regulating cell viability, apoptosis and drug resistance[193]. *TP53* is thus inhibited by four miRNAs and interacts with different drug resistances discussed in two distinct articles[189, 194]. The involvement of MYC in 5-FU resistance was reported by two different articles via different mechanisms[185, 187]. The miR-149/5-FU relation was also independently validated[187, 188], although, again, there was no agreement about the involved protein targets. Notch and WNT signaling are over-represented here, together with angiogenesis (FDR <0.05) (Table 4.3).

PANTHER Pathways	observed	expected	Fold Enrichment	+/-	raw P value	FDR
Notch signaling pathway	2	0.03	72.01	+	3.74E-04	1.56E-02
p53 pathway feedback loops 2	2	0.03	62.13	+	4.97E-04	1.66E-02
Interleukin signaling pathway	2	0.05	36.84	+	1.36E-03	3.80E-02
Angiogenesis	3	0.11	27.16	+	1.70E-04	9.46E-03
Wnt signaling pathway	4	0.2	19.99	+	3.70E-05	6.17E-03

Table 4.3. The Pathways over-represented by the genes included in the miR-34a/TP53 network.

4.3 The miR-514b and miR128 activities converge on CDH1

MiR-514 and miR-128, as well as miR-340, regulate the proteins involved in CDDP, CPT11 and L-OHP resistance in colon cancer (Figure 4.4).

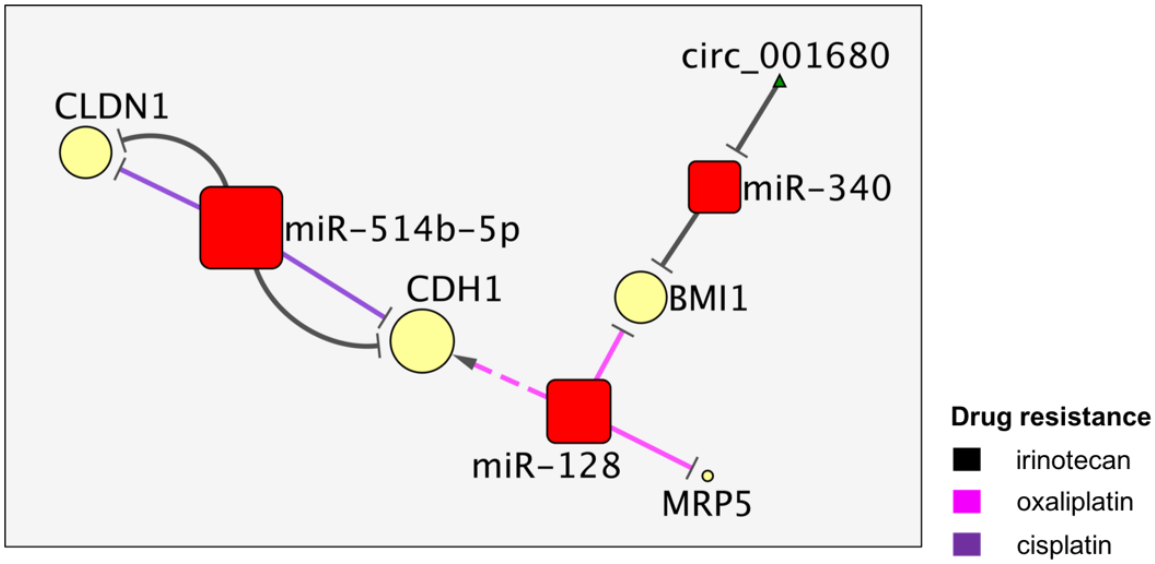

Figure 4.4. The miR-514b and miR128 microRNA niches are connected by CDH1.

Ren *et al.* investigated the antagonist effects of the miR-514b-5p and miR-514b-3p products, respectively, a promoter and suppressor of metastasis, EMT and CPT11/CDDP resistance, by regulating cadherin 1 (*CDH1)* and claudin 1 (*CLDN)*, the targets of miR-514b-5p, frizzled class receptor 4 (*FZD4*) and netrin 1 (*NTN1*), the targets of miR-514-5b-3p (previously shown in Figure 4.1)[195]. On the other hand, miR-128 was associated with L-OHP sensitivity by its indirect enhancing of *CDH1* expression and the downregulation of multidrug resistance-associated protein 5 (*MRP5*) and the *BMI1* Polycomb Ring Finger proto-oncogene. This activity was reported to also be present in the exosomes secreted by L-OHP-resistant cell lines[196]. BMI1 is a promoter of stemness traits of cancer cells and represents a key mutual target linking miR-128 and miR-340, both suppressors of tumorigenesis in CRC. In particular, miR-340 appeared to be sponged by circ_001680, leading to an upregulation of *BMI1* and to an increase of both the cancer stem cell (CSC) population and CPT11 resistance[197]. Among the key factors of this network, CDH1, an important onco-suppressor, was confirmed by two research groups. In fact, *CDH1* was downregulated by miR-514, promoting CPT11 and CDDP resistance, while it was indirectly upregulated by miR-128, which contrasted the oxaliplatin resistance. In addition, BMI was suppressed by either miR-340 or miR-128 to sensitize CRC cells, respectively, to C and to L-OHP treatments.

4.4 Smaller miRNA networks involved in CRC drug resistance

Some smaller networks reported in Figure 4.1 were not discussed above, but in our opinion, they should be carefully noted. We list and discuss them briefly in the following paragraphs.

MiR-195. The role of miR-195 in drug resistance, depicted in Figure 4.1, was the object of divergent conclusions. Kim *et al*. sustained that miR-195-5p promotes 5-FU resistance by suppressing the WEE1 G2 checkpoint kinase (*WEE1)* and checkpoint kinase 1 (*CHK1*) in CRC[198]. Jin *et al*. affirmed that miR-195-5p enhanced 5-FU sensitivity and apoptosis, involving the suppression of mechanisms induced downstream by NOTCH2 and the recombination signal-binding protein for immunoglobulin kappa J region (*RBPJ*)[199]. Qu *et al.* concorded with the latter hypothesis of miR-195 as promoter of CRC chemosensitivity; in particular, they investigated the relation between the suppression of BCL2-like 2 (*BCL2L2*) by miR-195 and the sensitivity to DOXO[200].

MiR-194. This miRNA was reported to be downregulated by HMGA2 as a consequence of *VAPA* suppression by miR-194, thus leading to the sensitization of cancer cells to CPT11 and L-OHP[201].

MiR-15b. The overexpression of miR-15b determined the proapoptotic and antiproliferative effects and is associated with a major sensitivity to 5-FU treatment by suppressing either the Pim-1 proto-oncogene, serine/threonine kinase (*PIM1*)[202] or doublecortin-like kinase 1 (*DCLK1*)[203].

4.5 UNCONFIRMED ASSOCIATIONS OF MIRNAS WITH DRUG RESISTANCE IN CRC

The three networks we discussed above were those including 'validated' miRNA/drug or miRNA/target interactions, i.e., those described by at least two unrelated research teams. Nonetheless, Figure 4.1 also contains interactions that have not been independently confirmed. We describe below these findings, albeit with a cautionary note, grouping them by drug.

5-Fluorouracil resistance. MiR-372/373 acted as promoters of stemness and 5-FU resistance in CRC cells by silencing the genes implicated in the differentiation process, such as the speckle-type BTB/POZ protein (*SPOP*), SET domain containing 7, histone lysine methyltransferase (*SETD7*) and vitamin D receptor (*VDR*) targets[204]. MiR-377 downregulated the Wnt/β-catenin pathway by targeting the X-linked inhibitor of apoptosis (*XIAP*) and *ZEB2*, with a positive effect on apoptosis and 5-FU chemosensitivity[205]. MiR-587 was considered as a 5-FU antagonist by repressing the protein phosphatase 2 scaffold subunit A beta (*PPP2R1B*) with an increased *XIAP* expression and AKT pathway activity[206]. This effect was reversed by the overexpression of *PPP2R1B* associated with a promotion of apoptosis. MiR-501 was downregulated by the KH-type splicing regulatory protein (*KHSRP*), with a consequent upregulation of its ERBB receptor feedback inhibitor 2 (*ERRFI2*) target, thus determining the 5-FU cell resistance and CRC proliferation[207]. Both effects were contrasted by either *ERRFI2* knockdown or miR-501 overexpression. MiR-199b was commonly downregulated in colon cancer, while the miR target SET nuclear proto-oncogene (*SET*) was highly expressed and correlated to 5-FU resistance in advanced rectal cancer (LARC)[208]. The ectopic expression of miR-199b determined the 5-FU sensitivity and represented a frontier to prevent drug resistance. MiR-1290 expression was highly detectable in deficient mismatch repair (dMMR) colon cancer and was associated with 5-FU resistance[209]. The silencing of miR-1290 determined an upregulation of its direct target mutS homolog 2 (*MSH2*) and a relative 5-FU sensitivity in CRC cells. Liu *et al.* demonstrated that LINC01296 downregulates miR-26a and indirectly upregulates the polypeptide N-acetylgalactosaminyl transferase 3 (*GALNT3*) miR target, thus promoting the PI3K/AKT pathway by the catalysis of mucin 1 (*MUC1*) and 5-FU resistance[210]. Tumor suppressor miR-22 was related to autophagy inhibition and a proapoptotic effect that led to a promoted 5-FU sensitivity[211]. From a molecular point of view, miR-22 suppressed the BTG antiproliferation factor 1 (*BTG1*) target and, indirectly, thymidylate synthetase (*TYMS*) and upregulated sequestosome 1 (*SQSTM1*), a downstream target.

Irinotecan resistance. Sun *et al.* investigated the promoting effect of calcitriol on the miR-627 expression and demonstrated a relation between the suppression of its target, cytochrome P450 family 3 subfamily A member 4 (*CYP3A4*), and the CPT11 sensitivity in CRC cells with a relative inhibition of cell growth and an increase of apoptosis[212]. The loss of miR-4454 expression was correlated with the activation of the G protein nucleolar 3-like (GNL3L)/NFKB pathway, resulting in a resistance to CPT11[213]. The overexpression of miR-4454 restored GNL3L silencing and reduced chemoresistance and cancer aggression *in vitro*.

Cetuximab resistance. MiR-100 and miR-125b promoted CET resistance by suppressing the negative modulators of Wnt signaling, such as dickkopf WNT signaling pathway inhibitor (*DKK1*), *DKK3* (miR-100 targets) and APC regulator of WNT signaling pathway 2 (*APC2*), GATA-binding protein 6 (*GATA6*), ring finger protein 43 (*RNF43*) and zinc and ring finger 3 (*ZNRF3*) (miR-125b targets)[214]. MiR-302a was generally downregulated in colon cancer; its overexpression directly inhibits metastasis and CET resistance by silencing nuclear factor I B (*NFIB*) and CD44 targets[215].

Doxorubicin resistance. MiR-135b acted as promoter of DOXO resistance and antiapoptotic programs by directly targeting the tumor suppressor kinase 2 (*LATS2*)[216]. These results were also confirmed in a xenograft model.

Oxaliplatin resistance. LATS2 was silenced by miR-31, itself upregulated by forkhead box C1 (*FOXC1*) in L-OHP-resistant cells[217]. MiR-107 was also a promoter of L-OHP resistance by suppressing calcium-binding protein 39 (*CAB39*) and activating the protein kinase AMP-activated (AMPK) mTOR pathway; these events could be reversed by dichloroacetate, which promoted the chemosensitivity[218]. An additional study found that high levels of miR-153, detected in 21 (out of 30) colorectal cancer patients, correlated with L-OHP resistance, as well as a sustained cellular proliferation[219]. Mir-19b acted as onco-miRNA and as a promoter of L-OHP resistance by targeting SMAD family member 4 (*SMAD4*); this link was firstly identified by bioinformatics and later confirmed *in vitro*[220]. MiR-203 was also correlated with the enhancement of L-OHP resistance; a high expression of miR-203 was present in three colorectal cell lines where the ATM protein kinase was its direct target[221]. MiR-21 can play a pro-metastatic role and promote L-OHP resistance in CRC cells. In fact, Bullock *et al.* demonstrated that an ectopic expression of miR-21 increased the invasiveness by way of an indirect upregulation of matrix metallopeptidase 2 (*MMP2*), which was, in turn, negatively regulated by the reversion-inducing cysteine-rich protein with kazal motifs (*RECK*) miR-21 target[222]. On the contrary, miR-27b, detected at low levels in L-OHP-resistant CRC cells due to c-MYC binding in the promoter of the miR-27B gene, was involved in chemosensitivity by repressing the autophagy-related 10 (*ATG10*) target, as well in the negative regulation of autophagy[223]. Rasmussen *et al.* investigated another key factor in the poor outcome of colon cancer patient, the downregulation of mitogen-activated protein kinase kinase 6 (*MAP2K6)* by miR-625 and the reduction of p38 signaling linked to the evasion from apoptosis and to L-OHP resistance[224]. A last miRNA involved in the promotion of L-OHP resistance was miR-122, which also activated glycolysis by an indirect upregulation of the pyruvate kinase M1/2 (*PKM2*) miR target and was proposed as a competitive 'sponged effect' by a circular RNA, hsa_circ_0005963[225].

5-FU and Cisplatin resistance (Multidrug). A lower expression of miR-223 was detected in colon cancer cells presenting mutated TP53. The ectopic expression of miR-223 in p53-mutant CRCs promoted 5-FU and CDDP sensitivity by targeting stathmin 1 (*STMN1*) and enhanced apoptosis[226]. When overexpressed, miR-497 targeted the 3'UTR site of the insulin-like growth factor 1 receptor (*IGF1R*)

oncogene and determined an increase in cell death and 5-FU and CDDP sensitivity[227]. Gu *et al.* investigated a possible tumor suppressor role for miR-532, found to be downregulated in colorectal adenoma. Its ectopic expression determined a decrease of CRC aggressiveness *in vitro* and of a resistance to 5-FU and CDDP by suppressing the ETS proto-oncogene 1 transcription factor (*ETS1*)/transglutaminase 1 (*TGM1*) axis and the Wnt/β-catenin pathways[228].

5-FU and L-OHP resistance (Multidrug). The expression of miR-4802 and miR-18a was indirectly repressed by Fusobacterium (F.) *nucleatum*, a component of the gut microbiota highly represented in drug-resistant colon cancer patients, resulting in the upregulation of autophagy-related 7 (*ATG7*) and unc-51-like autophagy activating kinase 1 (*ULK1*) targets, two activators of autophagy, as well as a resistance to 5-FU and L-OHP[229]. MiR-92a, secreted by cancer-associated fibroblasts in exosomes, was positively correlated with the tumorigenesis of colon cancer. It promoted stemness, metastasis, 5-FU and L-OHP resistance and inhibited mitochondrial apoptosis mediators, such as F-box and WD repeat domain containing 7 (*FBXW7*) and the modulator of apoptosis 1 (*MOAP1*)[230].

Finally, the non-validated interactions for drugs that have not been the object of more than one study and for this reason not included in the networks of Figure 4.1 are listed in Table 4.4.

PMID	miRNA	Target	Drug Name	Ref.
29844307	miR-550a	YAP1	vemurafenib	[231]
28327152	miR-106b, miR-17	miR-34a, MYCN, TP53, TRIM8	sorafenib, nutlin-3, axitinib	[186]
33585440	miR-214	KPNA3	mitomycin	[232]
28069878	miR-218	MALAT1	FOLFOX	[233]
30831320	miR-192, miR-215	NID1	doxicyclin	[234]
31208913	miR-338	IL6	cyclophosphamide	[235]
28189050	miR-675	VDR	calcitriol	[236]
30103475	miR-324	SOD2	4-acetylantroquinonol B	[237]
25928322	miR-145, miR-21	NUMB, CD44, KRT20, SOX2	5-FU and L-OHP mix	[238]

Table 4.4. List of miRNA target interactions and relative drugs not included in the Figure 4.1 networks.

4.6 Drug-Centric network and clusters of miRNA/targets interactions in CRC

In this paper, we have hitherto discussed the miRNAs and their interactions, either the first or higher order, to understand the mechanisms underlying various types of chemoresistance in CRC. Protein targets were included in the network and provided the connections of non-coding RNAs with the molecular effectors in apoptosis, cell proliferation and other major cellular processes of CRC. In some of these networks, members of the other classes of non-coding RNAs, such as lncRNAs or circular RNAs, also participated. At this stage, we wished to dig further into the intricate web of gene networks by using a different point of view, namely that of an all-in drug interaction. We obtained such a view by considering the drug nodes rather than, as above, edges. The resulting network is quite complex, and we report it integrally in Figure 4.5, highlighting the most connected drug

resistance (green rhombuses) and their relations with the miRNAs (red squares) and miRNA targets (yellow circles) in CRC.

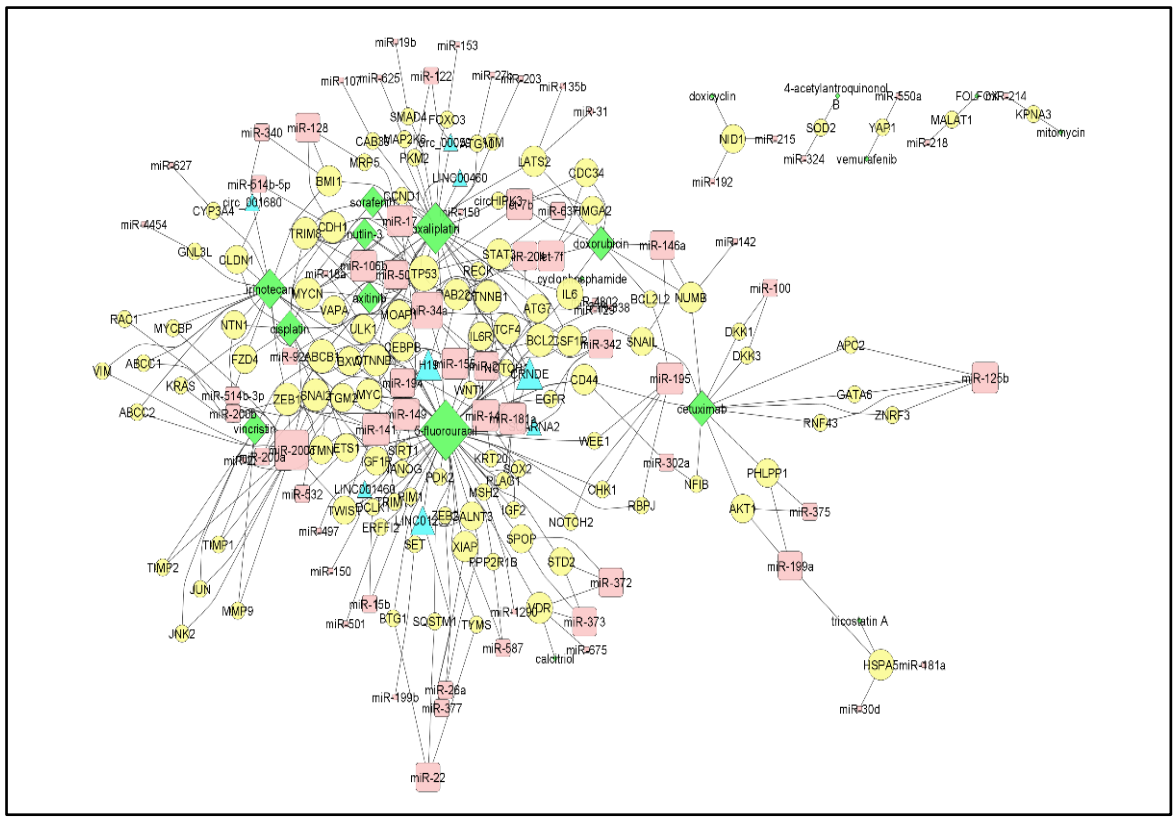

Figure 4.5. Network of miRNAs and their targets connected to the drugs discussed in our review. In the network we included miRNAs (red rectangle), their target (yellow circle) and miRNA regulators (sky-blue triangle) connected to the drug resistances. The map node size was dependent to degree

The upstream regulators of miRNAs are indicated as sky-blue triangles. The map node size was proportional to the node's degree. Since this drug-centric network is highly connected, unlike the one of Figure 4.1, we looked for embedded clusters, using a community analysis, implemented by the GLay plugin in Cytoscape. Figure 4.5 shows the six major clusters identified within the drug-centric network. The largest cluster, on the top left, includes the miRNAs and proteins regulating the resistance to 5-FU: miR-155, miR-342 and miR-204 are the miRNAs with the highest degrees, while BCL2 and ABCB1 are the most prominent among proteins. In the L-OHP cluster miR-92, miR-181a and miR-506 are the most connected, and CTNNB1 is the protein with the highest degree. While, in the previous two clusters, there was only one drug, CPT11 and VCR share together another cluster, with EMT gene representation (miR-200c/miR141 and ZEB1/SNAI2 and VIM). DOXO, axitinib, sorafenib and nutlin are all in another cluster, which comprises miR-17, miR-106b, let-7b/f, miR-34a and miR-146a, alongside TP53, TRIM8, MYCN and CDC34. The biological process for the seven genes in this cluster is the 'positive regulation of cell death' (FDR = 9.2 E-3) as calculated using the PANTHER Over-representation Test. The CET and TSA cluster includes miR-125b and miR-199a and AKT1 as a protein target. The CET/TSA cluster corresponds to Wnt signaling

in the GO biological process (FDR = 1.2xE-4). CDDP spans miR-514 and miR-532, and the GO analysis points to gland development and other processes involved in cell differentiation.

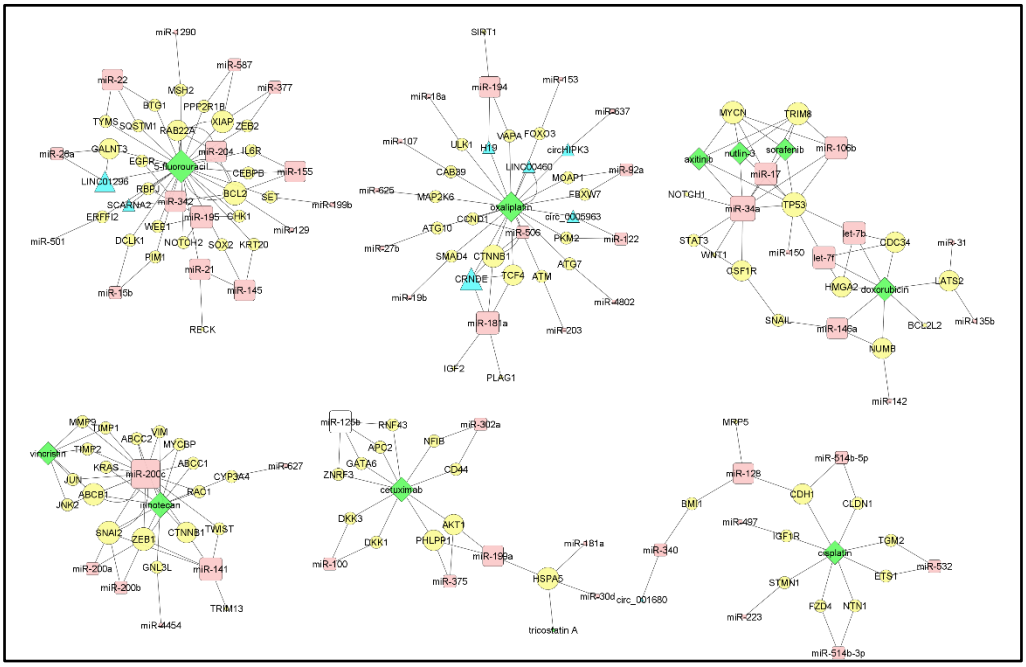

Figure 4.6. Clusters of miRNAs/targets/upstream regulators connected to the most-studied drugs in the treatment of CRC. Each subnetwork represents a separate cluster of the major drug-centric network (Figure 4.5). We included miRNAs (red square), their targets (yellow circle) and miRNA and target upstream regulators (sky-blue triangle) connected to the most-studied drug resistances (green rhombus). The map node size was dependent on the nodes' degree. To build the network, we arbitrarily linked the protein targets or the ncRNA regulator with the drug and the miRNAs to either their targets or ncRNA regulator. The edges here are undirected and, thus, represent associations. Drug abbreviations: 5-FU, 5-fluorouracil; L-OHP, oxaliplatin; CPT11, irinotecan; CET, cetuximab, CDDP: cisplatin.

4.7 Discussion

Our data-driven and machine learning-assisted review distilled some well-defined genetic networks involved in the drug resistance of CRC. The largest miRNA network in CRC drug resistance spanned miR-200s/miR-181a, among others, and was implicated in the action of six different anticancer treatments (Figure 4.2). In this network, CTNNB1 plays a pivotal role, and it is at the interface of two miRNA subnetworks. CTNNB1 is part of a complex of proteins forming adherens junctions, which are important for the establishment and maintenance of epithelial cell layers by regulating cell growth and adhesion between adjacent cells[239]. *CTNNB1* is altered in 4.81% of colorectal carcinoma patients mutations, which are commonly homo- or hemizygous, indicating a higher threshold of CTNNB1 stabilization to be required for transformation in the colon as compared to extracolonic sites[240]. Moreover, different mutational hotspots in *CTNNB1* for MSI-H and MSS CRCs suggest different effects on CTNNB1 stabilization. Reduced E-cadherin may also contribute to higher levels of transcriptionally active CTNNB1,

and it is not directly linked to the *CTNNB1* mutational status. Another target shared by both miR-181a and miR-200s is ABCB1, a membrane transport involved in multidrug resistance. ABCB1 links the larger portion of this network to the miR-155 lobe. MiR-155 is expressed both in CRC cells and in the tumor immune infiltrates, with the presence of CEBPB pointing to tumor-associated macrophages as additional actors in drug resistance. The potency of miR-155 indirectly regulates IL6R, which also suggests the inclusion of granulocytes in the relevant immune cells. Finally, there is a higher-order downregulation of the *BCL2* and *EGFR* oncogenes by both miR-155 and miR-342. The molecular mechanisms underlying multiple drug resistance are revealed here as crossing different types of cells and some of them appearing to be exosome-mediated.

Another network that stands out, albeit a smaller one, is highly concentrated around miR-34a[241] and comprises heavy-weight cancer genes, namely TP53 and MYC, together with some other outstanding oncoproteins, such as MYCN, NOTCH1, WNT1, CSF1R, CDC34 and the stem cell regulator NANOG (Figure 4.3). The notorious onco-miR-17, which is transcribed by MYC[241], seems to have an opposite influence when compared to miR-34a. This small network has been reported in the resistance to five different cancer drugs.

A small number of microRNAs and proteins in the networks and clusters that we defined through our work are critically involved in major anticancer treatments for colon cancer. In particular, the family of miR-200, miR-34a, miR-155 and miR-17 appear among the key microRNAs. Thus, the regulation of these miRNAs and their downstream targets or effectors might help to interfere with several drug resistance mechanisms in CRC. As evidenced by our study, few miRNAs seem to have pleiotropic effects on different anticancer drugs. These miRNAs and their partners might also be used in predictive hybrid coding/non-coding gene signatures to address patients to the most effective therapy.

CONCLUSION

Summarizing these three years of studies we were able to prove our hypotheses identifying a sizeable group of circular RNAs that have the potential to generate novel protein components in the cellular circuitry. We also demonstrated that T-UCRs sustain cell cycle modulation in two cell line models of breast cancer, in particular uc.183, uc.110, and uc.84 are mutually exclusive of miR-221, and seem to be components of alternative cell cycle circuits. We have further unveiled some of the most important networks embracing ncRNA/target interactions, and described their involvement in breast development and in colon cancer drug-resistance.

FURTHER DEVELOPMENT

-Whether the circRNAs might constitute a core of more stable mRNA forms, be mass regulated by somatic mutations in the splicing machinery genes, and really impact in some key cancer pathways remains to be experimentally determined. Certainly, this work can represent an hint for a deep investigation in *in vitro* and *in vivo* models and a new frontier for clinical applications.

-T-UCRs as well as circRNAs were considered as “dark genome” elements. In fact, the role of this class of ncRNAs is under scrutiny. With our data-mining study and *in vitro* experiments we demonstrated the influence of three T-UCRs in cell cycle circuitry and in the most dysregulated pathways in breast cancer cell lines. Consistently such a combined approach can be relevant to investigate on the potential role of these transcriptomics regulators in other cancer types.

-Our data-driven and machine learning-assisted review can be a useful and flexible strategy to synthesize the fragmented information about molecular relations, from literature. Such a systematic approach can help to quickly filter the eligible articles and to create a network composed by the molecular connections involved in different type of disease.

ABBREVIATIONS

BC: Breast cancer; BIM: BCL2 like 11; BLBC: Basal like breast cancer; BRK: Protein tyrosine kinase 6; CDDP: cisplatin; ceRNA: Competing endogenous RNA; CET: cetuximab; circRNA: Circular RNA; CPT11: irinotecan; CRC: colorectal cancer; CSCs: Cancer stem cells; DOXO: doxorubicin; EMT: Epithelial mesenchymal transition; ER: Estrogen receptor; ETR: Endocrine therapy resistant; EV: Exosomal vesicles; HBXIP: Late endosomal/lysosomal adaptorMAPK and MTOR activator 5; IDC: Invasive ductal carcinoma; IMP1: Insulin-like growth factor 2 messenger RNA binding protein; JAM1: F11 receptor; LINCRNA:Large intergenic non-coding RNAs; L-OHP: oxaliplatin; LN1:Laminin111; lncRNA:Long noncoding RNAs; LSD1:Lysine demethylase 1A; LSH:Helicase lymphoid specific; MCT-1:MCTS1 re-initiation and release factor; miR:Microrna; ncRNA:Non-coding

RNA; nSMase:Sphingomyelin phosphodiesterase 2; ORF: open reading frame; PIP3:Phosphatidylinositol-3,4,5-trisphosphate dependent Rac exchange factor; PNUTS:Protein phosphatase 1 regulatory subunit 10; RNA:Ribonucleic acid; SAH:Acyl-CoA synthetase medium chain family member 3; SAHH:Adenosylhomocysteinase; SCA1:Ataxin 1; SLUG:Snail family transcriptional repressor 2; SNP:Single nucleotide polymorphism; T-UCR:transcribed ultra-conserved region; TNBC:Triple negative breast cancer; TSA: trichostatin A; UBC13:Ubiquitin conjugating enzyme E2 N; UCR: ultra-conserved region; VCR: vincristine; 5-FU: 5-fluorouracil

REFERENCES

[1] Yildirim, O.; Izgu, E. C.; Damle, M.; Chalei, V.; Ji, F.; Sadreyev, R. I.; Szostak, J. W.; Kingston, R. E. S-Phase Enriched Non-Coding RNAs Regulate Gene Expression and Cell Cycle Progression. *Cell Rep*, **2020**, *31* (6), 107629. https://doi.org/10.1016/j.celrep.2020.107629.

[2] Volinia, S.; Galasso, M.; Costinean, S.; Tagliavini, L.; Gamberoni, G.; Drusco, A.; Marchesini, J.; Mascellani, N.; Sana, M. E.; Abu Jarour, R.; et al. Reprogramming of MiRNA Networks in Cancer and Leukemia. *Genome Res.*, **2010**, *20* (5), 589–599. https://doi.org/10.1101/gr.098046.109.

[3] Bejerano, G.; Pheasant, M.; Makunin, I.; Stephen, S.; Kent, W. J.; Mattick, J. S.; Haussler, D. Ultraconserved Elements in the Human Genome. *Science*, **2004**, *304* (5675), 1321–1325. https://doi.org/10.1126/science.1098119.

[4] Mestdagh, P.; Fredlund, E.; Pattyn, F.; Rihani, A.; Van Maerken, T.; Vermeulen, J.; Kumps, C.; Menten, B.; De Preter, K.; Schramm, A.; et al. An Integrative Genomics Screen Uncovers NcRNA T-UCR Functions in Neuroblastoma Tumours. *Oncogene*, **2010**, *29* (24), 3583–3592. https://doi.org/10.1038/onc.2010.106.

[5] Wojcik, S. E.; Rossi, S.; Shimizu, M.; Nicoloso, M. S.; Cimmino, A.; Alder, H.; Herlea, V.; Rassenti, L. Z.; Rai, K. R.; Kipps, T. J.; et al. Non-CodingRNA Sequence Variations in Human Chronic Lymphocytic Leukemia and Colorectal Cancer. *Carcinogenesis*, **2010**, *31* (2), 208–215. https://doi.org/10.1093/carcin/bgp209.

[6] Calin, G. A.; Liu, C.; Ferracin, M.; Hyslop, T.; Spizzo, R.; Sevignani, C.; Fabbri, M.; Cimmino, A.; Lee, E. J.; Wojcik, S. E.; et al. Ultraconserved Regions Encoding NcRNAs Are Altered in Human Leukemias and Carcinomas. *Cancer Cell*, **2007**, *12* (3), 215–229. https://doi.org/10.1016/j.ccr.2007.07.027.

[7] Takahashi, K.; Yan, I.; Haga, H.; Patel, T. Long Noncoding RNA in Liver Diseases. *Hepatology*, **2014**, *60* (2), 744–753. https://doi.org/10.1002/hep.27043.

[8] Galasso, M.; Dama, P.; Previati, M.; Sandhu, S.; Palatini, J.; Coppola, V.; Warner, S.; Sana, M. E.; Zanella, R.; Abujarour, R.; et al. A Large Scale Expression Study Associates Uc.283-plus LncRNA with Pluripotent Stem Cells and Human Glioma. *Genome Med*, **2014**, *6* (10), 76. https://doi.org/10.1186/s13073-014-0076-4.

[9] Scaruffi, P.; Stigliani, S.; Moretti, S.; Coco, S.; De Vecchi, C.; Valdora, F.; Garaventa, A.; Bonassi, S.; Tonini, G. P. Transcribed-Ultra Conserved Region Expression Is Associated with Outcome in High-Risk Neuroblastoma. *BMC Cancer*, **2009**, *9*, 441. https://doi.org/10.1186/1471-2407-9-441.

[10] Esteller, M. Non-Coding RNAs in Human Disease. *Nat Rev Genet*, **2011**, *12* (12), 861–874. https://doi.org/10.1038/nrg3074.

[11] Ni, J. Z.; Grate, L.; Donohue, J. P.; Preston, C.; Nobida, N.; O'Brien, G.; Shiue, L.; Clark, T. A.; Blume, J. E.; Ares, M. Ultraconserved Elements Are Associated with Homeostatic Control of

Splicing Regulators by Alternative Splicing and Nonsense-Mediated Decay. *Genes Dev*, **2007**, *21* (6), 708–718. https://doi.org/10.1101/gad.1525507.
[12] Pauli, A.; Rinn, J. L.; Schier, A. F. Non-Coding RNAs as Regulators of Embryogenesis. *Nat Rev Genet*, **2011**, *12* (2), 136–149. https://doi.org/10.1038/nrg2904.
[13] Kapranov, P.; Cheng, J.; Dike, S.; Nix, D. A.; Duttagupta, R.; Willingham, A. T.; Stadler, P. F.; Hertel, J.; Hackermüller, J.; Hofacker, I. L.; et al. RNA Maps Reveal New RNA Classes and a Possible Function for Pervasive Transcription. *Science*, **2007**, *316* (5830), 1484–1488. https://doi.org/10.1126/science.1138341.
[14] Katayama, S.; Tomaru, Y.; Kasukawa, T.; Waki, K.; Nakanishi, M.; Nakamura, M.; Nishida, H.; Yap, C. C.; Suzuki, M.; Kawai, J.; et al. Antisense Transcription in the Mammalian Transcriptome. *Science*, **2005**, *309* (5740), 1564–1566. https://doi.org/10.1126/science.1112009.
[15] Mercer, T. R.; Dinger, M. E.; Mattick, J. S. Long Non-Coding RNAs: Insights into Functions. *Nat Rev Genet*, **2009**, *10* (3), 155–159. https://doi.org/10.1038/nrg2521.
[16] Kretz, M.; Siprashvili, Z.; Chu, C.; Webster, D. E.; Zehnder, A.; Qu, K.; Lee, C. S.; Flockhart, R. J.; Groff, A. F.; Chow, J.; et al. Control of Somatic Tissue Differentiation by the Long Non-Coding RNA TINCR. *Nature*, **2013**, *493* (7431), 231–235. https://doi.org/10.1038/nature11661.
[17] Pilyugin, M.; Irminger-Finger, I. Long Non-Coding RNA and MicroRNAs Might Act in Regulating the Expression of BARD1 MRNAs. *Int J Biochem Cell Biol*, **2014**, *54*, 356–367. https://doi.org/10.1016/j.biocel.2014.06.018.
[18] Gibb, E. A.; Brown, C. J.; Lam, W. L. The Functional Role of Long Non-Coding RNA in Human Carcinomas. *Mol Cancer*, **2011**, *10*, 38. https://doi.org/10.1186/1476-4598-10-38.
[19] Wapinski, O.; Chang, H. Y. Long Noncoding RNAs and Human Disease. *Trends Cell Biol*, **2011**, *21* (6), 354–361. https://doi.org/10.1016/j.tcb.2011.04.001.
[20] Sana, J.; Hankeova, S.; Svoboda, M.; Kiss, I.; Vyzula, R.; Slaby, O. Expression Levels of Transcribed Ultraconserved Regions Uc.73 and Uc.388 Are Altered in Colorectal Cancer. *Oncology*, **2012**, *82* (2), 114–118. https://doi.org/10.1159/000336479.
[21] Huarte, M. The Emerging Role of LncRNAs in Cancer. *Nat Med*, **2015**, *21* (11), 1253–1261. https://doi.org/10.1038/nm.3981.
[22] Volinia, S.; Calin, G. A.; Liu, C.-G.; Ambs, S.; Cimmino, A.; Petrocca, F.; Visone, R.; Iorio, M.; Roldo, C.; Ferracin, M.; et al. A MicroRNA Expression Signature of Human Solid Tumors Defines Cancer Gene Targets. *Proc. Natl. Acad. Sci. U.S.A.*, **2006**, *103* (7), 2257–2261. https://doi.org/10.1073/pnas.0510565103.
[23] Kristensen, L. S.; Hansen, T. B.; Venø, M. T.; Kjems, J. Circular RNAs in Cancer: Opportunities and Challenges in the Field. *Oncogene*, **2018**, *37* (5), 555–565. https://doi.org/10.1038/onc.2017.361.
[24] Sanger, H. L.; Klotz, G.; Riesner, D.; Gross, H. J.; Kleinschmidt, A. K. Viroids Are Single-Stranded Covalently Closed Circular RNA Molecules Existing as Highly Base-Paired Rod-like Structures. *PNAS*, **1976**, *73* (11), 3852–3856. https://doi.org/10.1073/pnas.73.11.3852.
[25] Memczak, S.; Jens, M.; Elefsinioti, A.; Torti, F.; Krueger, J.; Rybak, A.; Maier, L.; Mackowiak, S. D.; Gregersen, L. H.; Munschauer, M.; et al. Circular RNAs Are a Large Class of Animal RNAs with Regulatory Potency. *Nature*, **2013**, *495* (7441), 333–338. https://doi.org/10.1038/nature11928.
[26] Guo, J. U.; Agarwal, V.; Guo, H.; Bartel, D. P. Expanded Identification and Characterization of Mammalian Circular RNAs. *Genome Biol.*, **2014**, *15* (7), 409. https://doi.org/10.1186/s13059-014-0409-z.
[27] Smid, M.; Wilting, S.; Uhr, K.; Rodriguez-Gonzalez, G.; Weerd, V. de; Smissen, W. P.-V. der; Vlugt -Daane, M. van der; Galen, A. van; Nik-Zainal, S.; Butler, A.; et al. The Circular RNome of Primary Breast Cancer. *Genome Res.*, **2019**, gr.238121.118. https://doi.org/10.1101/gr.238121.118.

[28] Vo, J. N.; Cieslik, M.; Zhang, Y.; Shukla, S.; Xiao, L.; Zhang, Y.; Wu, Y.-M.; Dhanasekaran, S. M.; Engelke, C. G.; Cao, X.; et al. The Landscape of Circular RNA in Cancer. *Cell*, **2019**, *176* (4), 869-881.e13. https://doi.org/10.1016/j.cell.2018.12.021.

[29] Papaioannou, D.; Volinia, S.; Nicolet, D.; Świerniak, M.; Petri, A.; Mrózek, K.; Bill, M.; Pepe, F.; Walker, C. J.; Walker, A. E.; et al. Clinical and Functional Significance of Circular RNAs in Cytogenetically Normal AML. *Blood Adv*, **2020**, *4* (2), 239–251. https://doi.org/10.1182/bloodadvances.2019000568.

[30] Qu, S.; Yang, X.; Li, X.; Wang, J.; Gao, Y.; Shang, R.; Sun, W.; Dou, K.; Li, H. Circular RNA: A New Star of Noncoding RNAs. *Cancer Lett.*, **2015**, *365* (2), 141–148. https://doi.org/10.1016/j.canlet.2015.06.003.

[31] Abe, N.; Matsumoto, K.; Nishihara, M.; Nakano, Y.; Shibata, A.; Maruyama, H.; Shuto, S.; Matsuda, A.; Yoshida, M.; Ito, Y.; et al. Rolling Circle Translation of Circular RNA in Living Human Cells. *Sci Rep*, **2015**, *5*, 16435. https://doi.org/10.1038/srep16435.

[32] Chen, L.; Huang, C.; Wang, X.; Shan, G. Circular RNAs in Eukaryotic Cells. *Curr Genomics*, **2015**, *16* (5), 312–318. https://doi.org/10.2174/1389202916666150707161554.

[33] Chen, X.; Han, P.; Zhou, T.; Guo, X.; Song, X.; Li, Y. CircRNADb: A Comprehensive Database for Human Circular RNAs with Protein-Coding Annotations. *Sci Rep*, **2016**, *6* (1), 1–6. https://doi.org/10.1038/srep34985.

[34] Wawrzyniak, O.; Zarębska, Ż.; Kuczyński, K.; Gotz-Więckowska, A.; Rolle, K. Protein-Related Circular RNAs in Human Pathologies. *Cells*, **2020**, *9* (8). https://doi.org/10.3390/cells9081841.

[35] Yang, Y.; Gao, X.; Zhang, M.; Yan, S.; Sun, C.; Xiao, F.; Huang, N.; Yang, X.; Zhao, K.; Zhou, H.; et al. Novel Role of FBXW7 Circular RNA in Repressing Glioma Tumorigenesis. *J Natl Cancer Inst*, **2017**, *110* (3), 304–315. https://doi.org/10.1093/jnci/djx166.

[36] Zhang, M.; Zhao, K.; Xu, X.; Yang, Y.; Yan, S.; Wei, P.; Liu, H.; Xu, J.; Xiao, F.; Zhou, H.; et al. A Peptide Encoded by Circular Form of LINC-PINT Suppresses Oncogenic Transcriptional Elongation in Glioblastoma. *Nature Communications*, **2018**, *9* (1), 4475. https://doi.org/10.1038/s41467-018-06862-2.

[37] Zhang, M.; Huang, N.; Yang, X.; Luo, J.; Yan, S.; Xiao, F.; Chen, W.; Gao, X.; Zhao, K.; Zhou, H.; et al. A Novel Protein Encoded by the Circular Form of the SHPRH Gene Suppresses Glioma Tumorigenesis. *Oncogene*, **2018**, *37* (13), 1805–1814. https://doi.org/10.1038/s41388-017-0019-9.

[38] Wu, P.; Mo, Y.; Peng, M.; Tang, T.; Zhong, Y.; Deng, X.; Xiong, F.; Guo, C.; Wu, X.; Li, Y.; et al. Emerging Role of Tumor-Related Functional Peptides Encoded by LncRNA and CircRNA. *Mol Cancer*, **2020**, *19* (1), 22. https://doi.org/10.1186/s12943-020-1147-3.

[39] Zhi, X.; Zhang, J.; Cheng, Z.; Bian, L.; Qin, J. CircLgr4 Drives Colorectal Tumorigenesis and Invasion through Lgr4-Targeting Peptide. *International Journal of Cancer*, *n/a* (n/a). https://doi.org/10.1002/ijc.32549.

[40] Mo, D.; Li, X.; Raabe, C. A.; Rozhdestvensky, T. S.; Skryabin, B. V.; Brosius, J. Circular RNA Encoded Amyloid Beta Peptides—A Novel Putative Player in Alzheimer's Disease. *Cells*, **2020**, *9* (10). https://doi.org/10.3390/cells9102196.

[41] Cieslik, M.; Chugh, R.; Wu, Y.-M.; Wu, M.; Brennan, C.; Lonigro, R.; Su, F.; Wang, R.; Siddiqui, J.; Mehra, R.; et al. The Use of Exome Capture RNA-Seq for Highly Degraded RNA with Application to Clinical Cancer Sequencing. *Genome Res*, **2015**, *25* (9), 1372–1381. https://doi.org/10.1101/gr.189621.115.

[42] Robinson, D.; Van Allen, E. M.; Wu, Y.-M.; Schultz, N.; Lonigro, R. J.; Mosquera, J.-M.; Montgomery, B.; Taplin, M.-E.; Pritchard, C. C.; Attard, G.; et al. Integrative Clinical Genomics of Advanced Prostate Cancer. *Cell*, **2015**, *161* (5), 1215–1228. https://doi.org/10.1016/j.cell.2015.05.001.

[43] Robinson, D. R.; Wu, Y.-M.; Lonigro, R. J.; Vats, P.; Cobain, E.; Everett, J.; Cao, X.; Rabban, E.; Kumar-Sinha, C.; Raymond, V.; et al. Integrative Clinical Genomics of Metastatic Cancer. *Nature*, **2017**, *548* (7667), 297–303. https://doi.org/10.1038/nature23306.

[44] Mody, R. J.; Wu, Y.-M.; Lonigro, R. J.; Cao, X.; Roychowdhury, S.; Vats, P.; Frank, K. M.; Prensner, J. R.; Asangani, I.; Palanisamy, N.; et al. Integrative Clinical Sequencing in the Management of Refractory or Relapsed Cancer in Youth. *JAMA*, **2015**, *314* (9), 913–925. https://doi.org/10.1001/jama.2015.10080.

[45] Desiere, F.; Deutsch, E. W.; King, N. L.; Nesvizhskii, A. I.; Mallick, P.; Eng, J.; Chen, S.; Eddes, J.; Loevenich, S. N.; Aebersold, R. The PeptideAtlas Project. *Nucleic Acids Research*, **2006**, *34* (suppl_1), D655–D658. https://doi.org/10.1093/nar/gkj040.

[46] Schwenk, J. M.; Omenn, G. S.; Sun, Z.; Campbell, D. S.; Baker, M. S.; Overall, C. M.; Aebersold, R.; Moritz, R. L.; Deutsch, E. W. The Human Plasma Proteome Draft of 2017: Building on the Human Plasma PeptideAtlas from Mass Spectrometry and Complementary Assays. *J Proteome Res*, **2017**, *16* (12), 4299–4310. https://doi.org/10.1021/acs.jproteome.7b00467.

[47] Brenner, S. E.; Chothia, C.; Hubbard, T. J. Assessing Sequence Comparison Methods with Reliable Structurally Identified Distant Evolutionary Relationships. *Proc Natl Acad Sci U S A*, **1998**, *95* (11), 6073–6078. https://doi.org/10.1073/pnas.95.11.6073.

[48] Mi, H.; Ebert, D.; Muruganujan, A.; Mills, C.; Albou, L.-P.; Mushayamaha, T.; Thomas, P. D. PANTHER Version 16: A Revised Family Classification, Tree-Based Classification Tool, Enhancer Regions and Extensive API. *Nucleic Acids Research*, **2021**, *49* (D1), D394–D403. https://doi.org/10.1093/nar/gkaa1106.

[49] Vo, J. N.; Cieslik, M.; Zhang, Y.; Shukla, S.; Xiao, L.; Zhang, Y.; Wu, Y.-M.; Dhanasekaran, S. M.; Engelke, C. G.; Cao, X.; et al. The Landscape of Circular RNA in Cancer. *Cell*, **2019**, *176* (4), 869-881.e13. https://doi.org/10.1016/j.cell.2018.12.021.

[50] Hansen, T. B.; Jensen, T. I.; Clausen, B. H.; Bramsen, J. B.; Finsen, B.; Damgaard, C. K.; Kjems, J. Natural RNA Circles Function as Efficient MicroRNA Sponges. *Nature*, **2013**, *495* (7441), 384–388. https://doi.org/10.1038/nature11993.

[51] Kulcheski, F. R.; Christoff, A. P.; Margis, R. Circular RNAs Are MiRNA Sponges and Can Be Used as a New Class of Biomarker. *Journal of Biotechnology*, **2016**, *238*, 42–51. https://doi.org/10.1016/j.jbiotec.2016.09.011.

[52] Li, J.; Sun, D.; Pu, W.; Wang, J.; Peng, Y. Circular RNAs in Cancer: Biogenesis, Function, and Clinical Significance. *Trends in Cancer*, **2020**, *6* (4), 319–336. https://doi.org/10.1016/j.trecan.2020.01.012.

[53] Fischer, J. W.; Leung, A. K. L. CircRNAs: A Regulator of Cellular Stress. *Critical Reviews in Biochemistry and Molecular Biology*, **2017**, *52* (2), 220–233. https://doi.org/10.1080/10409238.2016.1276882.

[54] Pamudurti, N. R.; Bartok, O.; Jens, M.; Ashwal-Fluss, R.; Stottmeister, C.; Ruhe, L.; Hanan, M.; Wyler, E.; Perez-Hernandez, D.; Ramberger, E.; et al. Translation of CircRNAs. *Mol Cell*, **2017**, *66* (1), 9-21.e7. https://doi.org/10.1016/j.molcel.2017.02.021.

[55] Wesselhoeft, R. A.; Kowalski, P. S.; Anderson, D. G. Engineering Circular RNA for Potent and Stable Translation in Eukaryotic Cells. *Nature Communications*, **2018**, *9* (1), 2629. https://doi.org/10.1038/s41467-018-05096-6.

[56] Legnini, I.; Di Timoteo, G.; Rossi, F.; Morlando, M.; Briganti, F.; Sthandier, O.; Fatica, A.; Santini, T.; Andronache, A.; Wade, M.; et al. Circ-ZNF609 Is a Circular RNA That Can Be Translated and Functions in Myogenesis. *Mol Cell*, **2017**, *66* (1), 22-37.e9. https://doi.org/10.1016/j.molcel.2017.02.017.

[57] Liang, W.-C.; Wong, C.-W.; Liang, P.-P.; Shi, M.; Cao, Y.; Rao, S.-T.; Tsui, S. K.-W.; Waye, M. M.-Y.; Zhang, Q.; Fu, W.-M.; et al. Translation of the Circular RNA Circβ-Catenin Promotes Liver Cancer Cell Growth through Activation of the Wnt Pathway. *Genome Biology*, **2019**, *20* (1), 84. https://doi.org/10.1186/s13059-019-1685-4.

[58] Ye, F.; Gao, G.; Zou, Y.; Zheng, S.; Zhang, L.; Ou, X.; Xie, X.; Tang, H. CircFBXW7 Inhibits Malignant Progression by Sponging MiR-197-3p and Encoding a 185-Aa Protein in Triple-Negative Breast Cancer. *Molecular Therapy - Nucleic Acids*, **2019**, *18*, 88–98. https://doi.org/10.1016/j.omtn.2019.07.023.

[59] Pineau, P.; Volinia, S.; McJunkin, K.; Marchio, A.; Battiston, C.; Terris, B.; Mazzaferro, V.; Lowe, S. W.; Croce, C. M.; Dejean, A. MiR-221 Overexpression Contributes to Liver Tumorigenesis. *Proc Natl Acad Sci U S A*, **2010**, *107* (1), 264–269. https://doi.org/10.1073/pnas.0907904107.

[60] Li, Y.; Liang, C.; Ma, H.; Zhao, Q.; Lu, Y.; Xiang, Z.; Li, L.; Qin, J.; Chen, Y.; Cho, W. C.; et al. MiR-221/222 Promotes S-Phase Entry and Cellular Migration in Control of Basal-like Breast Cancer. *Molecules*, **2014**, *19* (6), 7122–7137. https://doi.org/10.3390/molecules19067122.

[61] Corrà, F.; Crudele, F.; Baldassari, F.; Bianchi, N.; Galasso, M.; Minotti, L.; Agnoletto, C.; Di Leva, G.; Brugnoli, F.; Reali, E.; et al. UC.183, UC.110, and UC.84 Ultra-Conserved RNAs Are Mutually Exclusive with MiR-221 and Are Engaged in the Cell Cycle Circuitry in Breast Cancer Cell Lines. *Genes (Basel)*, **2021**, *12* (12), 1978. https://doi.org/10.3390/genes12121978.

[62] Speed, T. Mathematics. A Correlation for the 21st Century. *Science*, **2011**, *334* (6062), 1502–1503. https://doi.org/10.1126/science.1215894.

[63] Holliday, D. L.; Speirs, V. Choosing the Right Cell Line for Breast Cancer Research. *Breast Cancer Res*, **2011**, *13* (4), 1–7. https://doi.org/10.1186/bcr2889.

[64] Neve, R. M.; Chin, K.; Fridlyand, J.; Yeh, J.; Baehner, F. L.; Fevr, T.; Clark, L.; Bayani, N.; Coppe, J.-P.; Tong, F.; et al. A Collection of Breast Cancer Cell Lines for the Study of Functionally Distinct Cancer Subtypes. *Cancer Cell*, **2006**, *10* (6), 515–527. https://doi.org/10.1016/j.ccr.2006.10.008.

[65] Cardinali, B.; Castellani, L.; Fasanaro, P.; Basso, A.; Alemà, S.; Martelli, F.; Falcone, G. Microrna-221 and Microrna-222 Modulate Differentiation and Maturation of Skeletal Muscle Cells. *PLoS One*, **2009**, *4* (10), e7607. https://doi.org/10.1371/journal.pone.0007607.

[66] Zagalak, J. A.; Menzi, M.; Schmich, F.; Jahns, H.; Dogar, A. M.; Wullschleger, F.; Towbin, H.; Hall, J. Properties of Short Double-Stranded RNAs Carrying Randomized Base Pairs: Toward Better Controls for RNAi Experiments. *RNA*, **2015**, *21* (12), 2132–2142. https://doi.org/10.1261/rna.053637.115.

[67] Hernández-Vargas, H.; Palacios, J.; Moreno-Bueno, G. Molecular Profiling of Docetaxel Cytotoxicity in Breast Cancer Cells: Uncoupling of Aberrant Mitosis and Apoptosis. *Oncogene*, **2007**, *26* (20), 2902–2913. https://doi.org/10.1038/sj.onc.1210102.

[68] Sim, S. H.; Bae, C.-D.; Kwon, Y.; Hwang, H.-L.; Poojan, S.; Hong, H.-I.; Kim, K.; Kang, S.-H.; Kim, H.-S.; Um, T.-H.; et al. CKAP2 (Cytoskeleton-Associated Protein2) Is a New Prognostic Marker in HER2-Negative Luminal Type Breast Cancer. *PLoS One*, **2017**, *12* (8), e0182107. https://doi.org/10.1371/journal.pone.0182107.

[69] Baldassari, F.; Zerbinati, C.; Galasso, M.; Corrà, F.; Minotti, L.; Agnoletto, C.; Previati, M.; Croce, C. M.; Volinia, S. Screen for MicroRNA and Drug Interactions in Breast Cancer Cell Lines Points to MiR-126 as a Modulator of CDK4/6 and PIK3CA Inhibitors. *Front Genet*, **2018**, *9*, 174. https://doi.org/10.3389/fgene.2018.00174.

[70] Wang, X. A PCR-Based Platform for MicroRNA Expression Profiling Studies. *RNA*, **2009**, *15* (4), 716–723. https://doi.org/10.1261/rna.1460509.

[71] Song, L.; Langfelder, P.; Horvath, S. Comparison of Co-Expression Measures: Mutual Information, Correlation, and Model Based Indices. *BMC Bioinformatics*, **2012**, *13*, 328. https://doi.org/10.1186/1471-2105-13-328.

[72] Llopis, S.; Singleton, B.; Duplessis, T.; Carrier, L.; Rowan, B.; Williams, C. Dichotomous Roles for the Orphan Nuclear Receptor NURR1 in Breast Cancer. *BMC Cancer*, **2013**, *13*, 139. https://doi.org/10.1186/1471-2407-13-139.

[73] Scaruffi, P. The Transcribed-Ultraconserved Regions: A Novel Class of Long Noncoding RNAs Involved in Cancer Susceptibility https://www.hindawi.com/journals/tswj/2011/192193/ (accessed Sep 24, 2020). https://doi.org/10.1100/tsw.2011.35.

[74] Wang, L.; Feng, W.; Yang, X.; Yang, F.; Wang, R.; Ren, Q.; Zhu, X.; Zheng, G. Fbxw11 Promotes the Proliferation of Lymphocytic Leukemia Cells through the Concomitant Activation of NF-KB and β-Catenin/TCF Signaling Pathways. *Cell Death Dis*, **2018**, *9* (4), 427. https://doi.org/10.1038/s41419-018-0440-1.

[75] Chang, H.; Liu, Y.-H.; Wang, L.-L.; Wang, J.; Zhao, Z.-H.; Qu, J.-F.; Wang, S.-F. MiR-182 Promotes Cell Proliferation by Suppressing FBXW7 and FBXW11 in Non-Small Cell Lung Cancer. *Am J Transl Res*, **2018**, *10* (4), 1131–1142.

[76] Zheng, N.; Wang, Z.; Wei, W. Ubiquitination-Mediated Degradation of Cell Cycle-Related Proteins by F-Box Proteins. *Int. J. Biochem. Cell Biol.*, **2016**, *73*, 99–110. https://doi.org/10.1016/j.biocel.2016.02.005.

[77] Wang, Z.; Liu, P.; Inuzuka, H.; Wei, W. Roles of F-Box Proteins in Cancer. *Nat. Rev. Cancer*, **2014**, *14* (4), 233–247. https://doi.org/10.1038/nrc3700.

[78] Makowski, A. M.; Dutnall, R. N.; Annunziato, A. T. Effects of Acetylation of Histone H4 at Lysines 8 and 16 on Activity of the Hat1 Histone Acetyltransferase. *J. Biol. Chem.*, **2001**, *276* (47), 43499–43502. https://doi.org/10.1074/jbc.C100549200.

[79] Pogribny, I. P.; Tryndyak, V. P.; Muskhelishvili, L.; Rusyn, I.; Ross, S. A. Methyl Deficiency, Alterations in Global Histone Modifications, and Carcinogenesis. *J. Nutr.*, **2007**, *137* (1 Suppl), 216S-222S. https://doi.org/10.1093/jn/137.1.216S.

[80] Gruber, J. J.; Geller, B.; Lipchik, A. M.; Chen, J.; Salahudeen, A. A.; Ram, A. N.; Ford, J. M.; Kuo, C. J.; Snyder, M. P. HAT1 Coordinates Histone Production and Acetylation via H4 Promoter Binding. *Molecular Cell*, **2019**, *75* (4), 711-724.e5. https://doi.org/10.1016/j.molcel.2019.05.034.

[81] Xue, L.; Hou, J.; Wang, Q.; Yao, L.; Xu, S.; Ge, D. RNAi Screening Identifies HAT1 as a Potential Drug Target in Esophageal Squamous Cell Carcinoma. *Int J Clin Exp Pathol*, **2014**, *7* (7), 3898–3907.

[82] Liu, W.; Wang, X. Prediction of Functional MicroRNA Targets by Integrative Modeling of MicroRNA Binding and Target Expression Data. *Genome Biol*, **2019**, *20* (1), 18. https://doi.org/10.1186/s13059-019-1629-z.

[83] Miranda, K. C.; Huynh, T.; Tay, Y.; Ang, Y.-S.; Tam, W.-L.; Thomson, A. M.; Lim, B.; Rigoutsos, I. A Pattern-Based Method for the Identification of MicroRNA Binding Sites and Their Corresponding Heteroduplexes. *Cell*, **2006**, *126* (6), 1203–1217. https://doi.org/10.1016/j.cell.2006.07.031.

[84] Kertesz, M.; Iovino, N.; Unnerstall, U.; Gaul, U.; Segal, E. The Role of Site Accessibility in MicroRNA Target Recognition. *Nature Genetics*, **2007**, *39* (10), 1278–1284. https://doi.org/10.1038/ng2135.

[85] Zhang, Q.; Yin, X.; Zhang, Y. MicroRNA-221 Promotes Cell Proliferation and Inhibits Apoptosis in Osteosarcoma Cells by Directly Targeting FBXW11 and Regulating Wnt Signaling. *Archives of Medical Research*, **2021**, *52* (2), 191–199. https://doi.org/10.1016/j.arcmed.2020.10.017.

[86] Wu, X.; Huang, J.; Yang, Z.; Zhu, Y.; Zhang, Y.; Wang, J.; Yao, W. MicroRNA-221-3p Is Related to Survival and Promotes Tumour Progression in Pancreatic Cancer: A Comprehensive Study on Functions and Clinicopathological Value. *Cancer Cell Int*, **2020**, *20*, 443. https://doi.org/10.1186/s12935-020-01529-9.

[87] Zhou, Y.; Richards, A. M.; Wang, P. MicroRNA-221 Is Cardioprotective and Anti-Fibrotic in a Rat Model of Myocardial Infarction. *Mol Ther Nucleic Acids*, **2019**, *17*, 185–197. https://doi.org/10.1016/j.omtn.2019.05.018.

[88] Linck-Paulus, L.; Hellerbrand, C.; Bosserhoff, A. K.; Dietrich, P. Dissimilar Appearances Are Deceptive–Common MicroRNAs and Therapeutic Strategies in Liver Cancer and Melanoma. *Cells*, **2020**, *9* (1), 114. https://doi.org/10.3390/cells9010114.

[89] Jiang, C.-Y.; Gao, Y.; Wang, X.-J.; Ruan, Y.; Bei, X.-Y.; Wang, X.-H.; Jing, Y.-F.; Zhao, W.; Jiang, Q.; Li, J.; et al. Long Non-Coding RNA Lnc-MX1-1 Is Associated with Poor Clinical Features and Promotes Cellular Proliferation and Invasiveness in Prostate Cancer. *Biochem Biophys Res Commun*, **2016**, *470* (3), 721–727. https://doi.org/10.1016/j.bbrc.2016.01.056.

[90] Su, X.; Malouf, G. G.; Chen, Y.; Zhang, J.; Yao, H.; Valero, V.; Weinstein, J. N.; Spano, J.-P.; Meric-Bernstam, F.; Khayat, D.; et al. Comprehensive Analysis of Long Non-Coding RNAs in Human Breast Cancer Clinical Subtypes. *Oncotarget*, **2014**, *5* (20), 9864–9876. https://doi.org/10.18632/oncotarget.2454.

[91] Vannini, I.; Wise, P. M.; Challagundla, K. B.; Plousiou, M.; Raffini, M.; Bandini, E.; Fanini, F.; Paliaga, G.; Crawford, M.; Ferracin, M.; et al. Transcribed Ultraconserved Region 339 Promotes Carcinogenesis by Modulating Tumor Suppressor MicroRNAs. *Nat Commun*, **2017**, *8* (1), 1801. https://doi.org/10.1038/s41467-017-01562-9.

[92] Garofalo, M.; Quintavalle, C.; Romano, G.; Croce, C. M.; Condorelli, G. MiR221/222 in Cancer: Their Role in Tumor Progression and Response to Therapy. *Curr Mol Med*, **2012**, *12* (1), 27–33. https://doi.org/10.2174/156652412798376170.

[93] LoPiccolo, J.; Blumenthal, G. M.; Bernstein, W. B.; Dennis, P. A. Targeting the PI3K/Akt/MTOR Pathway: Effective Combinations and Clinical Considerations. *Drug Resist. Updat.*, **2008**, *11* (1–2), 32–50. https://doi.org/10.1016/j.drup.2007.11.003.

[94] Jiang, W.; He, T.; Liu, S.; Zheng, Y.; Xiang, L.; Pei, X.; Wang, Z.; Yang, H. The PIK3CA E542K and E545K Mutations Promote Glycolysis and Proliferation via Induction of the β-Catenin/SIRT3 Signaling Pathway in Cervical Cancer. *J Hematol Oncol*, **2018**, *11* (1), 139. https://doi.org/10.1186/s13045-018-0674-5.

[95] Crudele, F.; Bianchi, N.; Reali, E.; Galasso, M.; Agnoletto, C.; Volinia, S. The Network of Non-Coding RNAs and Their Molecular Targets in Breast Cancer. *Mol Cancer*, **2020**, *19* (1), 61. https://doi.org/10.1186/s12943-020-01181-x.

[96] Lu, Z.; Jiao, D.; Qiao, J.; Yang, S.; Yan, M.; Cui, S.; Liu, Z. Restin Suppressed Epithelial-Mesenchymal Transition and Tumor Metastasis in Breast Cancer Cells through Upregulating Mir-200a/b Expression via Association with P73. *Molecular Cancer*, **2015**, *14* (1), 102. https://doi.org/10.1186/s12943-015-0370-9.

[97] Humphries, B.; Wang, Z.; Li, Y.; Jhan, J.-R.; Jiang, Y.; Yang, C. ARHGAP18 Downregulation by MiR-200b Suppresses Metastasis of Triple-Negative Breast Cancer by Enhancing Activation of RhoA. *Cancer Res.*, **2017**, *77* (15), 4051–4064. https://doi.org/10.1158/0008-5472.CAN-16-3141.

[98] Chang, C.-C.; Wu, M.-J.; Yang, J.-Y.; Camarillo, I. G.; Chang, C.-J. Leptin-STAT3-G9a Signaling Promotes Obesity-Mediated Breast Cancer Progression. *Cancer Res.*, **2015**, *75* (11), 2375–2386. https://doi.org/10.1158/0008-5472.CAN-14-3076.

[99] Dang, T. T.; Esparza, M. A.; Maine, E. A.; Westcott, J. M.; Pearson, G. W. ΔNp63α Promotes Breast Cancer Cell Motility through the Selective Activation of Components of the Epithelial-to-Mesenchymal Transition Program. *Cancer Res.*, **2015**, *75* (18), 3925–3935. https://doi.org/10.1158/0008-5472.CAN-14-3363.

[100] Zhang, P.; Wang, L.; Rodriguez-Aguayo, C.; Yuan, Y.; Debeb, B. G.; Chen, D.; Sun, Y.; You, M. J.; Liu, Y.; Dean, D. C.; et al. MiR-205 Acts as a Tumour Radiosensitizer by Targeting ZEB1 and Ubc13. *Nat Commun*, **2014**, *5*, 5671. https://doi.org/10.1038/ncomms6671.

[101] Le, M. T. N.; Hamar, P.; Guo, C.; Basar, E.; Perdigão-Henriques, R.; Balaj, L.; Lieberman, J. MiR-200-Containing Extracellular Vesicles Promote Breast Cancer Cell Metastasis. *J. Clin. Invest.*, **2014**, *124* (12), 5109–5128. https://doi.org/10.1172/JCI75695.

[102] Croset, M.; Pantano, F.; Kan, C. W. S.; Bonnelye, E.; Descotes, F.; Alix-Panabières, C.; Lecellier, C.-H.; Bachelier, R.; Allioli, N.; Hong, S.-S.; et al. MiRNA-30 Family Members Inhibit

Breast Cancer Invasion, Osteomimicry, and Bone Destruction by Directly Targeting Multiple Bone Metastasis-Associated Genes. *Cancer Res.*, **2018**, *78* (18), 5259–5273. https://doi.org/10.1158/0008-5472.CAN-17-3058.

[103] di Gennaro, A.; Damiano, V.; Brisotto, G.; Armellin, M.; Perin, T.; Zucchetto, A.; Guardascione, M.; Spaink, H. P.; Doglioni, C.; Snaar-Jagalska, B. E.; et al. A P53/MiR-30a/ZEB2 Axis Controls Triple Negative Breast Cancer Aggressiveness. *Cell Death Differ.*, **2018**, *25* (12), 2165–2180. https://doi.org/10.1038/s41418-018-0103-x.

[104] Furuta, S.; Ren, G.; Mao, J.-H.; Bissell, M. J. Laminin Signals Initiate the Reciprocal Loop That Informs Breast-Specific Gene Expression and Homeostasis by Activating NO, P53 and MicroRNAs. *Elife*, **2018**, *7*. https://doi.org/10.7554/eLife.26148.

[105] Li, Y.; Kuscu, C.; Banach, A.; Zhang, Q.; Pulkoski-Gross, A.; Kim, D.; Liu, J.; Roth, E.; Li, E.; Shroyer, K. R.; et al. MiR-181a-5p Inhibits Cancer Cell Migration and Angiogenesis via Downregulation of Matrix Metalloproteinase-14. *Cancer Res.*, **2015**, *75* (13), 2674–2685. https://doi.org/10.1158/0008-5472.CAN-14-2875.

[106] Liu, K.; Xie, F.; Gao, A.; Zhang, R.; Zhang, L.; Xiao, Z.; Hu, Q.; Huang, W.; Huang, Q.; Lin, B.; et al. SOX2 Regulates Multiple Malignant Processes of Breast Cancer Development through the SOX2/MiR-181a-5p, MiR-30e-5p/TUSC3 Axis. *Mol. Cancer*, **2017**, *16* (1), 62. https://doi.org/10.1186/s12943-017-0632-9.

[107] D'Ippolito, E.; Plantamura, I.; Bongiovanni, L.; Casalini, P.; Baroni, S.; Piovan, C.; Orlandi, R.; Gualeni, A. V.; Gloghini, A.; Rossini, A.; et al. MiR-9 and MiR-200 Regulate PDGFRβ-Mediated Endothelial Differentiation of Tumor Cells in Triple-Negative Breast Cancer. *Cancer Res.*, **2016**, *76* (18), 5562–5572. https://doi.org/10.1158/0008-5472.CAN-16-0140.

[108] Shen, M.; Dong, C.; Ruan, X.; Yan, W.; Cao, M.; Pizzo, D.; Wu, X.; Yang, L.; Liu, L.; Ren, X.; et al. Chemotherapy-Induced Extracellular Vesicle MiRNAs Promote Breast Cancer Stemness by Targeting ONECUT2. *Cancer Res.*, **2019**, *79* (14), 3608–3621. https://doi.org/10.1158/0008-5472.CAN-18-4055.

[109] Taipaleenmäki, H.; Browne, G.; Akech, J.; Zustin, J.; van Wijnen, A. J.; Stein, J. L.; Hesse, E.; Stein, G. S.; Lian, J. B. Targeting of Runx2 by MiR-135 and MiR-203 Impairs Progression of Breast Cancer and Metastatic Bone Disease. *Cancer Res.*, **2015**, *75* (7), 1433–1444. https://doi.org/10.1158/0008-5472.CAN-14-1026.

[110] Li, G.-Y.; Wang, W.; Sun, J.-Y.; Xin, B.; Zhang, X.; Wang, T.; Zhang, Q.-F.; Yao, L.-B.; Han, H.; Fan, D.-M.; et al. Long Non-Coding RNAs AC026904.1 and UCA1: A "One-Two Punch" for TGF-β-Induced SNAI2 Activation and Epithelial-Mesenchymal Transition in Breast Cancer. *Theranostics*, **2018**, *8* (10), 2846–2861. https://doi.org/10.7150/thno.23463.

[111] Zhou, Y.; Meng, X.; Chen, S.; Li, W.; Li, D.; Singer, R.; Gu, W. IMP1 Regulates UCA1-Mediated Cell Invasion through Facilitating UCA1 Decay and Decreasing the Sponge Effect of UCA1 for MiR-122-5p. *Breast Cancer Res.*, **2018**, *20* (1), 32. https://doi.org/10.1186/s13058-018-0959-1.

[112] Zhang, J.; Sui, S.; Wu, H.; Zhang, J.; Zhang, X.; Xu, S.; Pang, D. The Transcriptional Landscape of LncRNAs Reveals the Oncogenic Function of LINC00511 in ER-Negative Breast Cancer. *Cell Death Dis*, **2019**, *10* (8), 599. https://doi.org/10.1038/s41419-019-1835-3.

[113] Ren, Y.; Wang, Y.-F.; Zhang, J.; Wang, Q.-X.; Han, L.; Mei, M.; Kang, C.-S. Targeted Design and Identification of AC1NOD4Q to Block Activity of HOTAIR by Abrogating the Scaffold Interaction with EZH2. *Clin Epigenetics*, **2019**, *11* (1), 29. https://doi.org/10.1186/s13148-019-0624-2.

[114] Lu, G.; Li, Y.; Ma, Y.; Lu, J.; Chen, Y.; Jiang, Q.; Qin, Q.; Zhao, L.; Huang, Q.; Luo, Z.; et al. Long Noncoding RNA LINC00511 Contributes to Breast Cancer Tumourigenesis and Stemness by Inducing the MiR-185-3p/E2F1/Nanog Axis. *J. Exp. Clin. Cancer Res.*, **2018**, *37* (1), 289. https://doi.org/10.1186/s13046-018-0945-6.

[115] Li, Y.; Wang, Z.; Shi, H.; Li, H.; Li, L.; Fang, R.; Cai, X.; Liu, B.; Zhang, X.; Ye, L. HBXIP and LSD1 Scaffolded by LncRNA Hotair Mediate Transcriptional Activation by C-Myc. *Cancer Res.*, **2016**, *76* (2), 293–304. https://doi.org/10.1158/0008-5472.CAN-14-3607.
[116] Li, M.; Li, X.; Zhuang, Y.; Flemington, E. K.; Lin, Z.; Shan, B. Induction of a Novel Isoform of the LncRNA HOTAIR in Claudin-Low Breast Cancer Cells Attached to Extracellular Matrix. *Mol Oncol*, **2017**, *11* (12), 1698–1710. https://doi.org/10.1002/1878-0261.12133.
[117] Peng, F.; Li, T.-T.; Wang, K.-L.; Xiao, G.-Q.; Wang, J.-H.; Zhao, H.-D.; Kang, Z.-J.; Fan, W.-J.; Zhu, L.-L.; Li, M.; et al. H19/Let-7/LIN28 Reciprocal Negative Regulatory Circuit Promotes Breast Cancer Stem Cell Maintenance. *Cell Death Dis*, **2017**, *8* (1), e2569. https://doi.org/10.1038/cddis.2016.438.
[118] Peng, F.; Wang, J.-H.; Fan, W.-J.; Meng, Y.-T.; Li, M.-M.; Li, T.-T.; Cui, B.; Wang, H.-F.; Zhao, Y.; An, F.; et al. Glycolysis Gatekeeper PDK1 Reprograms Breast Cancer Stem Cells under Hypoxia. *Oncogene*, **2018**, *37* (8), 1062–1074. https://doi.org/10.1038/onc.2017.368.
[119] Lin, A.; Li, C.; Xing, Z.; Hu, Q.; Liang, K.; Han, L.; Wang, C.; Hawke, D. H.; Wang, S.; Zhang, Y.; et al. The LINK-A LncRNA Activates Normoxic HIF1α Signalling in Triple-Negative Breast Cancer. *Nat. Cell Biol.*, **2016**, *18* (2), 213–224. https://doi.org/10.1038/ncb3295.
[120] Wang, J.; Xie, S.; Yang, J.; Xiong, H.; Jia, Y.; Zhou, Y.; Chen, Y.; Ying, X.; Chen, C.; Ye, C.; et al. The Long Noncoding RNA H19 Promotes Tamoxifen Resistance in Breast Cancer via Autophagy. *J Hematol Oncol*, **2019**, *12* (1), 81. https://doi.org/10.1186/s13045-019-0747-0.
[121] Lin, A.; Hu, Q.; Li, C.; Xing, Z.; Ma, G.; Wang, C.; Li, J.; Ye, Y.; Yao, J.; Liang, K.; et al. The LINK-A LncRNA Interacts with PtdIns(3,4,5)P3 to Hyperactivate AKT and Confer Resistance to AKT Inhibitors. *Nat. Cell Biol.*, **2017**, *19* (3), 238–251. https://doi.org/10.1038/ncb3473.
[122] Ingle, J. N.; Xie, F.; Ellis, M. J.; Goss, P. E.; Shepherd, L. E.; Chapman, J.-A. W.; Chen, B. E.; Kubo, M.; Furukawa, Y.; Momozawa, Y.; et al. Genetic Polymorphisms in the Long Noncoding RNA MIR2052HG Offer a Pharmacogenomic Basis for the Response of Breast Cancer Patients to Aromatase Inhibitor Therapy. *Cancer Res.*, **2016**, *76* (23), 7012–7023. https://doi.org/10.1158/0008-5472.CAN-16-1371.
[123] Cairns, J.; Ingle, J. N.; Kalari, K. R.; Shepherd, L. E.; Kubo, M.; Goetz, M. P.; Weinshilboum, R. M.; Wang, L. The LncRNA MIR2052HG Regulates ERα Levels and Aromatase Inhibitor Resistance through LMTK3 by Recruiting EGR1. *Breast Cancer Res.*, **2019**, *21* (1), 47. https://doi.org/10.1186/s13058-019-1130-3.
[124] Chen, H.; Pan, H.; Qian, Y.; Zhou, W.; Liu, X. MiR-25-3p Promotes the Proliferation of Triple Negative Breast Cancer by Targeting BTG2. *Mol. Cancer*, **2018**, *17* (1), 4. https://doi.org/10.1186/s12943-017-0754-0.
[125] Wu, M.-Z.; Cheng, W.-C.; Chen, S.-F.; Nieh, S.; O'Connor, C.; Liu, C.-L.; Tsai, W.-W.; Wu, C.-J.; Martin, L.; Lin, Y.-S.; et al. MiR-25/93 Mediates Hypoxia-Induced Immunosuppression by Repressing CGAS. *Nat. Cell Biol.*, **2017**, *19* (10), 1286–1296. https://doi.org/10.1038/ncb3615.
[126] Singh, R.; Pochampally, R.; Watabe, K.; Lu, Z.; Mo, Y.-Y. Exosome-Mediated Transfer of MiR-10b Promotes Cell Invasion in Breast Cancer. *Mol. Cancer*, **2014**, *13*, 256. https://doi.org/10.1186/1476-4598-13-256.
[127] Bahena-Ocampo, I.; Espinosa, M.; Ceballos-Cancino, G.; Lizarraga, F.; Campos-Arroyo, D.; Schwarz, A.; Maldonado, V.; Melendez-Zajgla, J.; Garcia-Lopez, P. MiR-10b Expression in Breast Cancer Stem Cells Supports Self-Renewal through Negative PTEN Regulation and Sustained AKT Activation. *EMBO Rep.*, **2016**, *17* (5), 648–658. https://doi.org/10.15252/embr.201540678.
[128] Yoo, B.; Kavishwar, A.; Ross, A.; Wang, P.; Tabassum, D. P.; Polyak, K.; Barteneva, N.; Petkova, V.; Pantazopoulos, P.; Tena, A.; et al. Combining MiR-10b-Targeted Nanotherapy with Low-Dose Doxorubicin Elicits Durable Regressions of Metastatic Breast Cancer. *Cancer Res.*, **2015**, *75* (20), 4407–4415. https://doi.org/10.1158/0008-5472.CAN-15-0888.

[129] Kim, J.; Siverly, A. N.; Chen, D.; Wang, M.; Yuan, Y.; Wang, Y.; Lee, H.; Zhang, J.; Muller, W. J.; Liang, H.; et al. Ablation of MiR-10b Suppresses Oncogene-Induced Mammary Tumorigenesis and Metastasis and Reactivates Tumor-Suppressive Pathways. *Cancer Res.*, **2016**, *76* (21), 6424–6435. https://doi.org/10.1158/0008-5472.CAN-16-1571.

[130] Tomita, S.; Abdalla, M. O. A.; Fujiwara, S.; Matsumori, H.; Maehara, K.; Ohkawa, Y.; Iwase, H.; Saitoh, N.; Nakao, M. A Cluster of Noncoding RNAs Activates the ESR1 Locus during Breast Cancer Adaptation. *Nat Commun*, **2015**, *6*, 6966. https://doi.org/10.1038/ncomms7966.

[131] Abdalla, M. O. A.; Yamamoto, T.; Maehara, K.; Nogami, J.; Ohkawa, Y.; Miura, H.; Poonperm, R.; Hiratani, I.; Nakayama, H.; Nakao, M.; et al. The Eleanor NcRNAs Activate the Topological Domain of the ESR1 Locus to Balance against Apoptosis. *Nat Commun*, **2019**, *10* (1), 3778. https://doi.org/10.1038/s41467-019-11378-4.

[132] Pruszko, M.; Milano, E.; Forcato, M.; Donzelli, S.; Ganci, F.; Di Agostino, S.; De Panfilis, S.; Fazi, F.; Bates, D. O.; Bicciato, S.; et al. The Mutant P53-ID4 Complex Controls VEGFA Isoforms by Recruiting LncRNA MALAT1. *EMBO Rep.*, **2017**, *18* (8), 1331–1351. https://doi.org/10.15252/embr.201643370.

[133] Ren, W.; Guan, W.; Zhang, J.; Wang, F.; Xu, G. Pyridoxine 5'-Phosphate Oxidase Is Correlated with Human Breast Invasive Ductal Carcinoma Development. *Aging (Albany NY)*, **2019**, *11* (7), 2151–2176. https://doi.org/10.18632/aging.101908.

[134] Kim, J.; Piao, H.-L.; Kim, B.-J.; Yao, F.; Han, Z.; Wang, Y.; Xiao, Z.; Siverly, A. N.; Lawhon, S. E.; Ton, B. N.; et al. Long Noncoding RNA MALAT1 Suppresses Breast Cancer Metastasis. *Nat. Genet.*, **2018**, *50* (12), 1705–1715. https://doi.org/10.1038/s41588-018-0252-3.

[135] Pakravan, K.; Babashah, S.; Sadeghizadeh, M.; Mowla, S. J.; Mossahebi-Mohammadi, M.; Ataei, F.; Dana, N.; Javan, M. MicroRNA-100 Shuttled by Mesenchymal Stem Cell-Derived Exosomes Suppresses in Vitro Angiogenesis through Modulating the MTOR/HIF-1α/VEGF Signaling Axis in Breast Cancer Cells. *Cell Oncol (Dordr)*, **2017**, *40* (5), 457–470. https://doi.org/10.1007/s13402-017-0335-7.

[136] Deng, L.; Shang, L.; Bai, S.; Chen, J.; He, X.; Martin-Trevino, R.; Chen, S.; Li, X.-Y.; Meng, X.; Yu, B.; et al. MicroRNA100 Inhibits Self-Renewal of Breast Cancer Stem-like Cells and Breast Tumor Development. *Cancer Res.*, **2014**, *74* (22), 6648–6660. https://doi.org/10.1158/0008-5472.CAN-13-3710.

[137] Li, X.; Xu, Y.; Ding, Y.; Li, C.; Zhao, H.; Wang, J.; Meng, S. Posttranscriptional Upregulation of HER3 by HER2 MRNA Induces Trastuzumab Resistance in Breast Cancer. *Mol. Cancer*, **2018**, *17* (1), 113. https://doi.org/10.1186/s12943-018-0862-5.

[138] Bailey, S. T.; Westerling, T.; Brown, M. Loss of Estrogen-Regulated MicroRNA Expression Increases HER2 Signaling and Is Prognostic of Poor Outcome in Luminal Breast Cancer. *Cancer Res.*, **2015**, *75* (2), 436–445. https://doi.org/10.1158/0008-5472.CAN-14-1041.

[139] Hsieh, T.-H.; Hsu, C.-Y.; Tsai, C.-F.; Long, C.-Y.; Wu, C.-H.; Wu, D.-C.; Lee, J.-N.; Chang, W.-C.; Tsai, E.-M. HDAC Inhibitors Target HDAC5, Upregulate MicroRNA-125a-5p, and Induce Apoptosis in Breast Cancer Cells. *Mol. Ther.*, **2015**, *23* (4), 656–666. https://doi.org/10.1038/mt.2014.247.

[140] Jin, K.; Park, S.; Teo, W. W.; Korangath, P.; Cho, S. S.; Yoshida, T.; Győrffy, B.; Goswami, C. P.; Nakshatri, H.; Cruz, L.-A.; et al. HOXB7 Is an ERα Cofactor in the Activation of HER2 and Multiple ER Target Genes Leading to Endocrine Resistance. *Cancer Discov*, **2015**, *5* (9), 944–959. https://doi.org/10.1158/2159-8290.CD-15-0090.

[141] Jiang, C.-F.; Shi, Z.-M.; Li, D.-M.; Qian, Y.-C.; Ren, Y.; Bai, X.-M.; Xie, Y.-X.; Wang, L.; Ge, X.; Liu, W.-T.; et al. Estrogen-Induced MiR-196a Elevation Promotes Tumor Growth and Metastasis via Targeting SPRED1 in Breast Cancer. *Mol. Cancer*, **2018**, *17* (1), 83. https://doi.org/10.1186/s12943-018-0830-0.

[142] Yu, J.; Lei, R.; Zhuang, X.; Li, X.; Li, G.; Lev, S.; Segura, M. F.; Zhang, X.; Hu, G. MicroRNA-182 Targets SMAD7 to Potentiate TGFβ-Induced Epithelial-Mesenchymal Transition and

Metastasis of Cancer Cells. *Nat Commun*, **2016**, *7*, 13884. https://doi.org/10.1038/ncomms13884.
[143] Velagapudi, S. P.; Cameron, M. D.; Haga, C. L.; Rosenberg, L. H.; Lafitte, M.; Duckett, D. R.; Phinney, D. G.; Disney, M. D. Design of a Small Molecule against an Oncogenic Noncoding RNA. *Proc. Natl. Acad. Sci. U.S.A.*, **2016**, *113* (21), 5898–5903. https://doi.org/10.1073/pnas.1523975113.
[144] Costales, M. G.; Matsumoto, Y.; Velagapudi, S. P.; Disney, M. D. Small Molecule Targeted Recruitment of a Nuclease to RNA. *J. Am. Chem. Soc.*, **2018**, *140* (22), 6741–6744. https://doi.org/10.1021/jacs.8b01233.
[145] Gilam, A.; Conde, J.; Weissglas-Volkov, D.; Oliva, N.; Friedman, E.; Artzi, N.; Shomron, N. Local MicroRNA Delivery Targets Palladin and Prevents Metastatic Breast Cancer. *Nat Commun*, **2016**, *7*, 12868. https://doi.org/10.1038/ncomms12868.
[146] Zhu, J.; Xiong, G.; Fu, H.; Evers, B. M.; Zhou, B. P.; Xu, R. Chaperone Hsp47 Drives Malignant Growth and Invasion by Modulating an ECM Gene Network. *Cancer Res.*, **2015**, *75* (8), 1580–1591. https://doi.org/10.1158/0008-5472.CAN-14-1027.
[147] Jia, J.; Shi, Y.; Chen, L.; Lai, W.; Yan, B.; Jiang, Y.; Xiao, D.; Xi, S.; Cao, Y.; Liu, S.; et al. Decrease in Lymphoid Specific Helicase and 5-Hydroxymethylcytosine Is Associated with Metastasis and Genome Instability. *Theranostics*, **2017**, *7* (16), 3920–3932. https://doi.org/10.7150/thno.21389.
[148] Zhao, H.; Wilkie, T.; Deol, Y.; Sneh, A.; Ganju, A.; Basree, M.; Nasser, M. W.; Ganju, R. K. MiR-29b Defines the pro-/Anti-Proliferative Effects of S100A7 in Breast Cancer. *Mol. Cancer*, **2015**, *14*, 11. https://doi.org/10.1186/s12943-014-0275-z.
[149] Müller, V.; Oliveira-Ferrer, L.; Steinbach, B.; Pantel, K.; Schwarzenbach, H. Interplay of LncRNA H19/MiR-675 and LncRNA NEAT1/MiR-204 in Breast Cancer. *Mol Oncol*, **2019**, *13* (5), 1137–1149. https://doi.org/10.1002/1878-0261.12472.
[150] Choudhry, H.; Albukhari, A.; Morotti, M.; Haider, S.; Moralli, D.; Smythies, J.; Schödel, J.; Green, C. M.; Camps, C.; Buffa, F.; et al. Tumor Hypoxia Induces Nuclear Paraspeckle Formation through HIF-2α Dependent Transcriptional Activation of NEAT1 Leading to Cancer Cell Survival. *Oncogene*, **2015**, *34* (34), 4482–4490. https://doi.org/10.1038/onc.2014.378.
[151] Li, W.; Zhang, Z.; Liu, X.; Cheng, X.; Zhang, Y.; Han, X.; Zhang, Y.; Liu, S.; Yang, J.; Xu, B.; et al. The FOXN3-NEAT1-SIN3A Repressor Complex Promotes Progression of Hormonally Responsive Breast Cancer. *J. Clin. Invest.*, **2017**, *127* (9), 3421–3440. https://doi.org/10.1172/JCI94233.
[152] Takahashi, R.; Miyazaki, H.; Takeshita, F.; Yamamoto, Y.; Minoura, K.; Ono, M.; Kodaira, M.; Tamura, K.; Mori, M.; Ochiya, T. Loss of MicroRNA-27b Contributes to Breast Cancer Stem Cell Generation by Activating ENPP1. *Nat Commun*, **2015**, *6*, 7318. https://doi.org/10.1038/ncomms8318.
[153] Eastlack, S. C.; Dong, S.; Ivan, C.; Alahari, S. K. Suppression of PDHX by MicroRNA-27b Deregulates Cell Metabolism and Promotes Growth in Breast Cancer. *Mol. Cancer*, **2018**, *17* (1), 100. https://doi.org/10.1186/s12943-018-0851-8.
[154] Hannafon, B. N.; Carpenter, K. J.; Berry, W. L.; Janknecht, R.; Dooley, W. C.; Ding, W.-Q. Exosome-Mediated MicroRNA Signaling from Breast Cancer Cells Is Altered by the Anti-Angiogenesis Agent Docosahexaenoic Acid (DHA). *Mol. Cancer*, **2015**, *14*, 133. https://doi.org/10.1186/s12943-015-0400-7.
[155] Bacci, M.; Lorito, N.; Ippolito, L.; Ramazzotti, M.; Luti, S.; Romagnoli, S.; Parri, M.; Bianchini, F.; Cappellesso, F.; Virga, F.; et al. Reprogramming of Amino Acid Transporters to Support Aspartate and Glutamate Dependency Sustains Endocrine Resistance in Breast Cancer. *Cell Rep*, **2019**, *28* (1), 104-118.e8. https://doi.org/10.1016/j.celrep.2019.06.010.

[156] Xing, Z.; Lin, A.; Li, C.; Liang, K.; Wang, S.; Liu, Y.; Park, P. K.; Qin, L.; Wei, Y.; Hawke, D. H.; et al. LncRNA Directs Cooperative Epigenetic Regulation Downstream of Chemokine Signals. *Cell*, **2014**, *159* (5), 1110–1125. https://doi.org/10.1016/j.cell.2014.10.013.
[157] Zheng, X.; Han, H.; Liu, G.-P.; Ma, Y.-X.; Pan, R.-L.; Sang, L.-J.; Li, R.-H.; Yang, L.-J.; Marks, J. R.; Wang, W.; et al. LncRNA Wires up Hippo and Hedgehog Signaling to Reprogramme Glucose Metabolism. *EMBO J.*, **2017**, *36* (22), 3325–3335. https://doi.org/10.15252/embj.201797609.
[158] Adams, B. D.; Wali, V. B.; Cheng, C. J.; Inukai, S.; Booth, C. J.; Agarwal, S.; Rimm, D. L.; Győrffy, B.; Santarpia, L.; Pusztai, L.; et al. MiR-34a Silences c-SRC to Attenuate Tumor Growth in Triple-Negative Breast Cancer. *Cancer Res.*, **2016**, *76* (4), 927–939. https://doi.org/10.1158/0008-5472.CAN-15-2321.
[159] Ito, Y.; Inoue, A.; Seers, T.; Hato, Y.; Igarashi, A.; Toyama, T.; Taganov, K. D.; Boldin, M. P.; Asahara, H. Identification of Targets of Tumor Suppressor MicroRNA-34a Using a Reporter Library System. *Proc. Natl. Acad. Sci. U.S.A.*, **2017**, *114* (15), 3927–3932. https://doi.org/10.1073/pnas.1620019114.
[160] Weng, Y.-S.; Tseng, H.-Y.; Chen, Y.-A.; Shen, P.-C.; Al Haq, A. T.; Chen, L.-M.; Tung, Y.-C.; Hsu, H.-L. MCT-1/MiR-34a/IL-6/IL-6R Signaling Axis Promotes EMT Progression, Cancer Stemness and M2 Macrophage Polarization in Triple-Negative Breast Cancer. *Mol. Cancer*, **2019**, *18* (1), 42. https://doi.org/10.1186/s12943-019-0988-0.
[161] Park, E. Y.; Chang, E.; Lee, E. J.; Lee, H.-W.; Kang, H.-G.; Chun, K.-H.; Woo, Y. M.; Kong, H. K.; Ko, J. Y.; Suzuki, H.; et al. Targeting of MiR34a-NOTCH1 Axis Reduced Breast Cancer Stemness and Chemoresistance. *Cancer Res.*, **2014**, *74* (24), 7573–7582. https://doi.org/10.1158/0008-5472.CAN-14-1140.
[162] Wang, B.; Li, D.; Kovalchuk, I.; Apel, I. J.; Chinnaiyan, A. M.; Wóycicki, R. K.; Cantor, C. R.; Kovalchuk, O. MiR-34a Directly Targets TRNAiMet Precursors and Affects Cellular Proliferation, Cell Cycle, and Apoptosis. *Proc. Natl. Acad. Sci. U.S.A.*, **2018**, *115* (28), 7392–7397. https://doi.org/10.1073/pnas.1703029115.
[163] Bayraktar, R.; Ivan, C.; Bayraktar, E.; Kanlikilicer, P.; Kabil, N. N.; Kahraman, N.; Mokhlis, H. A.; Karakas, D.; Rodriguez-Aguayo, C.; Arslan, A.; et al. Dual Suppressive Effect of MiR-34a on the FOXM1/EEF2-Kinase Axis Regulates Triple-Negative Breast Cancer Growth and Invasion. *Clin. Cancer Res.*, **2018**, *24* (17), 4225–4241. https://doi.org/10.1158/1078-0432.CCR-17-1959.
[164] Liu, R.; Liu, C.; Chen, D.; Yang, W.-H.; Liu, X.; Liu, C.-G.; Dugas, C. M.; Tang, F.; Zheng, P.; Liu, Y.; et al. FOXP3 Controls an MiR-146/NF-KB Negative Feedback Loop That Inhibits Apoptosis in Breast Cancer Cells. *Cancer Res.*, **2015**, *75* (8), 1703–1713. https://doi.org/10.1158/0008-5472.CAN-14-2108.
[165] Khawaled, S.; Suh, S. S.; Abdeen, S. K.; Monin, J.; Distefano, R.; Nigita, G.; Croce, C. M.; Aqeilan, R. I. WWOX Inhibits Metastasis of Triple-Negative Breast Cancer Cells via Modulation of MiRNAs. *Cancer Res.*, **2019**, *79* (8), 1784–1798. https://doi.org/10.1158/0008-5472.CAN-18-0614.
[166] Corrà, F.; Agnoletto, C.; Minotti, L.; Baldassari, F.; Volinia, S. The Network of Non-Coding RNAs in Cancer Drug Resistance. *Front Oncol*, **2018**, *8*, 327. https://doi.org/10.3389/fonc.2018.00327.
[167] Crudele, F.; Bianchi, N.; Astolfi, A.; Grassilli, S.; Brugnoli, F.; Terrazzan, A.; Bertagnolo, V.; Negrini, M.; Frassoldati, A.; Volinia, S. The Molecular Networks of MicroRNAs and Their Targets in the Drug Resistance of Colon Carcinoma. *Cancers (Basel)*, **2021**, *13* (17), 4355. https://doi.org/10.3390/cancers13174355.
[168] Sui, H.; Cai, G.-X.; Pan, S.-F.; Deng, W.-L.; Wang, Y.-W.; Chen, Z.-S.; Cai, S.-J.; Zhu, H.-R.; Li, Q. MiR200c Attenuates P-Gp-Mediated MDR and Metastasis by Targeting JNK2/c-Jun Signaling Pathway in Colorectal Cancer. *Mol Cancer Ther*, **2014**, *13* (12), 3137–3151. https://doi.org/10.1158/1535-7163.MCT-14-0167.

[169] Zhou, H.; Lin, C.; Zhang, Y.; Zhang, X.; Zhang, C.; Zhang, P.; Xie, X.; Ren, Z. MiR-506 Enhances the Sensitivity of Human Colorectal Cancer Cells to Oxaliplatin by Suppressing MDR1/P-Gp Expression. *Cell Proliferation*, **2017**, *50* (3), e12341. https://doi.org/10.1111/cpr.12341.

[170] Juang, V.; Chang, C.-H.; Wang, C.-S.; Wang, H.-E.; Lo, Y.-L. PH-Responsive PEG-Shedding and Targeting Peptide-Modified Nanoparticles for Dual-Delivery of Irinotecan and MicroRNA to Enhance Tumor-Specific Therapy. *Small*, **2019**, *15* (49), 1903296. https://doi.org/10.1002/smll.201903296.

[171] Senfter, D.; Holzner, S.; Kalipciyan, M.; Staribacher, A.; Walzl, A.; Huttary, N.; Krieger, S.; Brenner, S.; Jäger, W.; Krupitza, G.; et al. Loss of MiR-200 Family in 5-Fluorouracil Resistant Colon Cancer Drives Lymphendothelial Invasiveness in Vitro. *Hum Mol Genet*, **2015**, *24* (13), 3689–3698. https://doi.org/10.1093/hmg/ddv113.

[172] Moon, S. U.; Park, Y.; Park, M. G.; Song, S. K.; Jeong, S. H.; Lee, Y. S.; Heo, H. J.; Jung, W. Y.; Kim, S. Theragnosis by a MiR-141-3p Molecular Beacon: Simultaneous Detection and Sensitization of 5-Fluorouracil Resistant Colorectal Cancer Cells through the Activation of the TRIM13-Associated Apoptotic Pathway. *Chem Commun (Camb)*, **2019**, *55* (52), 7466–7469. https://doi.org/10.1039/c9cc01944h.

[173] Ren, J.; Ding, L.; Zhang, D.; Shi, G.; Xu, Q.; Shen, S.; Wang, Y.; Wang, T.; Hou, Y. Carcinoma-Associated Fibroblasts Promote the Stemness and Chemoresistance of Colorectal Cancer by Transferring Exosomal LncRNA H19. *Theranostics*, **2018**, *8* (14), 3932–3948. https://doi.org/10.7150/thno.25541.

[174] Wang, M.; Han, D.; Yuan, Z.; Hu, H.; Zhao, Z.; Yang, R.; Jin, Y.; Zou, C.; Chen, Y.; Wang, G.; et al. Long Non-Coding RNA H19 Confers 5-Fu Resistance in Colorectal Cancer by Promoting SIRT1-Mediated Autophagy. *Cell Death Dis*, **2018**, *9* (12), 1149. https://doi.org/10.1038/s41419-018-1187-4.

[175] Han, P.; Li, J.-W.; Zhang, B.-M.; Lv, J.-C.; Li, Y.-M.; Gu, X.-Y.; Yu, Z.-W.; Jia, Y.-H.; Bai, X.-F.; Li, L.; et al. The LncRNA CRNDE Promotes Colorectal Cancer Cell Proliferation and Chemoresistance via MiR-181a-5p-Mediated Regulation of Wnt/β-Catenin Signaling. *Mol Cancer*, **2017**, *16* (1), 9. https://doi.org/10.1186/s12943-017-0583-1.

[176] Shi, L.; Li, X.; Wu, Z.; Li, X.; Nie, J.; Guo, M.; Mei, Q.; Han, W. DNA Methylation-Mediated Repression of MiR-181a/135a/302c Expression Promotes the Microsatellite-Unstable Colorectal Cancer Development and 5-FU Resistance via Targeting PLAG1. *J Genet Genomics*, **2018**, *45* (4), 205–214. https://doi.org/10.1016/j.jgg.2018.04.003.

[177] Su, S.-F.; Chang, Y.-W.; Andreu-Vieyra, C.; Fang, J. Y.; Yang, Z.; Han, B.; Lee, A. S.; Liang, G. MiR-30d, MiR-181a and MiR-199a-5p Cooperatively Suppress the Endoplasmic Reticulum Chaperone and Signaling Regulator GRP78 in Cancer. *Oncogene*, **2013**, *32* (39), 4694–4701. https://doi.org/10.1038/onc.2012.483.

[178] Mussnich, P.; Rosa, R.; Bianco, R.; Fusco, A.; D'Angelo, D. MiR-199a-5p and MiR-375 Affect Colon Cancer Cell Sensitivity to Cetuximab by Targeting PHLPP1. *Expert Opin Ther Targets*, **2015**, *19* (8), 1017–1026. https://doi.org/10.1517/14728222.2015.1057569.

[179] Yin, Y.; Yao, S.; Hu, Y.; Feng, Y.; Li, M.; Bian, Z.; Zhang, J.; Qin, Y.; Qi, X.; Zhou, L.; et al. The Immune-Microenvironment Confers Chemoresistance of Colorectal Cancer through Macrophage-Derived IL6. *Clin Cancer Res*, **2017**, *23* (23), 7375–7387. https://doi.org/10.1158/1078-0432.CCR-17-1283.

[180] Yin, Y.; Zhang, B.; Wang, W.; Fei, B.; Quan, C.; Zhang, J.; Song, M.; Bian, Z.; Wang, Q.; Ni, S.; et al. MiR-204-5p Inhibits Proliferation and Invasion and Enhances Chemotherapeutic Sensitivity of Colorectal Cancer Cells by Downregulating RAB22A. *Clin Cancer Res*, **2014**, *20* (23), 6187–6199. https://doi.org/10.1158/1078-0432.CCR-14-1030.

[181] Karaayvaz, M.; Zhai, H.; Ju, J. MiR-129 Promotes Apoptosis and Enhances Chemosensitivity to 5-Fluorouracil in Colorectal Cancer. *Cell Death Dis*, **2013**, *4*, e659. https://doi.org/10.1038/cddis.2013.193.

[182] Zhang, P.-F.; Wu, J.; Wu, Y.; Huang, W.; Liu, M.; Dong, Z.-R.; Xu, B.-Y.; Jin, Y.; Wang, F.; Zhang, X.-M. The LncRNA SCARNA2 Mediates Colorectal Cancer Chemoresistance through a Conserved MicroRNA-342-3p Target Sequence. *J Cell Physiol*, **2019**, *234* (7), 10157–10165. https://doi.org/10.1002/jcp.27684.

[183] Mi, H.; Muruganujan, A.; Huang, X.; Ebert, D.; Mills, C.; Guo, X.; Thomas, P. D. Protocol Update for Large-Scale Genome and Gene Function Analysis with the PANTHER Classification System (v.14.0). *Nat Protoc*, **2019**, *14* (3), 703–721. https://doi.org/10.1038/s41596-019-0128-8.

[184] Dufresne, M.; Seva, C.; Fourmy, D. Cholecystokinin and Gastrin Receptors. *Physiol Rev*, **2006**, *86* (3), 805–847. https://doi.org/10.1152/physrev.00014.2005.

[185] Cai, M.-H.; Xu, X.-G.; Yan, S.-L.; Sun, Z.; Ying, Y.; Wang, B.-K.; Tu, Y.-X. Regorafenib Suppresses Colon Tumorigenesis and the Generation of Drug Resistant Cancer Stem-like Cells via Modulation of MiR-34a Associated Signaling. *J Exp Clin Cancer Res*, **2018**, *37* (1), 151. https://doi.org/10.1186/s13046-018-0836-x.

[186] Mastropasqua, F.; Marzano, F.; Valletti, A.; Aiello, I.; Di Tullio, G.; Morgano, A.; Liuni, S.; Ranieri, E.; Guerrini, L.; Gasparre, G.; et al. TRIM8 Restores P53 Tumour Suppressor Function by Blunting N-MYC Activity in Chemo-Resistant Tumours. *Mol Cancer*, **2017**, *16* (1), 67. https://doi.org/10.1186/s12943-017-0634-7.

[187] Findlay, V. J.; Wang, C.; Nogueira, L. M.; Hurst, K.; Quirk, D.; Ethier, S. P.; Staveley O'Carroll, K. F.; Watson, D. K.; Camp, E. R. SNAI2 Modulates Colorectal Cancer 5-Fluorouracil Sensitivity through MiR145 Repression. *Mol Cancer Ther*, **2014**, *13* (11), 2713–2726. https://doi.org/10.1158/1535-7163.MCT-14-0207.

[188] Liang, Y.; Hou, L.; Li, L.; Li, L.; Zhu, L.; Wang, Y.; Huang, X.; Hou, Y.; Zhu, D.; Zou, H.; et al. Dichloroacetate Restores Colorectal Cancer Chemosensitivity through the P53/MiR-149-3p/PDK2-Mediated Glucose Metabolic Pathway. *Oncogene*, **2020**, *39* (2), 469–485. https://doi.org/10.1038/s41388-019-1035-8.

[189] Meng, X.; Sun, W.; Yu, J.; Zhou, Y.; Gu, Y.; Han, J.; Zhou, L.; Jiang, X.; Wang, C. LINC00460-MiR-149-5p/MiR-150-5p-Mutant P53 Feedback Loop Promotes Oxaliplatin Resistance in Colorectal Cancer. *Mol Ther Nucleic Acids*, **2020**, *22*, 1004–1015. https://doi.org/10.1016/j.omtn.2020.10.018.

[190] Lee, J. Y.; Kim, H. J.; Yoon, N. A.; Lee, W. H.; Min, Y. J.; Ko, B. K.; Lee, B. J.; Lee, A.; Cha, H. J.; Cho, W. J.; et al. Tumor Suppressor P53 Plays a Key Role in Induction of Both Tristetraprolin and Let-7 in Human Cancer Cells. *Nucleic Acids Res*, **2013**, *41* (11), 5614–5625. https://doi.org/10.1093/nar/gkt222.

[191] Hwang, W.-L.; Jiang, J.-K.; Yang, S.-H.; Huang, T.-S.; Lan, H.-Y.; Teng, H.-W.; Yang, C.-Y.; Tsai, Y.-P.; Lin, C.-H.; Wang, H.-W.; et al. MicroRNA-146a Directs the Symmetric Division of Snail-Dominant Colorectal Cancer Stem Cells. *Nat Cell Biol*, **2014**, *16* (3), 268–280. https://doi.org/10.1038/ncb2910.

[192] Li, H.; Li, F. Exosomes from BM-MSCs Increase the Population of CSCs via Transfer of MiR-142-3p. *Br J Cancer*, **2018**, *119* (6), 744–755. https://doi.org/10.1038/s41416-018-0254-z.

[193] Zhang, Y.; Li, C.; Liu, X.; Wang, Y.; Zhao, R.; Yang, Y.; Zheng, X.; Zhang, Y.; Zhang, X. CircHIPK3 Promotes Oxaliplatin-Resistance in Colorectal Cancer through Autophagy by Sponging MiR-637. *EBioMedicine*, **2019**, *48*, 277–288. https://doi.org/10.1016/j.ebiom.2019.09.051.

[194] Shi, X.; Kaller, M.; Rokavec, M.; Kirchner, T.; Horst, D.; Hermeking, H. Characterization of a P53/MiR-34a/CSF1R/STAT3 Feedback Loop in Colorectal Cancer. *Cell Mol Gastroenterol Hepatol*, **2020**, *10* (2), 391–418. https://doi.org/10.1016/j.jcmgh.2020.04.002.

[195] Ren, L.-L.; Yan, T.-T.; Shen, C.-Q.; Tang, J.-Y.; Kong, X.; Wang, Y.-C.; Chen, J.; Liu, Q.; He, J.; Zhong, M.; et al. The Distinct Role of Strand-Specific MiR-514b-3p and MiR-514b-5p in Colorectal Cancer Metastasis. *Cell Death Dis*, **2018**, *9* (6), 687. https://doi.org/10.1038/s41419-018-0732-5.

[196] Liu, T.; Zhang, X.; Du, L.; Wang, Y.; Liu, X.; Tian, H.; Wang, L.; Li, P.; Zhao, Y.; Duan, W.; et al. Exosome-Transmitted MiR-128-3p Increase Chemosensitivity of Oxaliplatin-Resistant Colorectal Cancer. *Mol Cancer*, **2019**, *18* (1), 43. https://doi.org/10.1186/s12943-019-0981-7.

[197] Jian, X.; He, H.; Zhu, J.; Zhang, Q.; Zheng, Z.; Liang, X.; Chen, L.; Yang, M.; Peng, K.; Zhang, Z.; et al. Hsa_circ_001680 Affects the Proliferation and Migration of CRC and Mediates Its Chemoresistance by Regulating BMI1 through MiR-340. *Mol Cancer*, **2020**, *19* (1), 20. https://doi.org/10.1186/s12943-020-1134-8.

[198] Kim, C.; Hong, Y.; Lee, H.; Kang, H.; Lee, E. K. MicroRNA-195 Desensitizes HCT116 Human Colon Cancer Cells to 5-Fluorouracil. *Cancer Lett*, **2018**, *412*, 264–271. https://doi.org/10.1016/j.canlet.2017.10.022.

[199] Jin, Y.; Wang, M.; Hu, H.; Huang, Q.; Chen, Y.; Wang, G. Overcoming Stemness and Chemoresistance in Colorectal Cancer through MiR-195-5p-Modulated Inhibition of Notch Signaling. *Int J Biol Macromol*, **2018**, *117*, 445–453. https://doi.org/10.1016/j.ijbiomac.2018.05.151.

[200] Qu, J.; Zhao, L.; Zhang, P.; Wang, J.; Xu, N.; Mi, W.; Jiang, X.; Zhang, C.; Qu, J. MicroRNA-195 Chemosensitizes Colon Cancer Cells to the Chemotherapeutic Drug Doxorubicin by Targeting the First Binding Site of BCL2L2 MRNA. *J Cell Physiol*, **2015**, *230* (3), 535–545. https://doi.org/10.1002/jcp.24366.

[201] Chang, H.-Y.; Ye, S.-P.; Pan, S.-L.; Kuo, T.-T.; Liu, B. C.; Chen, Y.-L.; Huang, T.-C. Overexpression of MiR-194 Reverses HMGA2-Driven Signatures in Colorectal Cancer. *Theranostics*, **2017**, *7* (16), 3889–3900. https://doi.org/10.7150/thno.20041.

[202] Weirauch, U.; Beckmann, N.; Thomas, M.; Grünweller, A.; Huber, K.; Bracher, F.; Hartmann, R. K.; Aigner, A. Functional Role and Therapeutic Potential of the Pim-1 Kinase in Colon Carcinoma. *Neoplasia*, **2013**, *15* (7), 783–794. https://doi.org/10.1593/neo.13172.

[203] Ji, D.; Zhan, T.; Li, M.; Yao, Y.; Jia, J.; Yi, H.; Qiao, M.; Xia, J.; Zhang, Z.; Ding, H.; et al. Enhancement of Sensitivity to Chemo/Radiation Therapy by Using MiR-15b against DCLK1 in Colorectal Cancer. *Stem Cell Reports*, **2018**, *11* (6), 1506–1522. https://doi.org/10.1016/j.stemcr.2018.10.015.

[204] Wang, L.-Q.; Yu, P.; Li, B.; Guo, Y.-H.; Liang, Z.-R.; Zheng, L.-L.; Yang, J.-H.; Xu, H.; Liu, S.; Zheng, L.-S.; et al. MiR-372 and MiR-373 Enhance the Stemness of Colorectal Cancer Cells by Repressing Differentiation Signaling Pathways. *Mol Oncol*, **2018**, *12* (11), 1949–1964. https://doi.org/10.1002/1878-0261.12376.

[205] Huang, L.; Liu, Z.; Hu, J.; Luo, Z.; Zhang, C.; Wang, L.; Wang, Z. MiR-377-3p Suppresses Colorectal Cancer through Negative Regulation on Wnt/β-Catenin Signaling by Targeting XIAP and ZEB2. *Pharmacological Research*, **2020**, *156*, 104774. https://doi.org/10.1016/j.phrs.2020.104774.

[206] Zhang, Y.; Talmon, G.; Wang, J. MicroRNA-587 Antagonizes 5-FU-Induced Apoptosis and Confers Drug Resistance by Regulating PPP2R1B Expression in Colorectal Cancer. *Cell Death Dis*, **2015**, *6*, e1845. https://doi.org/10.1038/cddis.2015.200.

[207] Pan, R.; Cai, W.; Sun, J.; Yu, C.; Li, P.; Zheng, M. Inhibition of KHSRP Sensitizes Colorectal Cancer to 5-Fluoruracil through MiR-501-5p-Mediated ERRFI1 MRNA Degradation. *Journal of Cellular Physiology*, **2020**, *235* (2), 1576–1587. https://doi.org/10.1002/jcp.29076.

[208] Cristóbal, I.; Rubio, J.; Santos, A.; Torrejón, B.; Caramés, C.; Imedio, L.; Mariblanca, S.; Luque, M.; Sanz-Alvarez, M.; Zazo, S.; et al. MicroRNA-199b Downregulation Confers Resistance to 5-Fluorouracil Treatment and Predicts Poor Outcome and Response to Neoadjuvant Chemoradiotherapy in Locally Advanced Rectal Cancer Patients. *Cancers (Basel)*, **2020**, *12* (6). https://doi.org/10.3390/cancers12061655.

[209] Ye, L.; Jiang, T.; Shao, H.; Zhong, L.; Wang, Z.; Liu, Y.; Tang, H.; Qin, B.; Zhang, X.; Fan, J. MiR-1290 Is a Biomarker in DNA-Mismatch-Repair-Deficient Colon Cancer and Promotes

Resistance to 5-Fluorouracil by Directly Targeting HMSH2. *Mol Ther Nucleic Acids*, **2017**, *7*, 453–464. https://doi.org/10.1016/j.omtn.2017.05.006.

[210] Liu, B.; Pan, S.; Xiao, Y.; Liu, Q.; Xu, J.; Jia, L. LINC01296/MiR-26a/GALNT3 Axis Contributes to Colorectal Cancer Progression by Regulating O-Glycosylated MUC1 via PI3K/AKT Pathway. *Journal of Experimental & Clinical Cancer Research*, **2018**, *37* (1), 316. https://doi.org/10.1186/s13046-018-0994-x.

[211] Zhang, H.; Tang, J.; Li, C.; Kong, J.; Wang, J.; Wu, Y.; Xu, E.; Lai, M. MiR-22 Regulates 5-FU Sensitivity by Inhibiting Autophagy and Promoting Apoptosis in Colorectal Cancer Cells. *Cancer Lett*, **2015**, *356* (2 Pt B), 781–790. https://doi.org/10.1016/j.canlet.2014.10.029.

[212] Sun, M.; Zhang, Q.; Yang, X.; Qian, S. Y.; Guo, B. Vitamin D Enhances the Efficacy of Irinotecan through MiR-627-Mediated Inhibition of Intratumoral Drug Metabolism. *Mol Cancer Ther*, **2016**, *15* (9), 2086–2095. https://doi.org/10.1158/1535-7163.MCT-16-0095.

[213] Kannathasan, T.; Kuo, W.-W.; Chen, M.-C.; Viswanadha, V. P.; Shen, C.-Y.; Tu, C.-C.; Yeh, Y.-L.; Bharath, M.; Shibu, M. A.; Huang, C.-Y. Chemoresistance-Associated Silencing of MiR-4454 Promotes Colorectal Cancer Aggression through the GNL3L and NF-KB Pathway. *Cancers (Basel)*, **2020**, *12* (5). https://doi.org/10.3390/cancers12051231.

[214] Lu, Y.; Zhao, X.; Liu, Q.; Li, C.; Graves-Deal, R.; Cao, Z.; Singh, B.; Franklin, J. L.; Wang, J.; Hu, H.; et al. LncRNA MIR100HG-Derived MiR-100 and MiR-125b Mediate Cetuximab Resistance via Wnt/β-Catenin Signaling. *Nat Med*, **2017**, *23* (11), 1331–1341. https://doi.org/10.1038/nm.4424.

[215] Sun, L.; Fang, Y.; Wang, X.; Han, Y.; Du, F.; Li, C.; Hu, H.; Liu, H.; Liu, Q.; Wang, J.; et al. MiR-302a Inhibits Metastasis and Cetuximab Resistance in Colorectal Cancer by Targeting NFIB and CD44. *Theranostics*, **2019**, *9* (26), 8409–8425. https://doi.org/10.7150/thno.36605.

[216] He, Y.; Wang, J.; Wang, J.; Yung, V. Y.-W.; Hsu, E.; Li, A.; Kang, Q.; Ma, J.; Han, Q.; Jin, P.; et al. MicroRNA-135b Regulates Apoptosis and Chemoresistance in Colorectal Cancer by Targeting Large Tumor Suppressor Kinase 2. *Am J Cancer Res*, **2015**, *5* (4), 1382–1395.

[217] Hsu, H.-H.; Kuo, W.-W.; Shih, H.-N.; Cheng, S.-F.; Yang, C.-K.; Chen, M.-C.; Tu, C.-C.; Viswanadha, V. P.; Liao, P.-H.; Huang, C.-Y. FOXC1 Regulation of MiR-31-5p Confers Oxaliplatin Resistance by Targeting LATS2 in Colorectal Cancer. *Cancers (Basel)*, **2019**, *11* (10). https://doi.org/10.3390/cancers11101576.

[218] Liang, Y.; Zhu, D.; Hou, L.; Wang, Y.; Huang, X.; Zhou, C.; Zhu, L.; Wang, Y.; Li, L.; Gu, Y.; et al. MiR-107 Confers Chemoresistance to Colorectal Cancer by Targeting Calcium-Binding Protein 39. *Br J Cancer*, **2020**, *122* (5), 705–714. https://doi.org/10.1038/s41416-019-0703-3.

[219] Zhang, L.; Pickard, K.; Jenei, V.; Bullock, M. D.; Bruce, A.; Mitter, R.; Kelly, G.; Paraskeva, C.; Strefford, J.; Primrose, J.; et al. MiR-153 Supports Colorectal Cancer Progression via Pleiotropic Effects That Enhance Invasion and Chemotherapeutic Resistance. *Cancer Res*, **2013**, *73* (21), 6435–6447. https://doi.org/10.1158/0008-5472.CAN-12-3308.

[220] Jiang, T.; Ye, L.; Han, Z.; Liu, Y.; Yang, Y.; Peng, Z.; Fan, J. MiR-19b-3p Promotes Colon Cancer Proliferation and Oxaliplatin-Based Chemoresistance by Targeting SMAD4: Validation by Bioinformatics and Experimental Analyses. *J Exp Clin Cancer Res*, **2017**, *36* (1), 131. https://doi.org/10.1186/s13046-017-0602-5.

[221] Zhou, Y.; Wan, G.; Spizzo, R.; Ivan, C.; Mathur, R.; Hu, X.; Ye, X.; Lu, J.; Fan, F.; Xia, L.; et al. MiR-203 Induces Oxaliplatin Resistance in Colorectal Cancer Cells by Negatively Regulating ATM Kinase. *Mol Oncol*, **2014**, *8* (1), 83–92. https://doi.org/10.1016/j.molonc.2013.09.004.

[222] Bullock, M. D.; Pickard, K. M.; Nielsen, B. S.; Sayan, A. E.; Jenei, V.; Mellone, M.; Mitter, R.; Primrose, J. N.; Thomas, G. J.; Packham, G. K.; et al. Pleiotropic Actions of MiR-21 Highlight the Critical Role of Deregulated Stromal MicroRNAs during Colorectal Cancer Progression. *Cell Death Dis*, **2013**, *4*, e684. https://doi.org/10.1038/cddis.2013.213.

[223] Sun, W.; Li, J.; Zhou, L.; Han, J.; Liu, R.; Zhang, H.; Ning, T.; Gao, Z.; Liu, B.; Chen, X.; et al. The C-Myc/MiR-27b-3p/ATG10 Regulatory Axis Regulates Chemoresistance in Colorectal Cancer. *Theranostics*, **2020**, *10* (5), 1981–1996. https://doi.org/10.7150/thno.37621.
[224] Rasmussen, M. H.; Lyskjær, I.; Jersie-Christensen, R. R.; Tarpgaard, L. S.; Primdal-Bengtson, B.; Nielsen, M. M.; Pedersen, J. S.; Hansen, T. P.; Hansen, F.; Olsen, J. V.; et al. MiR-625-3p Regulates Oxaliplatin Resistance by Targeting MAP2K6-P38 Signalling in Human Colorectal Adenocarcinoma Cells. *Nat Commun*, **2016**, *7*, 12436. https://doi.org/10.1038/ncomms12436.
[225] Wang, X.; Zhang, H.; Yang, H.; Bai, M.; Ning, T.; Deng, T.; Liu, R.; Fan, Q.; Zhu, K.; Li, J.; et al. Exosome-Delivered CircRNA Promotes Glycolysis to Induce Chemoresistance through the MiR-122-PKM2 Axis in Colorectal Cancer. *Mol Oncol*, **2020**, *14* (3), 539–555. https://doi.org/10.1002/1878-0261.12629.
[226] Masciarelli, S.; Fontemaggi, G.; Di Agostino, S.; Donzelli, S.; Carcarino, E.; Strano, S.; Blandino, G. Gain-of-Function Mutant P53 Downregulates MiR-223 Contributing to Chemoresistance of Cultured Tumor Cells. *Oncogene*, **2014**, *33* (12), 1601–1608. https://doi.org/10.1038/onc.2013.106.
[227] Guo, S. T.; Jiang, C. C.; Wang, G. P.; Li, Y. P.; Wang, C. Y.; Guo, X. Y.; Yang, R. H.; Feng, Y.; Wang, F. H.; Tseng, H.-Y.; et al. MicroRNA-497 Targets Insulin-like Growth Factor 1 Receptor and Has a Tumour Suppressive Role in Human Colorectal Cancer. *Oncogene*, **2013**, *32* (15), 1910–1920. https://doi.org/10.1038/onc.2012.214.
[228] Gu, C.; Cai, J.; Xu, Z.; Zhou, S.; Ye, L.; Yan, Q.; Zhang, Y.; Fang, Y.; Liu, Y.; Tu, C.; et al. MiR-532-3p Suppresses Colorectal Cancer Progression by Disrupting the ETS1/TGM2 Axis-Mediated Wnt/β-Catenin Signaling. *Cell Death Dis*, **2019**, *10* (10), 739. https://doi.org/10.1038/s41419-019-1962-x.
[229] Yu, T.; Guo, F.; Yu, Y.; Sun, T.; Ma, D.; Han, J.; Qian, Y.; Kryczek, I.; Sun, D.; Nagarsheth, N.; et al. Fusobacterium Nucleatum Promotes Chemoresistance to Colorectal Cancer by Modulating Autophagy. *Cell*, **2017**, *170* (3), 548-563.e16. https://doi.org/10.1016/j.cell.2017.07.008.
[230] Hu, J. L.; Wang, W.; Lan, X. L.; Zeng, Z. C.; Liang, Y. S.; Yan, Y. R.; Song, F. Y.; Wang, F. F.; Zhu, X. H.; Liao, W. J.; et al. CAFs Secreted Exosomes Promote Metastasis and Chemotherapy Resistance by Enhancing Cell Stemness and Epithelial-Mesenchymal Transition in Colorectal Cancer. *Mol Cancer*, **2019**, *18* (1), 91. https://doi.org/10.1186/s12943-019-1019-x.
[231] Choe, M. H.; Yoon, Y.; Kim, J.; Hwang, S.-G.; Han, Y.-H.; Kim, J.-S. MiR-550a-3-5p Acts as a Tumor Suppressor and Reverses BRAF Inhibitor Resistance through the Direct Targeting of YAP. *Cell Death Dis*, **2018**, *9* (6), 640. https://doi.org/10.1038/s41419-018-0698-3.
[232] Chen, X.; Liu, Y.; Zhang, Q.; Liu, B.; Cheng, Y.; Zhang, Y.; Sun, Y.; Liu, J.; Gen, H. Exosomal Long Non-Coding RNA HOTTIP Increases Resistance of Colorectal Cancer Cells to Mitomycin via Impairing MiR-214-Mediated Degradation of KPNA3. *Front Cell Dev Biol*, **2020**, *8*, 582723. https://doi.org/10.3389/fcell.2020.582723.
[233] Li, P.; Zhang, X.; Wang, H.; Wang, L.; Liu, T.; Du, L.; Yang, Y.; Wang, C. MALAT1 Is Associated with Poor Response to Oxaliplatin-Based Chemotherapy in Colorectal Cancer Patients and Promotes Chemoresistance through EZH2. *Mol Cancer Ther*, **2017**, *16* (4), 739–751. https://doi.org/10.1158/1535-7163.MCT-16-0591.
[234] Rokavec, M.; Bouznad, N.; Hermeking, H. Paracrine Induction of Epithelial-Mesenchymal Transition Between Colorectal Cancer Cells and Its Suppression by a P53/MiR-192/215/NID1 Axis. *Cell Mol Gastroenterol Hepatol*, **2019**, *7* (4), 783–802. https://doi.org/10.1016/j.jcmgh.2019.02.003.
[235] Xu, K.; Zhan, Y.; Yuan, Z.; Qiu, Y.; Wang, H.; Fan, G.; Wang, J.; Li, W.; Cao, Y.; Shen, X.; et al. Hypoxia Induces Drug Resistance in Colorectal Cancer through the HIF-1α/MiR-338-5p/IL-6

Feedback Loop. *Mol Ther*, **2019**, *27* (10), 1810–1824. https://doi.org/10.1016/j.ymthe.2019.05.017.

[236] Chen, S.; Bu, D.; Ma, Y.; Zhu, J.; Chen, G.; Sun, L.; Zuo, S.; Li, T.; Pan, Y.; Wang, X.; et al. H19 Overexpression Induces Resistance to 1,25(OH)2D3 by Targeting VDR Through MiR-675-5p in Colon Cancer Cells. *Neoplasia*, **2017**, *19* (3), 226–236. https://doi.org/10.1016/j.neo.2016.10.007.

[237] Bamodu, O. A.; Yang, C.-K.; Cheng, W.-H.; Tzeng, D. T. W.; Kuo, K.-T.; Huang, C.-C.; Deng, L.; Hsiao, M.; Lee, W.-H.; Yeh, C.-T. 4-Acetyl-Antroquinonol B Suppresses SOD2-Enhanced Cancer Stem Cell-Like Phenotypes and Chemoresistance of Colorectal Cancer Cells by Inducing Hsa-MiR-324 Re-Expression. *Cancers (Basel)*, **2018**, *10* (8). https://doi.org/10.3390/cancers10080269.

[238] Yu, Y.; Nangia-Makker, P.; Farhana, L.; G. Rajendra, S.; Levi, E.; Majumdar, A. P. MiR-21 and MiR-145 Cooperation in Regulation of Colon Cancer Stem Cells. *Molecular Cancer*, **2015**, *14* (1), 98. https://doi.org/10.1186/s12943-015-0372-7.

[239] Hartsock, A.; Nelson, W. J. Adherens and Tight Junctions: Structure, Function and Connections to the Actin Cytoskeleton. *Biochim Biophys Acta*, **2008**, *1778* (3), 660–669. https://doi.org/10.1016/j.bbamem.2007.07.012.

[240] Arnold, A.; Tronser, M.; Sers, C.; Ahadova, A.; Endris, V.; Mamlouk, S.; Horst, D.; Möbs, M.; Bischoff, P.; Kloor, M.; et al. The Majority of β-Catenin Mutations in Colorectal Cancer Is Homozygous. *BMC Cancer*, **2020**, *20* (1), 1038. https://doi.org/10.1186/s12885-020-07537-2.

[241] Okada, N.; Lin, C.-P.; Ribeiro, M. C.; Biton, A.; Lai, G.; He, X.; Bu, P.; Vogel, H.; Jablons, D. M.; Keller, A. C.; et al. A Positive Feedback between P53 and MiR-34 MiRNAs Mediates Tumor Suppression. *Genes Dev*, **2014**, *28* (5), 438–450. https://doi.org/10.1101/gad.233585.113.